

**Friedrich-Schiller-Universität Jena**

Biologisch-Pharmazeutische Fakultät

**Max-Planck-Institut für chemische Ökologie (MPI-CE) Jena**



Max Planck Institute  
for Chemical Ecology

---

seit 1558

**Biosynthesis of (*Z,E*)-Farnesyl pyrophosphate in *Phyllotreta* flea beetles**

MASTERARBEIT

zur Erlangung des Grades

Master of Science Biochemistry

Vorgelegt von

**Michel Precht**

geb. am 28.05.1991 in Gera

Jena, im Februar 2017

Gutachter:

1. Gutachter: Prof. Dr. Wilhelm Boland
2. Gutachter: Dr. Franziska Beran

## Table of contents

<b>I. LIST OF FIGURES</b> .....	<b>IV</b>
<b>II. LIST OF TABLES</b> .....	<b>VI</b>
<b>III. LIST OF ABBREVIATIONS</b> .....	<b>VII</b>
<b>SUMMARY</b> .....	<b>1</b>
<b>ZUSAMMENFASSUNG</b> .....	<b>2</b>
<b>1 INTRODUCTION</b> .....	<b>3</b>
<b>1.1 The biosynthesis of terpenes</b> .....	<b>3</b>
<b>1.2 Isopentenyl diphosphate synthases</b> .....	<b>4</b>
<b>1.3 Terpene synthases</b> .....	<b>6</b>
<b>1.4 The role of terpenes in insects</b> .....	<b>7</b>
<b>1.5 The biosynthesis of (Z,E)-FPP in flea beetles</b> .....	<b>9</b>
<b>1.6 Master project</b> .....	<b>13</b>
<b>2 MATERIAL AND METHODS</b> .....	<b>14</b>
<b>2.1 Plants and Insects</b> .....	<b>14</b>
<b>2.2 Heterologous expression of IDS enzymes</b> .....	<b>14</b>
2.2.1 Ligation and Cloning.....	14
2.2.2 Expression and co-expression in <i>Escherichia coli</i> .....	16
2.2.3 Interaction studies with recombinant PsIDS .....	17
2.2.4 Bradford assay .....	19
2.2.5 Enzyme activity assays with recombinant IDSs.....	19
2.2.6 SDS-PAGE .....	19
2.2.7 Western Blot.....	20

<b>2.3</b>	<b>Liquid chromatography-MS<sup>E</sup> analysis.....</b>	<b>20</b>
2.3.1	Sample preparation.....	21
2.3.2	LC-MS <sup>E</sup> analysis.....	21
2.3.3	Data processing and database searching.....	22
<b>2.4</b>	<b>Knock-down of IDS genes via RNA interference.....</b>	<b>23</b>
2.4.1	Selection of RNAi targets.....	24
2.4.2	Template preparation and dsRNA synthesis.....	25
2.4.3	Injection of dsRNA.....	27
<b>2.5</b>	<b>Volatile collection.....</b>	<b>28</b>
<b>2.6</b>	<b>Gas chromatography- mass-spectrometry.....</b>	<b>29</b>
<b>2.7</b>	<b>Protein extraction from <i>P. striolata</i>.....</b>	<b>30</b>
<b>2.8</b>	<b>Enzyme activity assays with beetle crude extracts.....</b>	<b>30</b>
<b>2.9</b>	<b>Analysis of gene expression.....</b>	<b>31</b>
<b>2.10</b>	<b>Liquid chromatography- mass-spectrometry.....</b>	<b>32</b>
2.10.1	Analysis of enzyme assays.....	32
2.10.2	Spike-in experiments.....	33
<b>3</b>	<b>RESULTS.....</b>	<b>34</b>
<b>3.1</b>	<b>Expression and co-expression of <i>PaIDSs</i>.....</b>	<b>34</b>
3.1.1	Product identification of individually expressed <i>PaIDS</i> .....	35
3.1.2	Influence of metal ions on recombinant <i>PaIDS</i> .....	37
3.1.3	Identification of co-expressed <i>PaIDS</i> products.....	38
3.1.4	The influence of metal ions on co-expressed <i>PaIDSs</i> .....	39
<b>3.2</b>	<b>Experiments with recombinant <i>PsIDS</i> enzymes.....</b>	<b>41</b>
3.2.1	MS <sup>E</sup> analysis.....	42
3.2.2	Enzyme activity of individually expressed <i>PsIDS1</i> and <i>PsIDS3</i> .....	44
3.2.3	Identification of co-expressed <i>PsIDS</i> products.....	46
3.2.4	Product identification of individually expressed <i>PsIDS1</i> and <i>PsIDS3</i> +His-tag with mixed crude extracts.....	47
3.2.5	Product identification of individually expressed <i>PsIDS1</i> and <i>PsIDS3</i> with mixed elution fractions.....	48
3.2.6	Enzyme assays with combinations of <i>PsIDS1</i> and <i>PsIDS3</i> .....	49

3.3	Knock-down of <i>PsIDS1</i> , <i>PsIDS2</i> and <i>PsIDS3</i> via RNAi.....	50
3.3.1	Single knock-down of <i>PsIDS3</i> .....	50
3.3.2	Knock-down of <i>PsIDS1</i> , <i>PsIDS2</i> and <i>PsIDS3</i> .....	54
4	<b>DISCUSSION</b> .....	<b>58</b>
4.1	<i>P. armoraciae</i> and <i>P. striolata</i> IDS exhibit similar activities .....	58
4.2	Metal ions regulate overall enzyme activity of IDSs in <i>P. armoraciae</i> .....	59
4.3	Co-expressed IDS-isozymes produce (Z,E)-FPP in crucifer flea beetles.....	60
4.4	RNAi revealed that <i>PsIDS1</i> and <i>PsIDS3</i> are involved in the biosynthesis of (Z,E)-FPP...	62
5	<b>SUMMARY AND OUTLOOK</b> .....	<b>63</b>
6	<b>REFERENCES</b> .....	<b>I</b>
7	<b>SUPPLEMENTARY INFORMATION</b> .....	<b>VI</b>
8	<b>ACKNOWLEDGEMENTS</b> .....	<b>XXII</b>
9	<b>STATEMENT OF AUTHORSHIP</b> .....	<b>XXIII</b>

## I. List of Figures

Figure 1: The biosynthesis of isoprenoids .....	4
Figure 2: Comparison of <i>trans</i> - and <i>cis</i> - IDSs.....	5
Figure 3: Structure of (6 <i>R</i> -7 <i>S</i> )-Himachala-9,11-diene .....	7
Figure 4: GC-MS analysis of volatiles emitted by male <i>P. striolata</i> .....	8
Figure 5: GC-MS analysis of volatiles emitted by <i>P. armoraciae</i> .....	8
Figure 6: <i>Phyllotreta armoraciae</i> .....	9
Figure 7: <i>Phyllotreta striolata</i> .....	9
Figure 8: TPS and IDS activity in beetle crude extracts of <i>P. striolata</i> .....	10
Figure 9: Phylogenetic tree of IDS, IDS-like and TPS enzymes of flea beetles .....	11
Figure 10: Proposed pathway for the production of (6 <i>R</i> ,7 <i>S</i> )-himachala-9,11-diene .....	12
Figure 11: Setup of a Western Blot .....	20
Figure 12: siRNA pathway .....	23
Figure 13: Injection of dsRNA into the gap between thoracic and abdominal part .....	27
Figure 14: Setup used for volatile collection.....	28
Figure 15: Protein detection of individually and co-expressed <i>PaIDS1</i> , <i>PaIDS2</i> and <i>PaIDS3</i> .....	34
Figure 16: Spike-in experiments with enzymatic assays of heterologously expressed <i>PaIDS1</i> .....	35
Figure 17 Spike-in experiments with enzymatic assays from heterologously expressed <i>PaIDS3</i> .....	36
Figure 18: Relative activity of heterologously expressed and purified <i>PaIDS1</i> and <i>PaIDS3</i> .....	37
Figure 19: Spike-in experiments from heterologously co-expressed <i>PaIDS1</i> and <i>PaIDS3</i> .....	38
Figure 20: Spike-in experiments from heterologously co-expressed <i>PaIDS2</i> and <i>PaIDS3</i> .....	38
Figure 21: Relative activity of co-expressed and purified <i>PaIDS1</i> , <i>PaIDS2</i> and <i>PaIDS3</i> .....	40
Figure 22: Protein detection of expressed and co-expressed <i>PsIDS1</i> and <i>PsIDS3</i> .....	42
Figure 23: Coomassie-stained gel used for MS <sup>E</sup> analysis.....	42
Figure 24: Relative activity of individually expressed and purified <i>PsIDS</i> enzymes ....	45

Figure 25: Spike-in experiments from heterologously co-expressed <i>PsIDS1</i> and <i>PsIDS3</i> .....	46
Figure 26: Spike-in experiments from individually expressed <i>PsIDS1</i> and <i>PsIDS3</i> +His- tag with mixed crude extracts .....	47
Figure 27: Spike-in experiments from heterologously expressed <i>PsIDS1</i> and <i>PsIDS3</i> with mixed elution fractions. ....	48
Figure 28: Relative activity of heterologously expressed and purified <i>PsIDS1</i> and <i>PsIDS3</i> .....	50
Figure 29: ( <i>Z,E</i> )-FPP production in crude beetle extracts after <i>PsIDS3</i> knock-down via RNAi .....	51
Figure 30: Volatile emission 14 d after knock-down of <i>PsIDS3</i> .....	52
Figure 31: Transcript levels of <i>PsIDS</i> and <i>TPS1</i> after <i>PsIDS3</i> knock-down.....	53
Figure 32: GPP production in crude beetle extracts after <i>PsIDS1</i> , <i>PsIDS2</i> or <i>PsIDS3</i> knock-down via RNAi .....	54
Figure 33: ( <i>E,E</i> )-FPP production in crude beetle extracts after <i>PsIDS1-3</i> knock-down via RNAi .....	55
Figure 34: ( <i>Z,E</i> )-FPP production in crude beetle extracts after <i>PsIDS1-3</i> knock-down via RNAi .....	56
Figure 35: Transcript levels of <i>PsIDS1-3</i> and <i>TPS1</i> 14 days after knock-down .....	57
Figure 36: Spike-in experiments with <i>PaIDS1</i> .....	IX
Figure 37: Spike-in experiments with <i>PaIDS1</i> .....	X
Figure 38: Spike-in experiments with enzymatic assays with <i>PaIDS3</i> .....	XI
Figure 39: Spike-in experiments with co-expressed <i>PaIDS1</i> and <i>PaIDS3</i> .....	XII
Figure 40: Spike-in experiments with co-expressed <i>PaIDS2</i> and <i>PaIDS3</i> .....	XIII
Figure 41: Spike-in experiments with <i>PsIDS3</i> .....	XIV
Figure 42: Spike-in experiments with co-expressed <i>PsIDS1</i> and <i>PsIDS3</i> .....	XV
Figure 43: Spike-in experiments with co-expressed <i>PsIDS1</i> and <i>PsIDS3</i> .....	XVI
Figure 44: Spike-in experiments with co-expressed <i>PsIDS1</i> and <i>PsIDS3</i> with mixed crude extracts .....	XVII
Figure 45: Spike-in experiments with co-expressed <i>PsIDS1</i> and <i>PsIDS3</i> with mixed crude extracts .....	XVIII

Figure 46: Spike-in experiments of co-expressed <i>PsIDS1</i> and <i>PsIDS3</i> with mixed elution fractions .....	XIX
Figure 47: Spike-in experiments of co-expressed <i>PsIDS1</i> and <i>PsIDS3</i> with mixed elution fractions .....	XX
Figure 48: Cutout from the amino acid sequence alignment of <i>PsIDS1</i> , <i>PsIDS2</i> and <i>PsIDS3</i> .....	XXI
Figure 49: Full amino acid sequence alignment of <i>PaIDS1</i> , <i>PaIDS2</i> and <i>PaIDS3</i> ....	XXI

## II. List of Tables

Table 1: Primer used for amplification of <i>IDS</i> genes from <i>P. armoraciae</i> cDNA .....	15
Table 2: Experiments with recombinant <i>PaIDS</i> and <i>PsIDS</i> .....	18
Table 3: Primers used for dsRNA design .....	26
Table 4: GC-MS detection of volatile sesquiterpenes from <i>P. striolata</i> .....	29
Table 5: Primers used for qRT-PCR .....	32
Table 6: LC-gradient program for enzymatic assays .....	32
Table 7: Analysis parameters of terpenoid precursor molecules by LC-MS/MS .....	33
Table 8: LC-gradient program for spike-in experiments .....	33
Table 9: Results MS <sup>E</sup> analysis .....	43
Table 10: dsRNA sequences .....	VI
Table 11: Statistics RNAi targeting <i>PsIDS3</i> .....	VII
Table 12: Statistics RNAi targeting <i>PsIDS1</i> , <i>PsIDS2</i> and <i>PsIDS3</i> .....	VIII



### III. List of Abbreviations

AGE	Agarose gel electrophoresis
<i>B. juncea</i>	<i>Brassica juncea</i>
cDNA	Complimentary DNA
ddH <sub>2</sub> O	Double distilled water
dsRNA	Double stranded RNA
DNA	Desoxyribonucleic acid
<i>E. coli</i>	<i>Escherichia coli</i>
FA	formaldehyde
FARM	First aspartate rich motif
Fig.	Figure
fw	Forward
HPLC	High performance liquid chromatography
IMPI	Insect metallo protease inhibitor
L/D	Light/dark
LC	Liquid chromatography
MeOH	Methanol
MES	2-(N-Morpholino)ethansulfonic acid
MRM	Multiple reaction monitoring
mRNA	Messenger RNA
MS	Mass spectrometry
MS/MS	Tandem mass spectrometry
NI	Not injected
rev	Reverse
RH	Relative humidity
RNA	Ribonucleic acid
<i>P. armoraciae</i>	<i>Phyllotreta armoraciae</i>
<i>P. striolata</i>	<i>Phyllotreta striolata</i>
Rpm	Revolutions per minute
qRT-PCR	Quantitative real-time PCR
SDS	Sodium dodecyl sulfate
SI	Supplementary information

PAGE	Polyacrylamide gel electrophoresis
PCR	Polymerase-chain-reaction
PCR <sub>P</sub>	PCR-product
RISC	RNA-induced silencing complex
RT	Room temperature
SARM	Second aspartate rich motif
SEM	Standard error of the mean
siRNA	Small interfering RNA
TIC	Total ion chromatogram
TAE	Tris-Acetate-EDTA

## Summary

The biosynthesis of terpenes involves isopentenyl diphosphate synthases (IDS), which convert Dimethyl allyl pyrophosphate (DMAPP) and Isopentenyl pyrophosphate (IPP) into terpenoid precursor molecules. These precursor molecules are used as substrate by terpene synthases (TPS) to produce terpenes. Male individuals of the closely related flea beetles species *Phyllotreta striolata* and *Phyllotreta armoraciae*, emit a blend of volatile sesquiterpenes. For *P. striolata* it has been shown that some of these volatile compounds act as aggregation pheromones. TPS in these beetle species are known to convert the unusual substrate (*Z,E*)-Farnesyl pyrophosphate (FPP) into sesquiterpenes. Experiments with recombinant IDS from *P. striolata* exhibited that *PsIDS3* converts Geranyl pyrophosphate (GPP) and IPP into (*Z,E*)-FPP, suggesting this enzyme to be involved in the biosynthesis of aggregation pheromone volatiles. However, no recombinant *PsIDS* was able to produce GPP when provided with DMAPP and IPP. The aim of this study was to investigate the IDS enzymes from *P. armoraciae* and *P. striolata*, with respect to the biosynthesis of (*Z,E*)-FPP. Therefore, enzymatic assays with recombinant IDSs and knock-down experiments, targeting the IDS genes of *P. striolata*, were performed. In this master's thesis *IDS1*, *IDS2* and *IDS3* from *P. armoraciae* as well as *IDS1* and *IDS3* from *P. striolata* were heterologously expressed and co-expressed in *Escherichia coli*. Enzymatic assays confirmed that recombinant *IDS1* and *IDS3* from both species possess the same product spectrum. Assays with individually and co-expressed *PaIDS*, revealed an impact of different metal ion co-factors on the overall activity. Nevertheless, the product spectrum of these enzymes remained mostly unchanged. Enzymatic assays with co-expressed *IDS1* and *IDS3* from either beetle species showed that these enzymes combined are able to produce (*Z,E*)-FPP from the provided substrates DMAPP and IPP. To investigate the biosynthesis of (*Z,E*)-FPP *in vivo*, RNA interference (RNAi) was used. Therefore, double-stranded RNA targeting *IDS1*, *IDS2* and *IDS3* was injected in male *P. striolata* beetles. Crude extracts of dsRNA-injected beetles were tested for IDS activity. The knock-down experiments provided evidence that *PsIDS1* is responsible for GPP formation and that both, *PsIDS1* as well as *PsIDS3*, are involved in the biosynthesis of (*Z,E*)-FPP.

## Zusammenfassung

Die Biosynthese von Terpenen involviert Isopentenylidiphosphatsynthasen (IDS), welche Dimethylallylpyrophosphat (DMAPP) und Isopentenylpyrophosphat (IPP) in Terpenvorstufen umwandeln. Diese Vorstufen dienen als Substrat für Terpensynthasen (TPS) zur Herstellung von Terpenen. Männliche Vertreter der verwandten Flohkäfer *Phyllotreta striolata* und *Phyllotreta armoraciae* sondern ein Gemisch aus flüchtigen Sesquiterpenen ab. Experimente zeigten, dass zwei dieser flüchtigen Stoffe als Aggregationspheromon in *P. striolata* dienen. Es ist außerdem bekannt, dass TPSs in beiden Käferarten das ungewöhnliche Substrat (*Z,E*)-Farnesylpyrophosphat (FPP) in genannte flüchtige Sesquiterpene umwandeln können. Experimente mit rekombinanten IDS von *P. striolata* lieferten den Beweis, dass IDS3 (*Z,E*)-FPP aus Geranylpyrophosphat (GPP) und IPP herstellt, was auf eine Beteiligung von *PsIDS3* an der Biosynthese des Aggregationspheromons hinweist. Jedoch ist kein rekombinantes IDS Enzym aus *P. striolata* bekannt, welches GPP aus DMAPP und IPP herstellt. Das Ziel dieser Studie war es herauszufinden, welche IDS-Enzyme von *P. armoraciae* und *P. striolata* in die Biosynthese von (*Z,E*)-FPP involviert sind. Dafür wurden Assays mit rekombinanten IDS-Enzymen und *knock-down* Experimente, welche auf die IDS-Gene von *P. striolata* zielten, durchgeführt. In dieser Masterarbeit wurden IDS1, IDS2 und IDS aus *P. armoraciae* sowie IDS1 und IDS3 aus *P. striolata* heterolog in *Escherichia coli* exprimiert und co-exprimiert. Enzymassays haben dabei gezeigt, dass IDS1 und IDS3 aus beiden Käferarten die gleichen Produktspektren besitzen. Der Einfluss verschiedener Metallionen auf die Produktspezifität wurde mit IDS-Enzymen aus *P. armoraciae* getestet. Dies zeigte, dass Metallionen zwar die Enzymaktivität steigern können, jedoch keinen großen Einfluss auf die Produktspezifität haben. Enzymassays mit co-exprimierten Proteinen konnten nachweisen, dass beide Enzyme, IDS1 und IDS3 zur Herstellung von (*Z,E*)-FPP aus DMAPP und IPP, notwendig sind. Um die Biosynthese von (*Z,E*)-FPP *in vivo* zu prüfen wurde RNA-Interferenz genutzt. Dafür wurde doppelsträngige RNA in männliche *P. striolata* injiziert, welche die Expression der Gene *IDS1*, *IDS2* und *IDS3* herunterreguliert. Nach der Injektion wurden die Käferhextrakte auf IDS-Aktivität getestet. Die *knock-down* Experimente erbrachten Hinweise, dass *PsIDS1* GPP herstellt und, dass *PsIDS1* und *PsIDS3*, in die Biosynthese von (*Z,E*)-FPP involviert sind.

# 1 Introduction

Terpenes form a huge and heterogeneous group of biomolecules comprising about 55,000 different compounds. Following a proposal from August Kekulé and Marcellin Berthelot, this group of molecules was named after turpentine, the resin of conifers. Terpenes occur as primary and secondary metabolites in nearly every living organism, such as plants, fungi, vertebrates or insects and play various roles, for instance, as defense compounds or messenger molecules (Gershenson and Dudareva, 2007).

## 1.1 The biosynthesis of terpenes

In general, terpenes derive from five-carbon isoprene subunits. In detail, these subunits derive from their biologically activated forms dimethyl allyl pyrophosphate (DMAPP) and its double-bond isomer isopentenyl pyrophosphate (IPP). These basic structures are produced in the mevalonate pathway (Goldstein and Brown, 1990; Zeki *et al.*, 2015; Yang *et al.*, 2015) or in the methyl erythritol phosphat (MEP) pathway, which is restricted to bacteria, plant plastids and archaea (Rohmer, 1999). The further biosynthesis is mainly achieved by two classes of enzymes: isopentenyl diphosphate synthases (IDS) and terpene synthases (TPS). IDSs use DMAPP and IPP as substrates to produce acyclic precursor molecules. TPSs, which use IDS-products as substrates, are involved in the direct synthesis of terpenes. Both enzymes share a carbocationic-driven catalytic mechanism (Gao *et al.*, 2012).

## 1.2 Isopentenyl diphosphate synthases

IDS enzymes, also called prenyltransferases, couple DMAPP and IPP units to form terpenoid precursor molecules.

A conserved family of prenyltransferases, named short-chain IDSs (scIDSs), produces transoid terpene-precursors containing 10-20 carbon atoms (**Figure 1**). Their products represent the precursor molecules of mono-, sesqui-, and diterpenes, respectively.

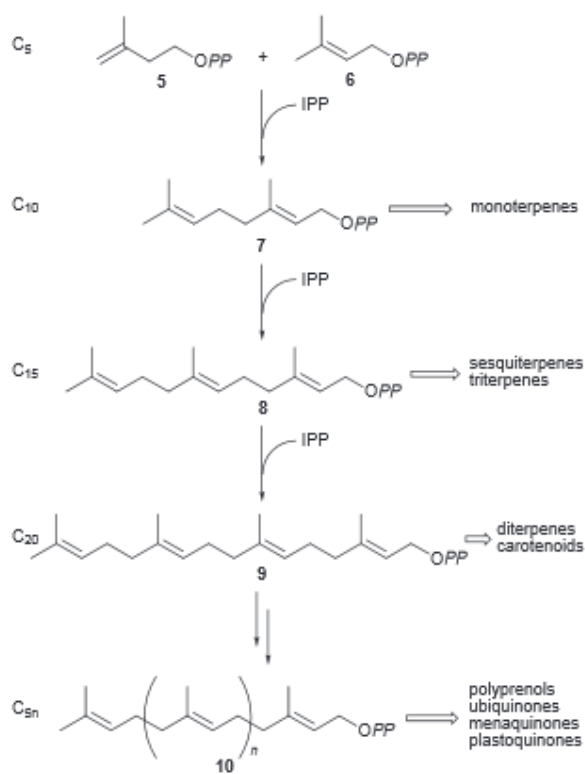


**Figure 1: The biosynthesis of isoprenoids**

The formation of terpenes starts with the molecules isopentenyl pyrophosphate (5) and dimethyl allyl pyrophosphate (6), which are used as substrates by IDS enzymes (Rohmer, 1999).

Furthermore, IDSs are categorized due to their ability of generating either *trans*-, or *cis*-carbon-carbon double bonds. *Trans*- and *cis*-IDSs belong to evolutionary distinct families of prenyltransferases (**Figure 2**) and exhibit a completely different tertiary fold (Fujiwara *et al.*, 2004).

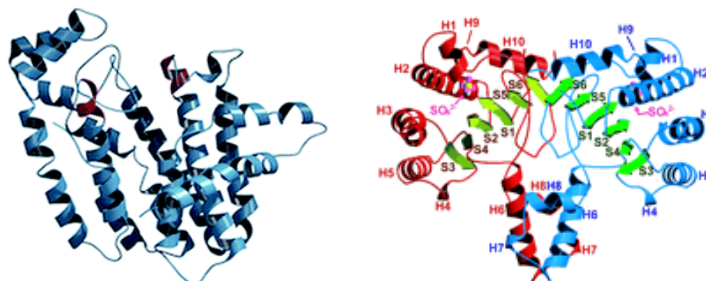


**Figure 2: Comparison of *trans*- and *cis*- IDSs**

*Trans*-IDS, such as the avian (*E,E*)-farnesyl pyrophosphate synthase (left) and *cis*-IDSs, such as the undecaprenyl synthase (right) of *Micrococcus. luteus* exhibit a different tertiary folding (avian FPPS (Tarshis *et al.*, 1994); UPS (Fujihashi *et al.*, 2001)).

IDSs ionize an allylic diphosphate precursor to generate an allylic carbocation. Subsequently, an intermolecular addition to a carbon-carbon double-bond takes place, followed by a deprotonation at C2 of the IPP. During this reaction, the pyrophosphate of DMAPP acts as leaving group. The enzymatic reaction typically occurs from C1 of the allylic carbocation to C4 of IPP (Gao *et al.*, 2012) and is named “head-to-tail” linkage.

The catalytic center of IDSs is hidden in a hydrophobic pocket and exhibits two aspartate-rich motifs (DDxxD), the first- and second-aspartate rich motif (FARM and SARM). These motifs chelate a trio of divalent metal ions (Hosfield *et al.*, 2004), which are involved in the binding and ionization of the allylic substrate (Gao *et al.*, 2012). In general, IDSs require divalent metal ions, such as Magnesium, for their catalytic activity (Tarshis *et al.*, 1996). Site-directed mutagenesis experiments have shown that amino-acid residues, 4 and 5 positions upstream of the FARM motif, play a crucial role in product chain length determination (Liang, 2009). The presence of bulky aromatic residues results in a bottom-like structure in the active cavity which restricts the chain length and may lead to shorter products.

The catalytic activity and product specificity of IDSs can be regulated by different factors. The ratio of DMAPP and IPP for example influences product formation of IDS enzymes in aphids (Vandermoten *et al.*, 2009). The formation of either homodimers or heterodimers can influence the overall enzyme activity in lepidopteran species (Sen *et al.*, 2007a), or enzyme activity and product specificity in *Humulus lupulus* (Wang and Dixon, 2009). Although Magnesium seems to be the usual cofactor of IDSs, it has been described that other divalent metal ions such as Manganese and Cobalt are capable to serve as cofactors.  $\text{Co}^{2+}$  and  $\text{Mn}^{2+}$  are, for example, able to influence catalytic activity and product specificity of IDS1 in *Phaedon cochleariae* (Frick *et al.*, 2013), which results in a product shift from FPP to GPP.

### **1.3 Terpene synthases**

The next step in the biosynthesis of terpenes is performed by TPSs. As already mentioned, the catalytic mechanism of TPS is similar to IDS enzymes. Here, the initially formed allylic carbocation binds to an intramolecular carbon-carbon double-bond, resulting in a variety of complex cyclization and/or rearrangement reactions (Gao *et al.*, 2012). Although cyclizations are often catalyzed by TPS, this type of reaction does not necessarily take place, which would result in linear products such as Farnesene. In general, TPSs exhibit a broad range of catalytic promiscuity. While some are specific, others have a wide product spectrum using one distinct substrate (Steele *et al.*, 1998).



## 1.4 The role of terpenes in insects

Terpenes play essential roles in development, defense and communication of insects. Sesquiterpenes, such as juvenile hormones and the triterpene ecdysone, regulate larval molting and pupation (Cymborowski and Stolarz, 1979). Iridoids, a group of biomolecules, which belong to the class of monoterpenes, serve as defense compounds in certain insect species such as ants (*e.g. Formica rufa*) or stick insects (*e.g. Peruphasma schultei*) (Dyer and Bowers, 1996; Dossey *et al.*, 2008).

In many cases the chemical communication between insects depends on small, often volatile molecules. A variety of chemicals, such as derivatives of fatty acids (Butenandt and Hecker, 1961), pyrrolizidine alkaloids (Boppre, 1978), but also terpenoids can act as messengers.

In many insect species sesquiterpenes serve as pheromones. For instance, the isomers (*E,E*)- $\alpha$  and (*E*)- $\beta$ -farnesene act as alarm pheromones in termites and aphids, respectively (Sobotnik *et al.*, 2008; Wientjen.Wh *et al.*, 1973). Periplanone, the well-studied sex pheromone of the American cockroach (*Periplaneta americana*), is another example for a sesquiterpene acting as messenger molecule in insects (Picimbon and Leal, 1999).

Male beetles of the genus *Phyllotreta* emit a species-specific blend of sesquiterpenes and some of these compounds have been identified to act as aggregation pheromones, attracting both sexes of the same species (Bartelt *et al.*, 2001; Beran *et al.*, 2011). Most of these volatiles are described as molecules with a himachalene basic structure. For instance, (*6R-7S*)-Himachala-9,11-diene (**Figure 3**) is identified as the major compound of emitted volatiles from *Phyllotreta striolata* (Beran *et al.*, 2011).

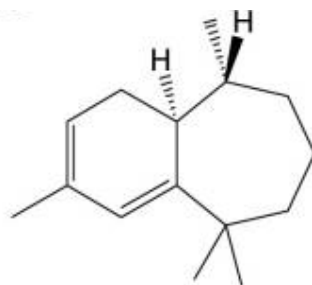


**Figure 3: Structure of (*6R-7S*)-Himachala-9,11-diene**

Beran *et al.* (2016a) showed that male individuals of the striped flea beetle *P. striolata* emit a blend of sesquiterpenes, out of which two compounds act as aggregation pheromone (**Figure 4 A and G**).

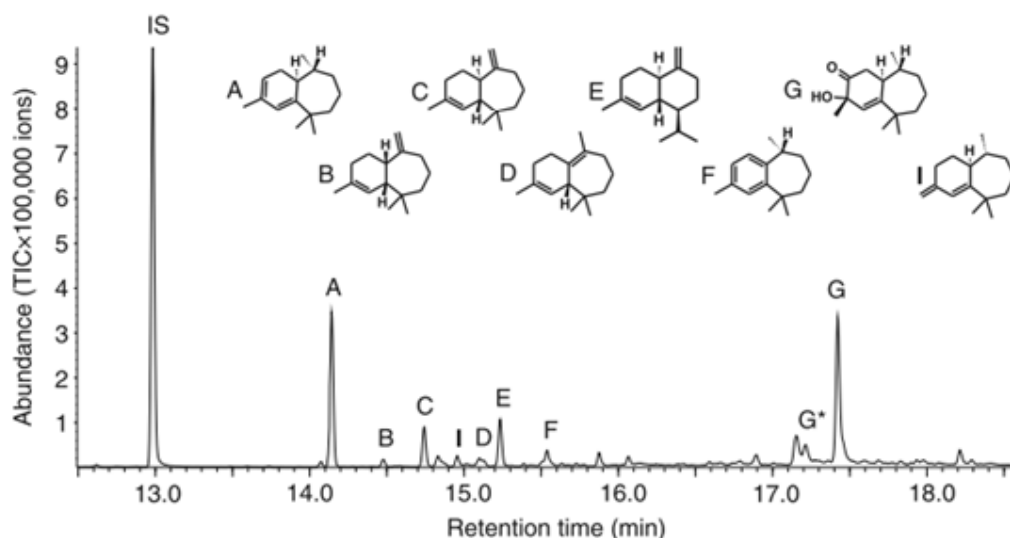


**Figure 4: GC-MS analysis of volatiles emitted by male *P. striolata***

IS, internal standard; A, (6*R*,7*S*)-himachala-9,11-diene; B,  $\alpha$ -himachalene; C, *trans*- $\alpha$ -himachalene; D,  $\beta$ -himachalene; E,  $\gamma$ -cadinene; F, (*R*)-*ar*-himachalene; G, (3*S*,9*R*,9*aS*)-3-hydroxy-3,5,5,9-tetramethyl-5,6,7,8,9,9*a*-hexahydro-1*H*-benzo[7]annulen-2(3*H*)-one; G\*, thermal rearrangement product of compound G; I (6*R*,7*S*)-2,2,6-trimethyl-10-methylene-bicyclo[5.4.0]undec-1,11-ene (Beran *et al.*, 2016b).

The horseradish flea beetle *Phyllotreta armoraciae* is a closely related species to *P. striolata*. Volatile collections of feeding *P. armoraciae* have shown that males of also emit a blend of volatiles (**Figure 5**, by Dr. Franziska Beran), in which some compounds are identical to volatiles emitted by *P. striolata*. Nevertheless, neither of these compounds has been confirmed to act as aggregation pheromone.

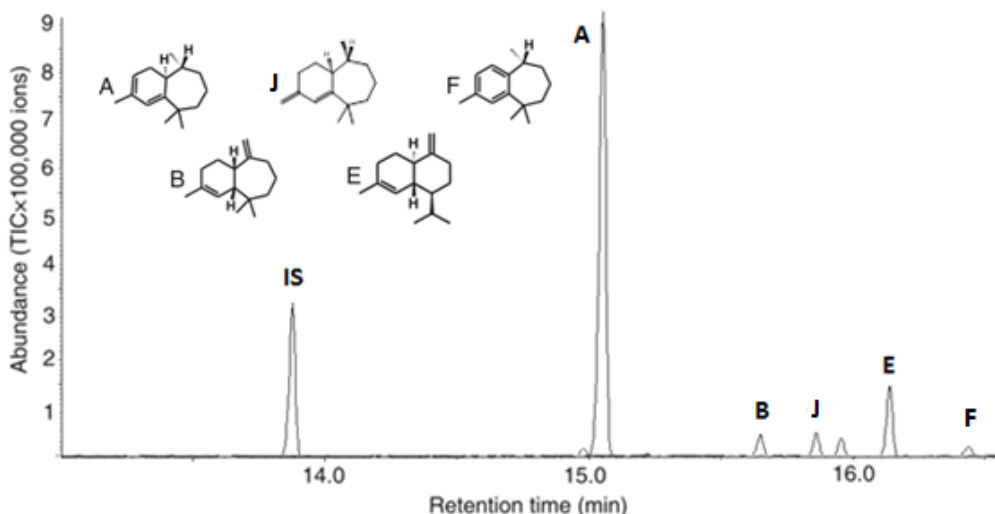


**Figure 5: GC-MS analysis of volatiles emitted by *P. armoraciae***

IS, internal standard; A, (6*R*,7*S*)-himachala-9,11-diene; B, *trans*- $\alpha$ -himachalene; C, 3,5,5-Trimethyl-9-methylene-2,4*a*,5,6,7,8,9,9*a*-octahydro-1*H*-benzo[*a*]cycloheptene; D,  $\gamma$ -cadinene; E, *ar*-himachalene.

## 1.5 The biosynthesis of (Z,E)-FPP in flea beetles

*Phyllotreta armoraciae* (**Figure 6**) is a monophagous beetle, naturally feeding on *Armoracia rusticana* (Nielsen *et al.*, 1979). Adult beetles are 4 - 5 mm long, possess yellowish elytra with a black stripe in the middle and feed on leaves of their host plant. Oviposition takes place on the petioles of young leaves in May. The larvae burrow into petioles for mine-feeding and pupate afterwards in the soil (Nielsen *et al.*, 1979). The new generation of beetles emerges in August and continues feeding. Adult beetles overwinter in the soil near their host plants (Vig, 2002). In the laboratory, *P. armoraciae* can be reared on brassicaceous plants, such as *Brassica juncea* or *Brassica napus* (Vig and Verdyck, 2001), obtaining several generations per year.



**Figure 6: *Phyllotreta armoraciae***  
(Source: <http://baza.biomap.pl>, January 2017)

The striped flea beetle *Phyllotreta striolata* (**Figure 7**) is a serious pest of *Brassica* crops in Southeast Asia and North America (Lamb, 1989). Adult beetles are 1.5 - 2.5 mm long and possess black elytra with a wavy yellowish line, respectively. They feed on the leaves of their host plant. Oviposition takes place on the plant-soil interface. Larvae feed on root hairs of host plants and pupate in the soil (Burgess, 1977). Under natural conditions, *P. striolata* has up to 11 generations per year (Chen *et al.*, 1991). The rearing of this species in the laboratory is more challenging compared to *P. armoraciae*. *P. striolata* beetles can be kept on *B. juncea* plants. However, it was not possible to rear a new generation.



**Figure 7: *Phyllotreta striolata***  
(Source: <http://baza.biomap.pl>, January 2017)

Beran *et al.* (2016b) discovered a novel family of terpene synthases in the flea beetle *P. striolata*. The major finding of this paper was the identification of *Ps*TPS1 being responsible for the production of aggregation pheromone volatiles. The authors supplied beetle crude extracts with either (*E,E*)-FPP or (*Z,Z*)-FPP to test for putative TPS activity. No enzyme activity converting these substrates into volatile sesquiterpenes was evident. Surprisingly, they found an enzyme converting the unusual substrate (*Z,E*)-FPP into (*6R,7S*)-himachala-9,11-diene, the major compound emitted by male *P. striolata*. The enzyme activity was 11-fold higher in males compared to females (**Figure 8 A**). Furthermore, beetle crude extracts were tested for IDS activity. Therefore, DMAPP and IPP were added to crude extracts, which resulted in the production of (*E,E*)-FPP as well as (*Z,E*)-FPP. The IDS activity for the production of (*Z,E*)-FPP was 23-fold higher in males compared to females (**Figure 8 B**).

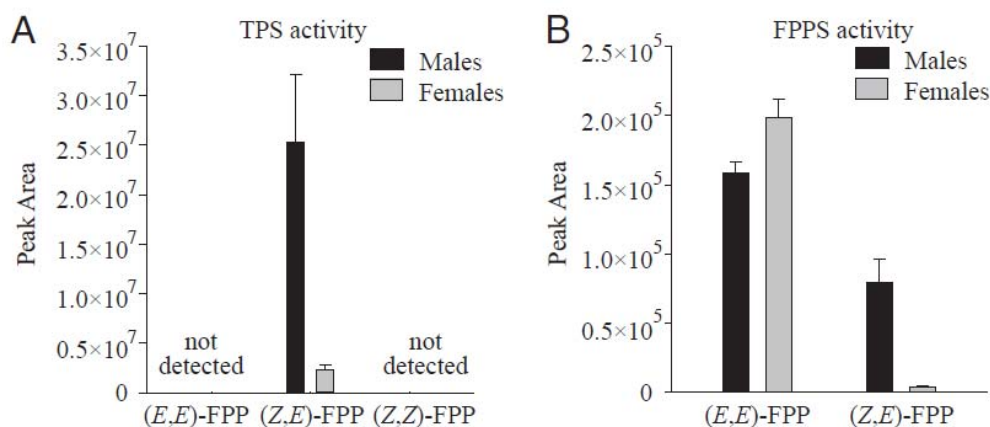


**Figure 8: TPS and IDS activity in beetle crude extracts of *P. striolata***

TPS activity (A) and FPP-synthase activity (B) in crude protein extracts of male and female *P. striolata* adults. Crude protein extracts were incubated with the substrates (*Z,E*)-FPP, (*E,E*)-FPP and (*Z,Z*)-FPP (A) or with IPP and DMAPP (B), respectively (Beran *et al.*, 2016b).

Beran *et al.* (2016b) searched a *P. striolata* transcriptome database for candidate genes encoding TPS enzymes. No amino acid homologies to known plant, fungal, or bacterial TPSs were found. However, nine transcripts were identified which were predicted to encode *trans*-IDSs (**Figure 9**).

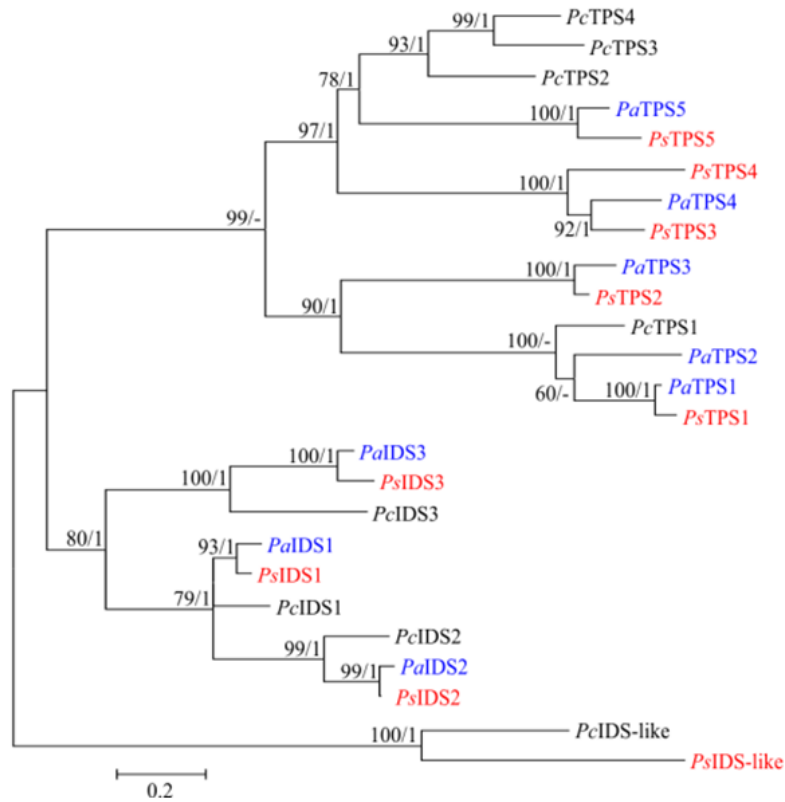


**Figure 9: Phylogenetic tree of IDS, IDS-like and TPS enzymes of flea beetles**

Phylogenetic tree of IDS, IDS-like and TPS enzymes from *P. striolata* (Ps), *P. armoraciae* (Pa) and *Psylliodes chrysocephala* (Pc), inferred by maximum-likelihood analysis (Beran *et al.*, 2016b).

Two of these candidates, *PsIDS1* and *PsIDS3* showed IDS activity. *PsIDS2*, a putative *trans*-IDS with high sequence similarity to *PsIDS1*, showed no enzyme activity. Sequence analysis revealed a modified DDxxD motif (**Figure 48, supplemental information (SI)**) that may explain the lack of activity. However, recombinant *PsIDS1* was capable to produce (*E,E*)-FPP when supplied with DMAPP and IPP. *PsIDS3*, predicted to be an *trans*-IDS, produced Neryl pyrophosphate (NPP) as well as (*Z,Z*)-FPP. Additionally, *PsIDS3* was able to produce (*Z,E*)-FPP when supplied with GPP and IPP (**Figure 10**). Which IDS enzyme is responsible for the production of GPP remains elusive.

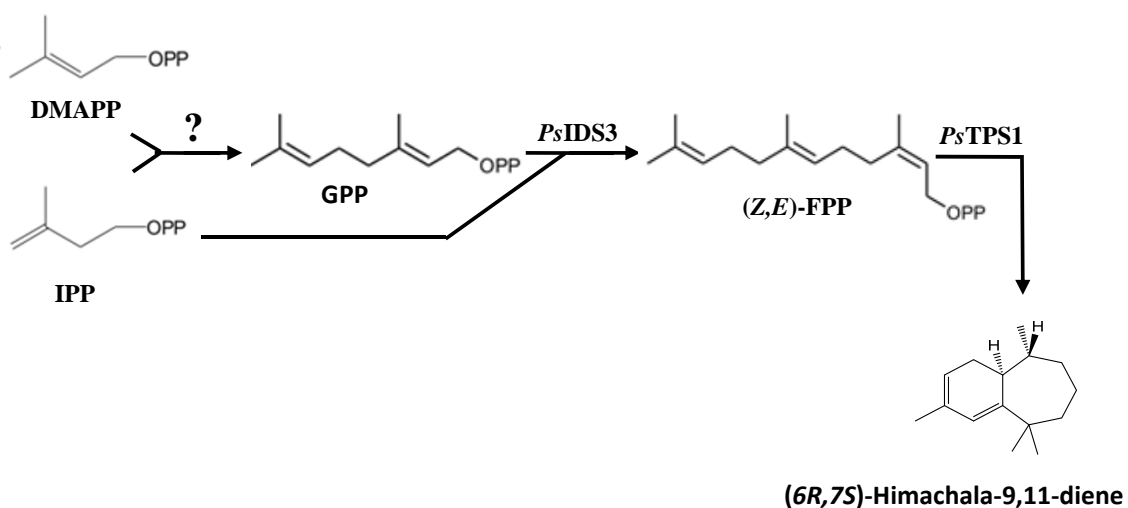


**Figure 10: Proposed pathway for the production of (6*R*,7*S*)-himachala-9,11-diene**

Recombinant *PsIDS3* converts GPP and IPP to (*Z,E*)-FPP, which is the substrate for *PsTPS1*. The production of GPP remains unclear (Modified from Beran *et al.*, 2016b).

## 1.6 Master project

During this project, the biosynthesis of (*Z,E*)-FPP in *Phyllotreta armoraciae* and *Phyllotreta striolata* was investigated.

The monophagous beetle *P. armoraciae* is a closely related species to *P. striolata*. In contrast to *P. armoraciae* is *P. striolata* a serious cabbage pest, especially in northern America and south-east Asia. Male individuals of this species emit a blend of volatile sesquiterpenes, in which some compounds are identified to act as aggregation pheromone. So far, it is known that the production of volatile sesquiterpenes by TPS1 in *P. striolata* depends on the presence of (*Z,E*)-FPP. Activity assays with recombinant *PsIDS3* have shown that this enzyme can produce (*Z,E*)-FPP by using GPP and IPP as substrates. Now, an IDS enzyme providing GPP for *PsIDS3* needs to be identified.

Understanding the biosynthesis of volatile sesquiterpenes in *Phyllotreta* subspecies would be the first step in finding a way to control the cabbage pest *P. striolata*, for instance with the help of pheromone-baited traps.

For this reason, IDS1, IDS2 and IDS3 from *P. armoraciae* as well as IDS1 and IDS3 from *P. striolata*, were expressed or co-expressed in *E. coli* and tested for IDS-activity in enzyme assays. Co-expressions were performed to investigate whether a combination of IDS isozymes is able produce (*Z,E*)-FPP under assay conditions. Assays with IDS enzymes from *P. armoraciae* were supplied with different metal ions to test whether these co-factors have an influence on the product specificity. Interaction studies with recombinant IDS from *P. striolata* were performed to test for putative heterodimerization, a factor which can influence the product spectrum of IDS enzymes. In another approach, RNAi experiments were performed to examine the role of IDS1, IDS2 and IDS3 of *P. striolata* in the synthesis of volatile sesquiterpenes.

## 2 Material and methods

### 2.1 Plants and Insects

“Yo Tsai Ching” strain *Brassica juncea* seeds were purchased from Known-You Seeds Co. LTD (Taiwan) and reared in a growth chamber (24 °C, 50-60% relative humidity (RH), 14 h / 10 h light/dark (L/D)). Adult *P. striolata* beetles were collected from *Brassica* crops and provided from the Entomology Unit of AVRDC-The World Vegetable Center in Shanhua, Taiwan, in February 2016. Adult *P. armoraciae* beetles were collected from *Armoracia rusticana* plants in Laasdorf (Thuringia, Germany). *Phyllotreta* beetles were reared in walk-in controlled environment chambers at the Max Planck Institute for Chemical Ecology (MPI-CE) in Jena, Germany. Adult beetles were kept in insect cages (45 × 45 × 45 cm, MegaView Science, Taiwan) with three to four weeks old potted *B. juncea* plants. Plants were exchanged in weekly intervals. Old plants from *P. armoraciae* rearing were kept in a separate cage for four weeks for larval development and pupation. After four weeks plant material was cut off and the soil with *B. juncea* roots was stored in plastic boxes (17.5 × 21 × 28 cm, Lock&Lock, Seocho-dong, South Korea) with a hole in the lid covered by a mesh (0.128 mm mesh size). The newly emerged beetles were transferred to new insect cages with potted *B. juncea* plants and used for experiments.

### 2.2 Heterologous expression of IDS enzymes

#### 2.2.1 Ligation and Cloning

The IDSs from *P. armoraciae* were amplified from total cDNA (provided by Dr. Franziska Beran; cDNA was synthesized using total RNA from adult beetles as described in 2.9) by polymerase chain reaction (PCR) using Phusion High-Fidelity DNA Polymerase (Thermo Fisher Scientific, Waltham, MA, USA) with gene-specific primers. The 5'-ends of the IDS genes were amplified in a truncated manner by using a gene-internal primer (**Table 1**) to prevent the influence of eukaryotic signal peptides which may affect protein expression in *E. coli* (Vander moten *et al.*, 2008). The amplified IDS sequences were purified via agarose gel electrophoresis using an 1.5% agarose gel (50 ml).



**Table 1: Primer used for amplification of *IDS* genes from *P. armoraciae* cDNA**

Target	Primer	Sequence (5' - 3')
<i>PaIDS1</i>	<i>PaIDS1-fw</i>	CACCACGATACAAACAAAAGTATTACCCAA
	<i>PaIDS1-rev</i>	TCAACAATCCCGCTTGTACAAC
<i>PaIDS2</i>	<i>PaIDS2-fw</i>	CACCACGATACAAACAAAAGTATTACCCAA
	<i>PaIDS2-rev</i>	TCTAATTCTATTTCGAACGCATACAATTCCCTC
<i>PaIDS3</i>	<i>PaIDS3-fw</i>	CACCCCTACGTTAGCTTCGTTTTCC
	<i>PaIDS3-rev</i>	TGGAGTTTTACTACTACAGTCTTATAAACCTGGT

The gel was stained using 2.5 µl of SYBR Safe (Thermo Fisher Scientific). The O'GeneRuler™ (Thermo Fisher Scientific) was used as a DNA marker. Resulting bands with correct product sizes were cut out of the gel and PCR products were recovered using the Zymoclean Gel DNA Recovery Kit (Zymo Research, Irvine, CA, USA). Concentrations of purified PCR products were determined using a Nanodrop ND-1000 spectrophotometer. Subsequently, PCR-products were ligated into expression vectors (pET100/D-TOPO, pET200/D-TOPO or pET101/D-TOPO (Thermo Fisher Scientific)). The pET100/200 vectors differ only in their selection markers (ampicillin and kanamycin, respectively) and encode an N-terminal His-tag. The pET101/D-TOPO vector, carrying an ampicillin resistance as selection marker, was used to express the proteins without His-tag. The ligation reaction was carried out in a 3 µl reaction containing 1 µl (10 ng/µl) of the respective PCR-product, 0.5 µl plasmid, 0.5 µl salt solution and 1 µl double distilled H<sub>2</sub>O (ddH<sub>2</sub>O). Ligation reactions were transformed into One Shot® TOP10 *E. coli* cells (Thermo Fisher Scientific). The first part of the transformation reaction was carried out on ice, by mixing 15 µl of *E. coli* cells with the ligation reaction. Subsequently, the transformation reactions were incubated for 30 min on ice before performing the heat shock for 30 s at 42 °C. The reactions were then supplied with 120 µl of SOC medium (Thermo Fisher Scientific) and incubated for 1 h at 37 °C shaking with 220 rpm. Finally, transformation reactions were plated on agar plates containing the respective antibiotics (50 µg/ml). Agar plates were incubated overnight at 37 °C. For every transformation, four to eight clones were picked for overnight cultures. Therefore, 15 ml reaction tubes with 5 ml LB medium, containing the respective antibiotics (50 ng/µl), were prepared. Overnight cultures were incubated shaking (220 rpm) at 37 °C. Then cultures were centrifuged for 2 min at 1000 × g. Plasmid DNA was isolated from the cells using the GeneJET Plasmid Miniprep Kit (Thermo Fisher Scientific) according to the manufacturer's instructions. Purified constructs

were sequenced using a 3730xl DNA Analyzer (Thermo Fisher Scientific) and the BigDye® Terminator v3.1 Cycle Sequencing Kit (Thermo Fisher Scientific) (by Domenica Schnabelrauch). The analysis of sequencing results was performed using the software Sequencher 5.2.4 (Gene Codes Corporation, Ann Arbor, MI, USA). Plasmids containing the correct IDS sequence were selected for heterologous gene expression. The pET100/101/200 plasmids containing the IDS genes from *P. striolata*, prepared as described, were provided by Dr. Franziska Beran.

### **2.2.2 Expression and co-expression in *Escherichia coli***

Heterologous expressions of IDSs from *P. armoraciae* and *P. striolata* were performed to investigate IDS activity under assay conditions and to compare the product spectrum of individually expressed IDS with co-expressions. Recombinant IDSs from *P. armoraciae* were supplied with different metal ions, to test, whether these co-factors influenced product specificity. Individually and co-expressed *PsIDS* were tested for a putative heterodimerization, described in **2.2.3**.

The enzymes IDS1, IDS2 and IDS3 from *P. armoraciae* as well as IDS1 and IDS3 from *P. striolata* were individually expressed in *E. coli*. Co-expressions were performed with *PaIDS1* and *PaIDS2*, *PaIDS1* and *PaIDS3*, *PaIDS2* and *PaIDS3* as well as *PsIDS1* and *PsIDS3*. Experiments, which were performed with recombinant *PaIDSs* or *PsIDSs* are listed in **Table 2**. Constructs with IDS genes were transformed into the *E. coli* strains BL21(DE3)pLysS (Thermo Fisher Scientific) or One Shot® BL21 Star™ (Thermo Fisher Scientific) for heterologous gene expression. In the case of co-expressions, two constructs with different selection markers (*e.g.* pET100 and pET200) were used. Transformation reactions were carried out as described in **2.2.1**, except that 0.1 µl of constructs were added to transformation reactions. A 5 ml pre-culture was inoculated with a single colony and incubated overnight at 18 °C and 220 rpm. The medium for protein expression of the main culture was prepared using the Overnight Express Auto-induction System 1 (Merck, Darmstadt, Germany; formerly Novagen). The pre-culture was centrifuged for 1 min at 1000 × g and the cell pellet was resuspended in 5 ml of the prepared expression medium. Subsequently, the 200 ml main culture was inoculated with the pre-culture to an  $OD_{600} \leq 0.05$  and cultivated for 2.5 d under the same conditions as the pre-culture. The cultivation step was done using a Certomat IS orbital shaker (Sartorius, Göttingen, Germany). For harvesting cells the whole culture medium was

centrifuged for 10 min at  $4000 \times g$  and  $4^\circ\text{C}$ . Cell pellets were resuspended in 10 ml of lysis buffer [50 mM Tris-HCl; 100 mM NaCl; 10% glycerol (vol/vol), 10 mM  $\text{MgCl}_2$ ; 2 mM DTT; 10 mM imidazole (pH 7.4)]. To support cell lysis and facilitate DNA degradation 0.3 g of lysozyme (AppliChem, GmbH, Darmstadt, Germany), and 1  $\mu\text{l}$  benzonase (2.5 U/ml; Merck) were added. To prevent protein degradation 250  $\mu\text{l}$  of protease inhibitor mix (Protease Inhibitor Cocktail Set V, EDTA-Free – Calbiochem, Merck) were added. The cell suspension was then incubated for 10 min at  $4^\circ\text{C}$  on a shaker. To ensure the complete cell wall disruption, a sonification step was carried out using a sonotrode (60% amplitude, 10 s pulse, 10 s pause, overall 100 s pulse duration, Bandelin, Berlin, Germany). Subsequently, cell lysates were centrifuged for 1 h at  $12500 \times g$  at  $4^\circ\text{C}$  to separate the cell debris from the soluble fraction. Recombinant IDS enzymes were purified via Ni-resin columns. Therefore, columns were filled with 1 ml of HisPur Ni-NTA Resin (Thermo Fisher Scientific) and washed three times its capacity with ddH<sub>2</sub>O. Columns were equilibrated with lysis buffer (one column volume). Afterwards, the total soluble fraction was added to the column. Columns were washed two times with lysis buffer. Protein elution was carried out by adding two times 750  $\mu\text{l}$  of elution-buffer [50 mM Tris-HCl; 100 mM NaCl; 10% glycerol (vol/vol), 10 mM  $\text{MgCl}_2$ ; 2 mM DTT; 200 mM imidazole (pH 7.4)]. To each elution-fraction 17.5  $\mu\text{l}$  of proteinase inhibitor mix was added. From each elution-fraction, 50  $\mu\text{l}$  were transferred to an Eppendorf-tube for protein detection by Western Blot.

### **2.2.3 Interaction studies with recombinant *PsIDS***

Interaction experiments were performed to test whether *PsIDS1* and *PsIDS3* can form a heterodimer. Therefore, *PsIDS3* was individually expressed without His-tag (*PsIDS3-ht*). Crude extracts of individually expressed *PsIDS3-ht* and *PsIDS1* (with His-tag) were mixed in the same ratio (1:1; vol/vol) and purified via Ni-Resin columns. Proteins without His-tag should not bind to Ni-resin columns during the purification step and, thus, *PsIDS3-ht* should just be present in elution fractions in the case of an interaction with *PsIDS1*.

Elution fractions were analyzed for the presence of recombinant IDSs in a proteomical approach using mass spectrometry (LC-MS<sup>E</sup>) described in 2.3. Elution fractions were further tested for IDS activity in enzymatic assays. Since it was not possible to predict in which ratio co-expressed *PsIDS1* and *PsIDS3* are produced in

*E. coli*, the elution fractions of individually expressed *PsIDS1* and *PsIDS3* were mixed in the same concentrations (1:1 c/c). IDS activity in this treatment was used as a reference control for co-expressed *PsIDS1* and *PsIDS3*, as well as individually expressed *PsIDSs* with mixed crude extracts.

**Table 2: Experiments with recombinant *PaIDS* and *PsIDS***  
 IDSs expressed without His-tag are tagged “-ht”; Co-expressions are labeled with “co”.

<b>Expressed enzyme</b>	<b>Experiment</b>
<i>PaIDS1</i>	Activity of recombinant <i>PaIDS</i> in enzymatic assays Influence of Mg <sup>2+</sup> , Mn <sup>2+</sup> , Co <sup>2+</sup> on IDS activity
<i>PaIDS2</i>	
<i>PaIDS3</i>	
<i>PaIDS1</i> and <i>PaIDS2</i> co	Activity of co-expressed <i>PaIDS</i> in enzymatic assays Influence of Mg <sup>2+</sup> , Mn <sup>2+</sup> , Co <sup>2+</sup> on IDS activity
<i>PaIDS1</i> and <i>PaIDS3</i> co	
<i>PaIDS2</i> and <i>PaIDS3</i> co	
<i>PsIDS1</i>	Activity of recombinant <i>PsIDS</i> in enzymatic assays with different protein concentrations
<i>PsIDS3</i>	
<i>PsIDS3</i> -ht	Negative control of interaction studies
<i>PsIDS1</i> and <i>PsIDS3</i> co	Activity of co-expressed <i>PsIDS</i> in enzymatic assays with different protein concentrations
<i>PsIDS1</i> and <i>PsIDS3</i> -ht mixed crude extracts	Interaction studies, Activity in enzymatic assays
<i>PsIDS1</i> and <i>PsIDS3</i> mixed crude extracts	Control for mixed crude extracts of <i>PsIDS1</i> and <i>PsIDS3</i> -ht
<i>PsIDS1</i> and <i>PsIDS3</i> mixed elution fractions	Reference control for co-expressed <i>PsIDS1</i> and <i>PsIDS3</i>
<i>PsIDS1</i> and <i>PsIDS3</i> (-) mixed elution fractions	Negative control for mixed elution fractions of <i>PsIDS1</i> and <i>PsIDS3</i>

#### **2.2.4 Bradford assay**

Determination of protein concentration in elution fractions was carried out using the Quick Start Bradford Protein Assay (Bio-Rad Laboratories, Hercules, CA, USA). An external standard curve was prepared from bovine gamma globulin (2 mg/ml stock solution, Bio-Rad) for quantification. The protein dilution series was set up by diluting the stock solution to 0, 125, 250, 500, 750, 1000 and 1500 µg/ml protein in elution buffer. The assay was performed by adding 250 µl of Bradford reagent to 5 µl of either the protein standard or protein elution fractions in a clear flat-bottom-96-well plate (Nunc, Roskilde, Denmark). Assays were incubated for 5 to 10 min at room temperature (RT) and absorbance at 595 nm was measured using a spectrophotometer (TECAN, Mennedorf, Switzerland). Samples were measured with three technical replicates, each.

#### **2.2.5 Enzyme activity assays with recombinant IDSs**

Enzymatic assays were carried out with a protein concentration of 10 µg/µl in a total volume of 100 µl assay buffer [MOPSO (pH 7.2); 10% Glycerol; and 10 mM MgCl<sub>2</sub>] and supplied with DMAPP (Sigma-Aldrich) and IPP (Sigma-Aldrich) or GPP (Sigma-Aldrich) and IPP, respectively. Assays were incubated at 30 °C for 15 min up to 1 h. Recombinant enzymes from *P. armoraciae* and *P. striolata* were tested for their catalytic activity. Individually and co-expressed IDSs from *P. armoraciae* were supplied with Magnesium, Manganese or Cobalt ions in concentrations of 0.1, 1 and 10 mM each, to investigate the influence of metal ions on the product specificity.

#### **2.2.6 SDS-PAGE**

Premanufactured polyacrylamide gels (Criterion XT-Gel, 4-12%; Bio-Rad) were used to run a sodium dodecyl sulfate polyacrylamide gel electrophoresis (SDS-PAGE, 75 min, 120 V). Samples were prepared with loading buffer [2 × XT-loading buffer; 1% SDS; 1 × reducing agent (Bio-Rad)] and boiled for 4 min at 95 °C while agitating (300 rpm). As marker 6 µl of the PageRuler™ Plus Prestained Protein Ladder (10 to 250 kDA; Thermo Fisher Scientific) was used. SDS-PAGE was carried out in 1 × 2-(N-Morpholino)ethansulfonic acid (MES) buffer.

### 2.2.7 Western Blot

To prepare the Western Blot, membranes (Bio-Rad) as well as the gel were equilibrated for 15 min in Tris-Glycine buffer containing 10% of Methanol (MeOH). The blotting cassette was built up as described in **Figure 11**. The blotting was carried out for 30 min at 100 V in the same TG-buffer mentioned before.

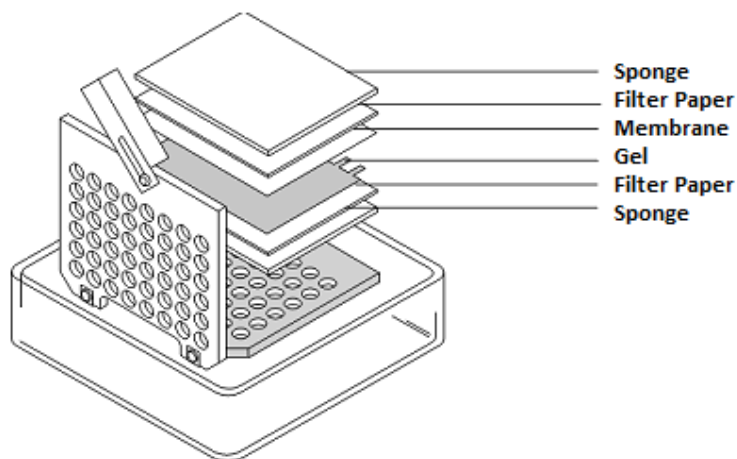


**Figure 11: Setup of a Western Blot**

(Source: <http://www.radio.cuci.udg.mx/bch/EN/Western.html>)

For the detection of heterologously expressed proteins, the His-tag antibody HRP Conjugate Kit (Merck) was used, according to manufacturer's instructions. To visualize proteins, membranes were incubated for 1 min with Solution A [100 mM Tris; 90 mM p-coumaric acid; 250 mM luminol (pH 8.5)] and Solution B [100 mM Tris; 0.024% [vol/vol)  $\text{H}_2\text{O}_2$  (pH 8.5)]. In presence of  $\text{H}_2\text{O}_2$  a horseradish peroxidase oxidized the luminol to its aminophthalate dianion which led to the release of photons, named chemiluminescence. The emitted light was then detected on a photo membrane (Amershan Hyperfilm ECL, GE Healthcare, Little Chalfont, UK) in a dark room.

### 2.3 Liquid chromatography-MS<sup>E</sup> analysis

In order to determine a putative heterodimerization of *PsIDS1* and *PsIDS3* (described in **2.2.3**) a proteomical approach using MS<sup>E</sup> was carried out. Sample preparation and LC-MS<sup>E</sup> analysis were performed by Dr. Natalie Wielsch and Yvonne Hupfer (Mass Spectrometry and Proteomics research group MPI-CE, Jena)

### 2.3.1 Sample preparation

For every sample, 10 µg of protein were separated by SDS-PAGE (1:15 h, 120 V) and stained using Roti-Blue (Carl Roth GmbH, Karlsruhe, Germany) according to the manufacturer's instructions. Protein bands were cut and in-gel digested as described by Shevchenko *et al.* (2006). Tryptic peptides were extracted, dried down in a vacuum centrifuge and dissolved in 50 µl of H<sub>2</sub>O containing 0.1% formaldehyde (FA).

### 2.3.2 LC-MS<sup>E</sup> analysis

One microliter of the peptide mixture was injected onto an UPLC M-class system (Waters, Milford, Massachusetts, US) online coupled to a Synapt G2-si mass spectrometer (Waters). Samples were first on-line pre-concentrated and desalted using a UPLC M-Class Symmetry C18 trap column (100 Å, 180 µm × 20 mm, 5 µm particle size) at a flow rate of 15 µl min<sup>-1</sup> (0.1% aqueous FA). Next, peptides were eluted onto a ACQUITY UPLC HSS T3 analytical column (100 Å, 75 µm × 200, 1.8 µm particle size) at a flow rate of 350 nl/min with the following gradient: 1–9% B over 10 min, 9-19% B over 10 min, 19–32% B over 10 min, 32-48% B over 10 min, 48-58% over 5 min, 70-95% over 5 min, isocratic at 95% B for 4 min, and a return to 1% B over 1 min (phases A and B composed of 0.1% FA and 100% acetonitrile in 0.1% FA, respectively). The analytical column was re-equilibrated for 9 min prior to the next injection. The eluted peptides were transferred into the mass spectrometer operated in V-mode with a resolving power of at least 20000 full widths at half height. The source temperature was set to 80 °C, cone gas flow to 20 l h<sup>-1</sup> and the nanoelectrospray voltage was 3.2 kV. A 100 fmol/µL human Glu-Fibrinopeptide B in 0.1% formic acid/acetonitrile (1:1 v/v) was infused at a flow rate of 0.5 µl min<sup>-1</sup> through the reference sprayer every 45 sec, to compensate for mass shifts in MS and MS/MS fragmentation mode. LC-MS data were collected using MassLynx v4.1 software (Waters) under data-independent acquisition that utilizes alternating scanning in low (MS) and elevated energy (MS<sup>E</sup>) mode. In low energy mode, data were collected at constant collision energy of 6 eV. In elevated MS<sup>E</sup> mode, collision energy was ramped from 20 to 45 eV. MS and MS<sup>E</sup> data were acquired over 0.5 sec intervals in the mass range of 50-2000 m/z.

### **2.3.3 Data processing and database searching**

The acquired data were processed using ProteinLynx Global Server Browser v.3.0.2 software (Waters) using the ion accounting algorithm as described by Li *et al.* (2009). Briefly, data were lock-mass corrected and product ion spectra were generated using following thresholds for low/high energy scan ions and peptide intensity: 150, 40, and 1000 counts, respectively. The peptide fragment spectra were searched against the Swissprot database combined with sequences of the *P. striolata* transcriptome. Database searching was restricted to tryptic peptides with a fixed carbamidomethyl modification for Cysteine residues, along with variable modifications for Lys with BEA residues. Further, default searching parameter specifying mass measurement accuracy were used, minimum number of product ion matches per peptide, minimum number of product ion matches per protein, minimum number of peptide matches, and maximum number of missed tryptic cleavage sites. Maximum false positive rate was set to 4% and all peptides matched under the 4% FDR were considered as correct assignments.



## 2.4 Knock-down of IDS genes via RNA interference

The gene silencing effect of double-stranded RNA (dsRNA) was first described in *Caenorhabditis elegans* by Fire *et al.* (1998). The presence of dsRNA inside of a eukaryotic cell leads to the activation of the short interfering RNA (siRNA) pathway (**Figure 12**). This mechanism is directed against viruses which may insert their dsRNA into a cell. The dsRNA is cleaved and leads to the degradation of the viral mRNA carrying the complementary nucleotide sequence to the dsRNA. In detail, the dsRNA is processed by the enzyme Dicer (RNase III enzyme) into 21-23 bp siRNAs. With the help of some binding proteins, siRNA and the Argonaute protein form the RNA induced silencing complex (RISC). The RISC degrades one strand (passenger strand) and selects the remaining one as guiding strand. With the help of the guiding strand the RISC complex is directed to the respective mRNA and leads to their degradation. Since the biological mechanism of the siRNA pathway was discovered and understood, the artificial insertion of siRNA into eukaryotic cells offers a tool to selectively knock-down genes.

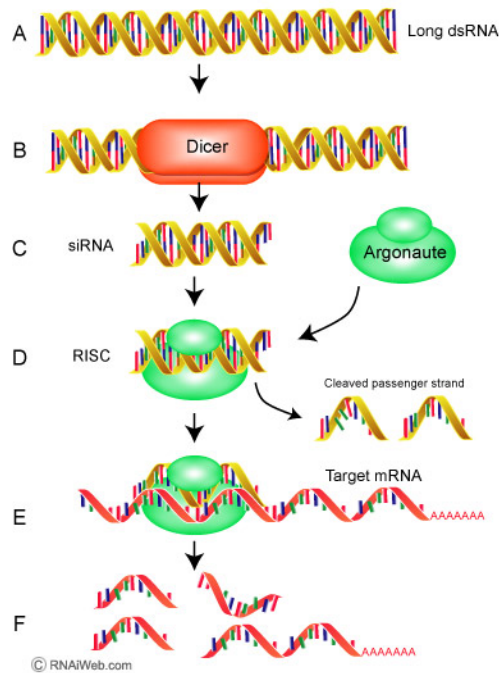


**Figure 12: siRNA pathway**

The siRNA pathway triggered by dsRNA leads to the degradation of mRNA.

(Source: <http://www.raniweb.com>, November 2016)

### 2.4.1 Selection of RNAi targets

The genes *PsIDS1*, *PsIDS2* and *PsIDS3* were used as RNAi targets. *IMPI* (insect metallo proteinase inhibitor), a gene occurring in lepidopteran species, was used as negative control for gene silencing experiments. The *IMPI* gene, originally discovered in *Galleria mellonella*, is not present in the flea beetles. The coding sequences of these genes were processed using the open source software siRNA Wizard v3.1 (<http://www.invitrogen.com/sirnawizard>, InvivoGen, San Diego, CA, USA). The program searched for motifs inside the gene which can mediate a proper siRNA binding. The resulting siRNAs were aligned to their target genes using the software Sequencher 5.2.4. (Gene Codes). For every target gene, dsRNA fragments containing several siRNA candidates were selected. Although, dsRNA should specifically silence the transcription of their corresponding gene, off-target effects are possible, resulting in the knock-down of other genes. The probability of off-target effects increases, when non-target genes contain regions with high similarity to the dsRNA sequence. To make sure the chosen dsRNA fragments only affect the respective *IDS* genes, off-target prediction was performed using the in-house software TagScan Server (developed by Steffi Gebauer-Jung). *In silico*, the software digested and aligned all possible 21-bp long siRNAs (forward (fw) and reverse (rev) strand) from the selected dsRNA fragments to the transcriptome of *P. striolata*. It calculated all possible matches to transcripts from the database, allowing up to two mismatches. The dsRNA fragments showing the least number of hits outside of the targets coding region were selected as target sequences. Here, it was possible to choose dsRNA fragments (**Table 10, SI**) targeting their respective genes.

#### 2.4.2 Template preparation and dsRNA synthesis

Templates used for dsRNA synthesis were amplified via PCR with forward and reverse primers, including the T7-promoter sequence at the 5'-end of each primer (**Table 3**). TOPO TA 2.1 vector (Thermo Fisher Scientific) containing the different *PsIDS* genes or the *IMPI* gene, were used as templates (provided by Dr. Franziska Beran). The PCR was performed using the Advantage 2 Polymerase (Takara Bio USA, inc., Mountain View, CA, USA) in a 50 µl total volume, containing 40 µl nuclease-free water, 5 µl buffer, 2 µl dNTPs, 1 µl forward and reverse primer (10 µM) each and 1 ng of plasmid DNA as a template. The PCR reaction was set up as follows: 94 °C for 2 min, 35 cycles of denaturation at 94 °C for 30 s, primer annealing at 60 °C for 30 s, elongation at 68 °C for 30 s, holding the temperature at 68 °C for 10 min and finally cooling down to 4 °C. PCR products were separated by agarose gel electrophoresis with an 1.5% (vol/vol) agarose gel at 100 V for 30 min. The gel was stained with SYBR Safe (Thermo Fisher Scientific) in a 1:20000 dilution. Bands with the estimated product size were cut out of the gel and purified using the Zymoclean Gel DNA Recovery Kit (Zymo Research). Double-stranded RNA was synthesized using the MEGAscript RNAi Kit (Thermo Fisher Scientific) according to the manufacturer's instructions. The transcription reaction was set up using 1 µg of template DNA, 2 µl 10× T7 Reaction Buffer, 2 µl T7 Enzyme Mix and 2 µl of each nucleotide solution, containing adenosine-, cytosine-, guanine- or uracil-triphosphate. The transcription reaction was performed for 16 h at 37 °C. Then, samples were incubated for 5 min at 75 °C to stop the reaction. Subsequent cooling to RT led to the annealing of the reaction products to double-stranded RNA (dsRNA). To digest remaining DNA or single-stranded RNA, 5 µl Digestion Buffer, 2 µl DNase I and 2 µl RNase were added to the reaction and incubated for 1 h at 37 °C. The synthesized dsRNA was purified according to the manufacturer's instruction. Concentration of dsRNA was determined using a Nanodrop ND-1000 spectrophotometer. If the dsRNA yield was lower than 1 ng/µl, an additional vacuum centrifugation step was performed to concentrate samples (Eppendorf concentrator 5301, Eppendorf AG, Hamburg, Germany).

**Table 3: Primers used for dsRNA design**

Full Primer sequences included T7 Promotor sequence TAATACGACTCACTATAGG at 5'-ends.

Target	Primer	Sequence (5' - 3')	Length [bp]	Tm [°C]	GC content	Product size [bp]
<i>PsIDS1</i>	<i>PsIDS1-fw</i>	GAGACGGAAGG AGTAGGTTTAA TAGCAGTCAAC	46	77.9	41	250
	<i>PsIDS1-rev</i>	GAGAATAGGAA GTCTTGTACTIONG ACGATGGTC	52	80.4	42	
<i>PsIDS2</i>	<i>PsIDS2-fw</i>	GAGGATCGAAC TGTTCCAAGAC AC	43	77.9	44	250
	<i>PsIDS2-rev</i>	GAGCTTTTGAA CTTGGAATAA TGCCCCATTTC	53	79.8	40	
<i>PsIDS3</i>	<i>PsIDS3-fw</i>	GAGAGCGGCTG ATTCCACGAG	40	78.9	50	362
	<i>PsIDS3-rev</i>	GAGTCGGATCC GCTTTGCCGTA	41	79	49	
IMPI	IMPI-fw	GAGCGGTGGAG CCTGCGATAAT G	42	79.9	50	310
	IMPI-rev	GAGCGACGGTG GAGGGGAGTCA A	42	80.7	52	

### 2.4.3 Injection of dsRNA

The dsRNA was injected using a Nanoliter 2010 injector and pulled glass capillaries (3.5", both World Precision Instruments, Sarasota, FL, USA). Capillaries were prepared using a P.2000 micropipette puller (Sutter Instrument Corporation, Novato, CA, USA) set to temperature of 425 °C; filament 4; velocity 40 m/s; delay 175 s, pull 30 s. Pulled capillaries were filled with mineral oil and subsequently mounted on the injector and filled with the dsRNA sample. 100 ng of dsRNA were injected between thoracic and abdominal part of male *P. striolata* beetles (**Figure 13**).

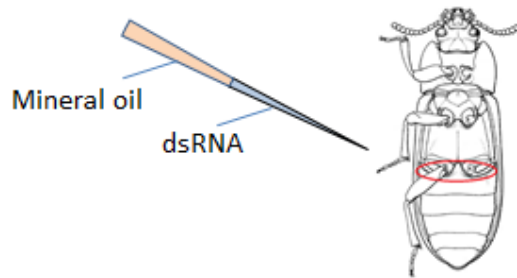


**Figure 13: Injection of dsRNA into the gap between thoracic and abdominal part**

The injection site is marked with a red circle (edited from <http://www.grainscanada.gc.ca>, November 2016).

In the first RNAi injection experiment, beetles were treated with dsRNA targeting *PsIDS3* or *IMPI*. Additionally, an untreated control group without injections (NI) was used as a control. The second knock-down experiment was performed targeting all three *IDS* genes. The injected beetles and the non-injected control group were kept in plastic tubes (4.5 × 10.5 cm, K-tk E.k., Retzstadt, Germany) for 14 d, together with a *B. juncea* leaf and moistened tissue paper inside a walk-in chamber (24 °C, 50-60% (RH), 14 h / 10 h (L/D)). Moistened tissue paper and leaves were exchanged every 2 days and plastic tubes were exchanged after 6 – 8 d to prevent molding. Injected beetles and non-injected control groups were used for volatile collections, enzyme activity assays and RNA isolation.

## 2.5 Volatile collection

The emission of volatile sesquiterpenes from *P. striolata* beetles injected with dsRNA and the non-injected control beetles was tested by headspace collection. Compressed air (8-10 bar, 2-3% humidity) was directed to a valve (**Figure 14 A**), reducing the pressure to 0.5 - 1 bar. Air was further directed to 10 flowmeters (**Figure 14 B**; 1-10 l/min; Ki-Instruments, Hatfield, PA, USA) where the flow was set to < 0.1 l/min. The air was now directed into glass jars (**Figure 14 C**; 100 ml, Schott, Jena, Germany) containing 50 ml of ddH<sub>2</sub>O. Then the air flow was charcoal cleaned (**Figure 14 D**) and conducted into silanized glass jars (100 ml, Schott) containing the beetles and one *B. juncea* leaf, respectively (**Figure 14 E**). Chemically inert materials were used to build up the system, to prevent the emission of other volatiles than these from beetles. This includes the usage of teflon tubes and polyether ketone stoppers on the collection jars. Volatile collections were carried out on 4 - 6 biological replicates. Each replicate comprised 20 beetles. Experiments were performed in the same walk-in chambers as described in 2.1. Volatiles were collected for 20 h on SuperQ filters (25 mg; ARS, Inc. Micanopy, FL, USA). Filters were eluted using 100 µl of hexane containing 10 ng/µl bromodecane as internal standard (Sigma Aldrich).

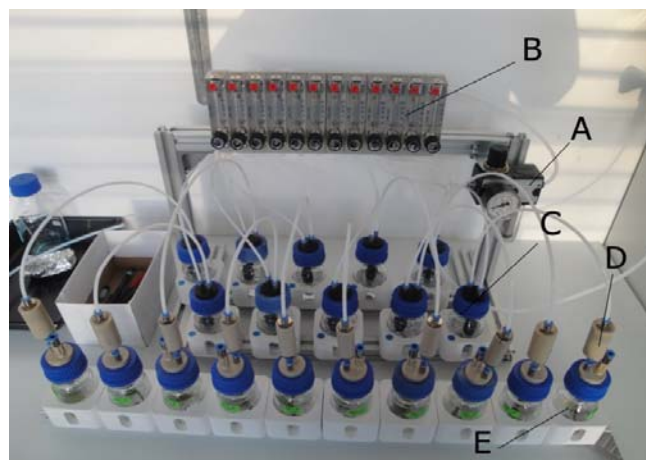


**Figure 14:** Setup used for volatile collection

## 2.6 Gas chromatography- mass spectrometry

Elution fractions from volatile collections were analyzed with an Agilent 6890 N gas chromatograph (GC) coupled to an Agilent 5973B quadrupole mass spectrometer. The gas chromatograph was equipped with an HP-5MS capillary column (30 m × 0.25 mm i.d., 0.25 μm film thickness, Agilent). Helium was used as carrier gas with a set flowrate of 1.0 ml/min. The oven program started at 40 °C, held for 2 min and increased by 10 °C/min up to 250 °C, which was used as injection temperature. Subsequently, temperature was increased to 300 °C and held for 2 min. One microliter of each sample was injected in splitless mode. MS conditions were set to electron impact mode (70 eV) and scanning mode detecting from 33 to 250 atomic mass units. Compounds (**Table 4**) were identified based on the comparison to known retention times and fragmentation patterns of volatile sesquiterpenes emitted by *P. striolata* (Beran *et al.*, 2011, 2016a). Analysis of GC-MS results was performed using the GCMS Chemstation software (Agilent). The sesquiterpene content was calculated as total ion chromatogram (TIC) peak area relative to the internal standard (bromodecane 10 ng/μl). Peak areas of all detected compounds were summed up to calculate the total amount of emitted volatile sesquiterpenes.

**Table 4: GC-MS detection of volatile sesquiterpenes from *P. striolata***

1	(6 <i>R</i> ,7 <i>S</i> )-Himachala-9,11-diene
2	α-Himachalene
3	<i>trans</i> -α-Himachalene
4	γ-Cadinene
5	( <i>R</i> )-ar-Himachalene
6	(3 <i>S</i> ,9 <i>R</i> ,9 <i>aS</i> )-3-hydroxy-3,5,5,9-tetramethyl-5,6,7,8,9,9 <i>a</i> -hexahydro-1 <i>H</i> -benzo[7]annulen-2(3 <i>H</i> )-one
7*	thermal rearrangement product of compound 6

## **2.7 Protein extraction from *P. striolata***

Adult beetles were anaesthetized for 5 min at -20 °C and homogenized in 250 µl of extraction buffer [25 mM 3-(N-morpholino)-2-hydroxy propanesulfonic acid (MOPSO) (pH 7.2); 10% Glycerol; protease inhibitor mix (Protease Inhibitor Cocktail Set V, EDTA-Free – Calbiochem, Merck)] using a 2 ml glas potter. Each replicate comprised 20 male *P. striolata* beetles. Homogenized samples were centrifuged at 4 °C and 16000 × g for 10 min. Supernatants were collected and ultracentrifuged at 4 °C and 48000 × g for 1 h. To determine protein concentration, Bradford assays were carried out as described in **2.2.4**.

## **2.8 Enzyme activity assays with beetle crude extracts**

Crude beetle extracts were tested for IDS activity to compare RNAi effects of dsRNA injected beetles and the non-injected control group. Activity assays were carried out by using 150 µg of protein in a total volume of 200 µl assay buffer [MOPSO (pH 7.2); 10% Glycerol; and 10 mM MgCl<sub>2</sub>] supplied with 50 µM DMAPP and 50 µM IPP. Assays were incubated at 30 °C for 1 h and analyzed via LC-MS/MS.



## 2.9 Analysis of gene expression

Quantitative real-time PCR (qRT-PCR) was performed to determine transcript levels of IDS genes in dsRNA injected male *P. striolata* beetles and the non-injected control group. Beetles were injected with dsRNA targeting *PsIDS1*, *PsIDS2* and *PsIDS3*. Six biological replicates and two technical replicates were tested. Biological replicates comprised eight adult beetles, each. RNA was extracted using the InnuPREP RNA Mini Kit (Analytik Jena, Jena, Germany). Samples were treated with TURBO DNase (Thermo Fisher Scientific) to remove remaining genomic DNA. A subsequent purification step was performed using the RNeasy MinElute Cleanup Kit (Qiagen, Venlo, Netherlands). RNA concentration was determined using a Nanodrop ND-1000 spectrophotometer. The cDNA synthesis was carried out with the Verso cDNA Synthesis Kit (Thermo Fisher Scientific). Therefore, random hexamer and anchored oligo-dT primers in a 3:1 ratio (vol/vol) were mixed with 400 ng of total RNA. Quantitative real-time PCR was done in optical 96-well plates (Bio-Rad) using Bio-Rad CFX Connect Real-Time System with Absolute Blue qPCR SYBR Green Kit (Thermo Fisher Scientific). The following PCR program was used: 15 min at 95 °C, 40 cycles for 15 s at 95 °C, 30 s at 57 °C, 30 s at 72 °C followed by a melt cycle from 55 to 95 °C in 0.5 s steps. Additionally, a cDNA pool was prepared by mixing 2 µl of each sample. The cDNA pool was then diluted in a range from 0.05-10 ng/µl to test the primer binding efficiency in a qRT-PCR run. The ribosomal protein L13a (*RPL13a*) and ribosomal protein S4e (*RPS4e*) were used as reference genes in the first RNAi experiment targeting *PsIDS3*, whereas the ribosomal protein L7 (*rpl7*) and the eukaryotic initiation factor 4a (*eIF4a*) were used as reference genes in the second RNAi experiments targeting *PsIDS1*, *PsIDS2* and *PsIDS3*. Expression levels of *PsIDS1*, *PsIDS2*, *PsIDS3* as well as *TPS1* were compared with 1000 molecules of PCR-product (PCR-P) of reference genes. The relative gene expression was statistically analyzed using One-Way ANOVA and Tukey's test. Analysis was done in SigmaPlot version 11.0.

**Table 5: Primers used for qRT-PCR**

Target	Primer	Sequence (5'-3')
<i>PsIDS1</i>	q <i>PsIDS1</i> fw	ACGATTTCTGGACGTGTT
	q <i>PsIDS1</i> rev	GTCGTTGTCCTTGCCGTAAT
<i>PsIDS2</i>	q <i>PsIDS2</i> fw	TACGCTACAGTTGCCAGTCG
	q <i>PsIDS2</i> rev	CCGAAGCAATTGAGGAAATC
<i>PsIDS3</i>	q <i>PsIDS3</i> fw	ACCGGAGAATCTCACACCAG
	q <i>PsIDS3</i> rev	CCGTCTCGTGAAGGAATTGT
<i>PsTPS1</i>	q <i>PsTPS1</i> fw	TCACCAGATCGAATTCACCA
	q <i>PsTPS1</i> rev	TCGTCCATTTCTGTGTTGAA

## 2.10 Liquid chromatography- mass-spectrometry

### 2.10.1 Analysis of enzyme assays

The analysis of enzymatic assay products was carried out using an Agilent 1260 HPLCsystem (Agilent) coupled to an API 5000 triple quadrupole mass spectrometer (AB Sciex, Darmstadt, Germany). As mobile phase a 5 mM ammonium bicarbonate solution in water (Solvent A) and acetonitrile (Solvent B) were used. The flow rate was set to 1.2 ml/min. Gradient details for the separation of assay products are listed in **Table 6**. Injection volume was set to 1 µl per sample. The MS was equipped with an electrospray ionization source (ESI) and used in the negative ionization mode. Ion spray voltage was maintained at -4200 eV. Heating gas was set to 70 psi resulting in a maintaining gas temperature of 700 °C. Nebulizing gas was set to 60 psi, curtain gas to 30 psi and collision gas to 7 psi. Multiple reaction monitoring (MRM) was applied to study the fragmentation of the parent ions to their respective product ions. Applied MRM parameters are listed in **Table 7**. For acquisition and processing of results the Analyst 1.6 software was used.

**Table 6: LC-gradient program for enzymatic assays**

Ammonium bicarbonate (5 mM) in water as mobile phase A and acetonitrile as mobile phase B were used.

Step	Time [min]	A [%]	B [%]
0	0	95	5
1	9	53	47
2	9.1	0	100
3	10	0	100
4	10.1	95	5
5	13	95	5

**Table 7: Analysis parameters of terpenoid precursor molecules by LC-MS/MS**

Displayed are the mass to charge ratios ( $m/z$ ) of quadrupole 1 (Q1) and 3 (Q3), retention time (min), voltage (V) of declustering potential (DP) and collision energy (CE) for IPP/DMAPP, GPP, FPP as well as GGPP.

Compound	Q1 [ $m/z$ ]	Q3 [ $m/z$ ]	DP [V]	CE [V]
IPP/DMAPP	244,800	79,100		
GPP	312,900	79,000	-40	-38
FPP	78,800	78,800	-40	-42
GGPP	78,900	78,900	-45	-50

### 2.10.2 Spike-in experiments

To determine the stereochemistry of assay products, spike-in experiments were carried out. Therefore, authentic standards were added to enzymatic assay samples and analyzed using LC-MS/MS. To achieve a proper separation of enantiomeric assay products, the LC-gradient program (**Table 8**) was modified according to Nagel *et al.* (2012). The flow rate of the liquid phase was set to 0.8 ml/min. Settings of the LC-MS are described in **2.10.1**.

**Table 8: LC-gradient program for spike-in experiments**

Ammonium bicarbonate (5 mM) in water as mobile phase A and acetonitrile as mobile phase B were used.

Step	Time [min]	A [%]	B [%]
0	0	100	0
1	2	90	10
2	9	58.5	41.5
3	9.1	0	100
4	10	0	100
5	10.1	100	0
6	15	100	0

### 3 Results

#### 3.1 Expression and co-expression of *PaIDS*s

All IDS enzymes from *P. armoraciae* were individually expressed or co-expressed in *E. coli* and purified via Ni-resin columns. The activity of purified proteins was tested in enzymatic assays and analyzed by LC-MS/MS. Assays were supplied with different metal ions to investigate whether these co-factors can influence product specificity and/or enzyme activity of recombinant *PaIDS*s.

Individual expressions of *PaIDS1* (42 kDa), *PaIDS2* (41 kDa) and *PaIDS3* (40.5 kDa) were detected in pellet fractions, crude extracts and elution fractions (Figure 15). Due to the similar molecular weight of recombinant *PaIDS*, these proteins cannot be distinguished on the western blot. Therefore, it was not clear whether both enzymes were successfully co-expressed. Membranes were stained with Coomassie Brilliant Blue. Coomassie-staining revealed bands in elution fractions, which did not superpose with bands from the protein detection, suggesting that the purification via Ni-resin columns did not remove all proteins without His-tag.

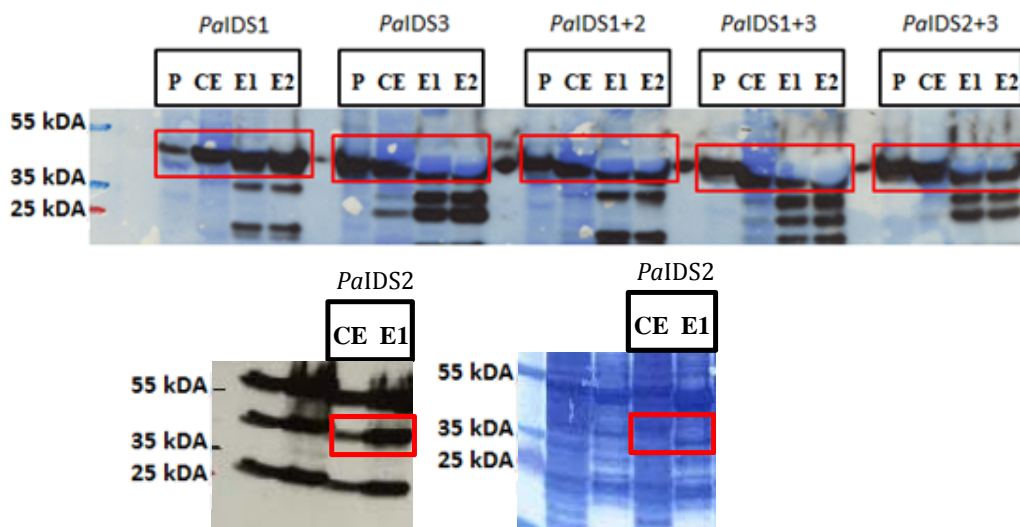


**Figure 15: Protein detection of individually and co-expressed *PaIDS1*, *PaIDS2* and *PaIDS3***  
All expressed enzymes were detected in pellet fractions (P), crude extract (CE) and elution fractions (E1-2). Coomassie-staining revealed a partially purification via Nickel-Resin columns.

### 3.1.1 Product identification of individually expressed *PaIDS*

Two products were detected in IDS activity assays performed with recombinant *PaIDS1* provided with DMAPP and IPP as substrates. These products were identified as (*E,E*)-FPP (**Figure 16 A**) and GPP (**Figure 16 B**). However, the peak area in original assays of FPP was on average 79 times higher compared to GPP, suggesting that (*E,E*)-FPP is the major product of *PaIDS1* under assay conditions.

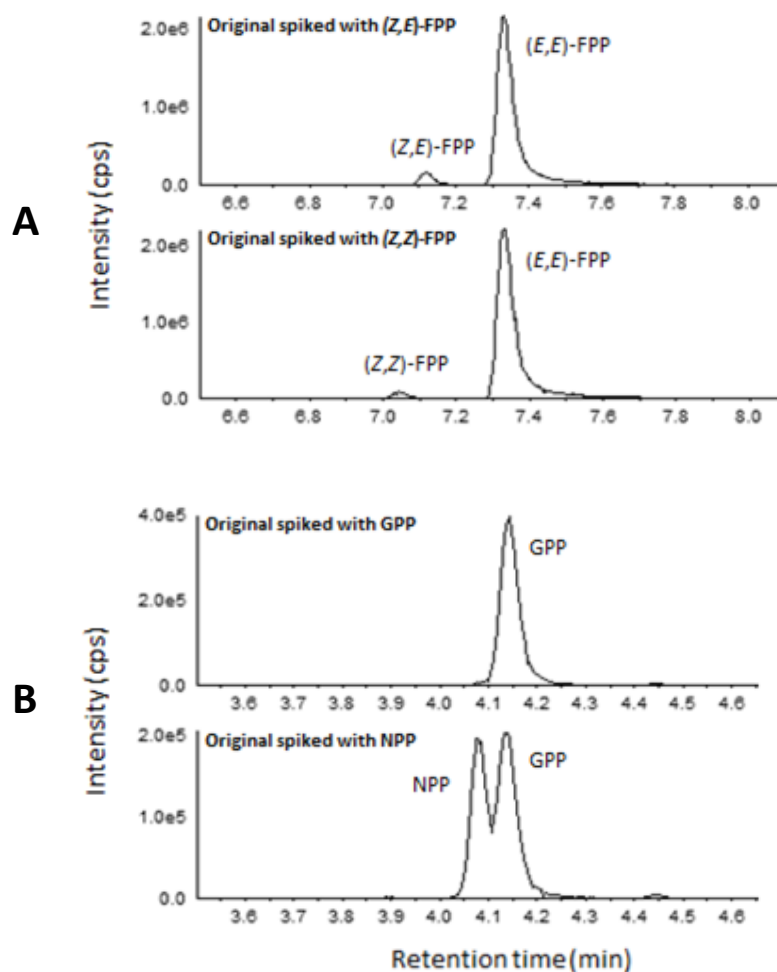


**Figure 16: Spike-in experiments with enzymatic assays of heterologously expressed *PaIDS1***

Heterologously expressed *PaIDS1* produced (*E,E*)-FPP (A); and GPP (B) when supplied with DMAPP and IPP. Authentic standards were added, to identify the stereochemistry of assay products.

Under assay conditions, recombinant *PaIDS3* produced FPP when supplied with GPP and IPP as substrates (**Figure 17**). The product was identified as (*Z,E*)-FPP.

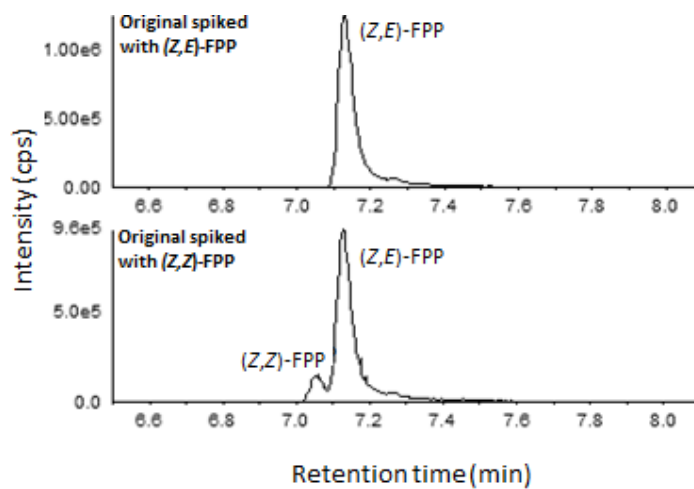


**Figure 17** Spike-in experiments with enzymatic assays from heterologously expressed *PaIDS3*. Heterologously expressed *PaIDS3* produced (*Z,E*)-FPP when supplied with GPP and IPP. Authentic standards were added to, identify the stereochemistry of FPP.

### 3.1.2 Influence of metal ions on recombinant *PaIDS*

Enzyme activity and product specificity of recombinant *PaIDS1* and *PaIDS3* was analyzed in the presence of the metal ion co-factors  $\text{Mg}^{2+}$ ,  $\text{Mn}^{2+}$  and  $\text{Co}^{2+}$ . Each metal ion was tested at concentrations of 0.1 mM, 1 mM, and 10 mM. For both, *PaIDS1* and *PaIDS3*, the overall highest enzyme activity was detected in assays with 1 mM  $\text{Mn}^{2+}$ , whereas in assays with  $\text{Mg}^{2+}$ , the highest activity was detected at a concentration of 10 mM (**Figure 18 A, B**). However, metal ions did not have a strong influence on the product specificity of *PaIDS1*. There was only a slight increase in GPP relative to (*E,E*)-FPP with  $\text{Mn}^{2+}$  and  $\text{Co}^{2+}$  as co-factors. The strongest shift in favor of GPP was evident in assays with 10 mM  $\text{Mn}^{2+}$  or  $\text{Co}^{2+}$ . In these assays, the peak area of FPP was 18 times ( $\text{Mn}^{2+}$ ) or 11 times ( $\text{Co}^{2+}$ ) larger than the peak area of GPP. In comparison, assays with  $\text{Mg}^{2+}$  possessed a 79 times larger peak area for FPP than for GPP. In enzyme assays with recombinant *PaIDS3*, only (*Z,E*)-FPP was detected (**Figure 18 B**). Enzymatic assays with heterologously expressed *PaIDS2* showed no activity.

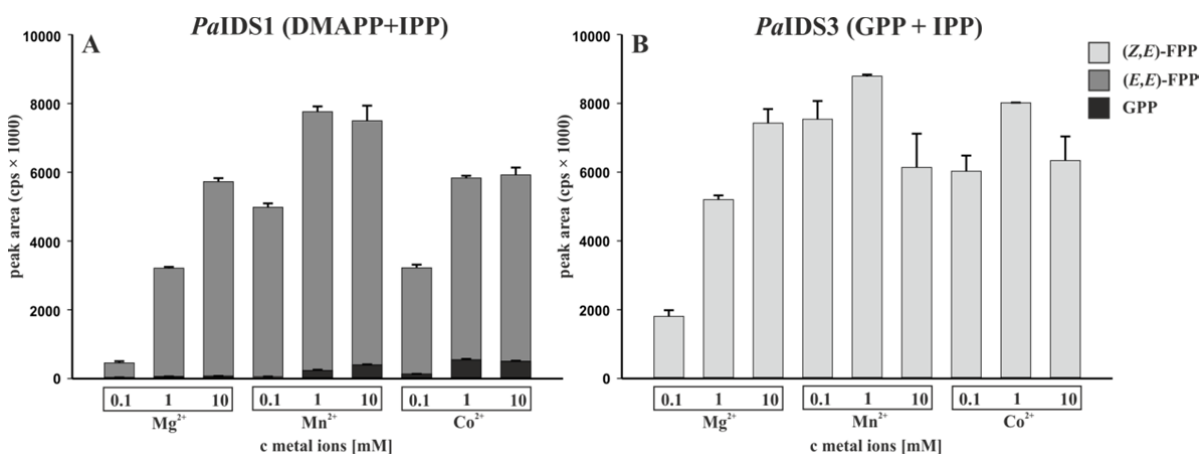


**Figure 18: Relative activity of heterologously expressed and purified *PaIDS1* and *PaIDS3***

Activities were measured by LC-MS/MS. Purified *PaIDS1* (A) and *PaIDS3* (B) were supplied with DMAPP and IPP or GPP and IPP, respectively. Additionally, treatments were supplied with  $\text{Mg}^{2+}$ ,  $\text{Mn}^{2+}$ ,  $\text{Co}^{2+}$  in the concentrations of 0.1, 1, 10 mM ( $N = 3$ ; mean + SD).

### 3.1.3 Identification of co-expressed *PaIDS* products

Co-expressed *PaIDS1* and *PaIDS3* produced two FPP isomers when supplied with DMAPP and IPP. Products were identified as (*Z,E*)-FPP and (*E,E*)-FPP (**Figure 19**).

One product was detected in activity assays performed with co-expressed *PaIDS2* and *PaIDS3*, supplied with DMAPP and IPP as substrates. This product was identified as NPP (**Figure 20**).

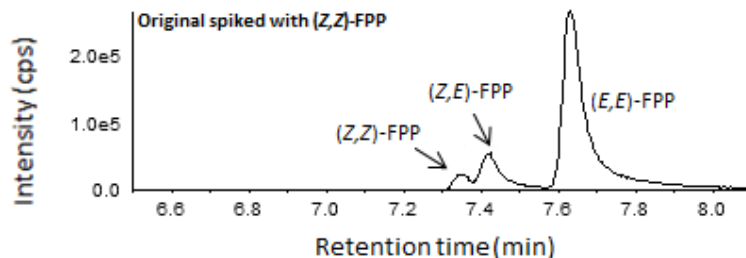


**Figure 19: Spike-in experiments from heterologously co-expressed *PaIDS1* and *PaIDS3***

Heterologously co-expressed *PaIDS1* and *PaIDS3* produced (*Z,E*)-FPP when supplied with the substrates DMAPP and IPP. Authentic standards were added to identify products.

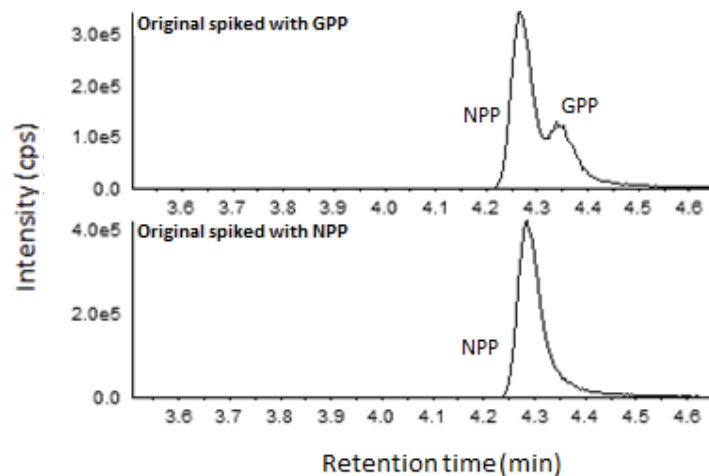


**Figure 20: Spike-in experiments from heterologously co-expressed *PaIDS2* and *PaIDS3***

Heterologously co-expressed *PaIDS2* and *PaIDS3* produced NPP when supplied with the substrates DMAPP and IPP. Authentic standards were added to identify products.



### 3.1.4 The influence of metal ions on co-expressed *PaIDS*s

The influence of metal ions on enzyme activity and product formation of co-expressed *PaIDS1* and *PaIDS2*, *PaIDS1* and *PaIDS3* as well as *PaIDS2* and *PaIDS3* was tested in enzyme activity assays with IPP and DMAPP as described in 3.1.2. For both, co-expressed *PaIDS1* and *PaIDS2* as well as co-expressed *PaIDS2* and *PaIDS3*, the overall highest enzyme activity was detected in assays with 1 mM  $Mn^{2+}$ , whereas assays with 10 mM  $Mn^{2+}$  exhibited the highest overall activity for co-expressed *PaIDS1* and *PaIDS3* (**Figure 21**). These results suggest that  $Mn^{2+}$  had the strongest positive impact on the overall enzyme activity. All assays supplied with 10 mM of  $Co^{2+}$  exhibited a lower enzyme activity when compared to assays with 10 mM  $Mg^{2+}$  or  $Mn^{2+}$ , suggesting that high concentrations of  $Co^{2+}$  had an inhibiting effect on enzyme activity of co-expressed *PaIDS*. For instance, co-expressed *PaIDS1* and *PaIDS2* exhibited a 3 times lower overall-activity in the presence of 10 mM  $Co^{2+}$  compared to assays with 10 mM  $Mg^{2+}$  or  $Mn^{2+}$ , respectively. However, co-expressed *PaIDS1* and *PaIDS2* produced (*E,E*)-FPP and low amounts of GPP (**Figure 21 A**). A slight shift in the product spectrum was evident when  $Co^{2+}$  was supplied. Assays with 10 mM  $Co^{2+}$  produced 10 times more FPP than GPP compared to assays with 10 mM  $Mn^{2+}$ , in which 55 times more FPP was produced than GPP. Co-expressed *PaIDS1* and *PaIDS3* (**Figure 21 B**) produced GPP, (*E,E*)-FPP, (*Z,E*)-FPP and GGPP under assay conditions. These results indicated that an interaction of *PaIDS1* and *PaIDS3* was necessary to produce (*Z,E*)-FPP by using only DMAPP and IPP as substrates. Additionally, GGPP was not detected as product in assays with individually expressed *PaIDS1* or *PaIDS3* (**Figure 18**), supporting the hypothesis that *PaIDS1* and *PaIDS3* interacted with each to produce the diterpene precursor. In assays with co-expressed *PaIDS2* and *PaIDS3* only NPP was detected as product (**Figure 21 C**).

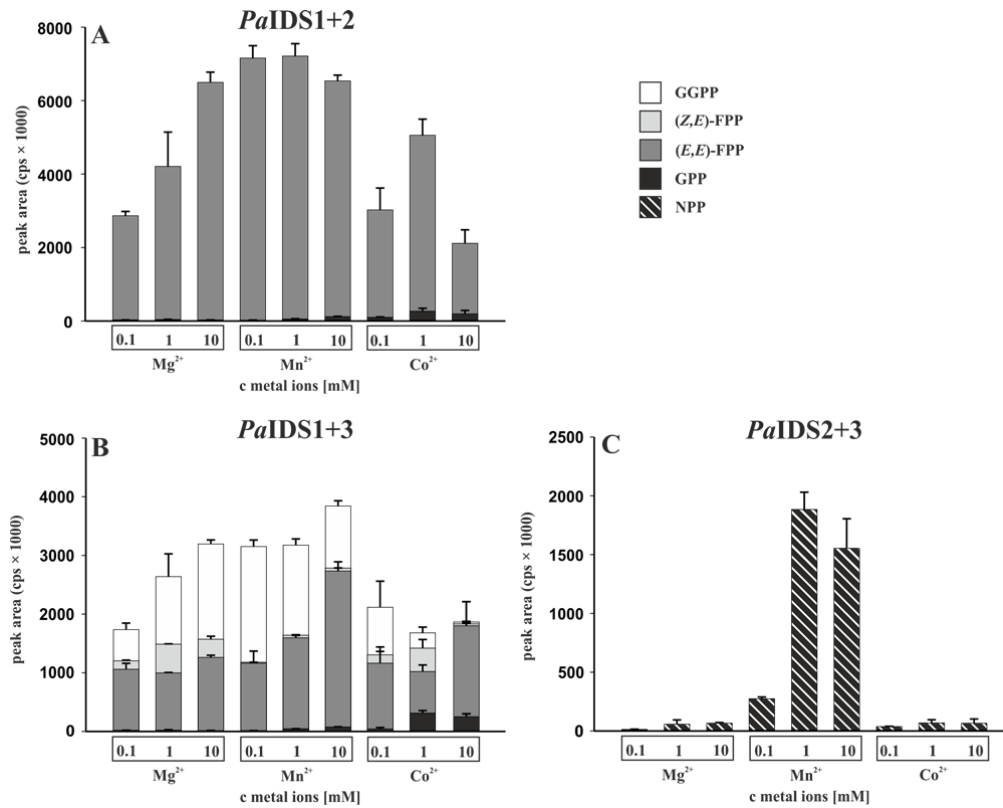


**Figure 21: Relative activity of co-expressed and purified *PaIDS1*, *PaIDS2* and *PaIDS3***  
 Activities were measured by LC-MS/MS. Purified *PaIDS1* and *PaIDS2* (A), *PaIDS1* and *PaIDS3* (B) and *PaIDS2* and *PaIDS3* (C) were supplied with DMAPP and IPP. Treatments were supplied with Mg<sup>2+</sup>, Mn<sup>2+</sup>, Co<sup>2+</sup> in concentrations of 0.1, 1, 10 mM (*N* = 3; mean + SD).

### 3.2 Experiments with recombinant *PsIDS* enzymes

IDS1 and IDS3 from *P. striolata* were heterologously expressed and co-expressed in *E. coli* and purified via Ni-resin columns. The activity of purified proteins was tested in enzymatic assays supplied with DMAPP and IPP and analyzed via LC-MS/MS. Interaction studies, described in 2.2.3, were performed to test whether *PsIDS1* and *PsIDS3* can form a heterodimer. Samples from interaction studies were analyzed via LC-MS<sup>E</sup> and in enzyme activity assays. An overview of experiments, which were carried out with recombinant *PsIDS*, is shown in **Table 2**.

Recombinant *PsIDS1* (45 kDa) and *PsIDS3* (41.5 kDa) as well as co-expressed *PsIDS1* and *PsIDS3* (*PsIDS1+3co*) were detected in pellet fractions (P), crude extracts (CE) and elution fractions (E) via Western Blot (**Figure 22** upper image). *PsIDS3* was individually expressed with or without His-tag (*PsIDS3+* or *PsIDS3-*, respectively). Crude extracts of individually expressed *PsIDS1* were mixed (1:1 vol/vol) with either *PsIDS3+* or *PsIDS3-* (1+3 mce). Mixed crude extracts of *PsIDS1* and *PsIDS3+* showed no band in elution fractions, whereas a band was detected in the elution fraction of mixed crude extracts of *PsIDS1* and *PsIDS3-*. Due to the similar molecular weight of *PsIDS1* and *PsIDS3*, these recombinant enzymes cannot be distinguished on the western blot. Therefore, it was not clear whether both enzymes were successfully co-expressed or present in elution fractions with mixed crude extracts. The presence of recombinant IDS in elution fractions was further analyzed by LC-MS<sup>E</sup> (3.2.1). With this, more sensitive method, co-expressed *PsIDS1* and *PsIDS3* were distinguishable.

However, the protein detection via Western Blot showed several bands in elution fractions, which did not match with the size of recombinant *PsIDS1* and *PsIDS3*, suggesting an unspecific binding of the His-tag antibody. Coomassie-staining of the membrane (**Figure 22** lower image) exhibited several protein bands in elution fractions, which suggest that the purification via Ni-resin columns did not remove all proteins without His-tag.

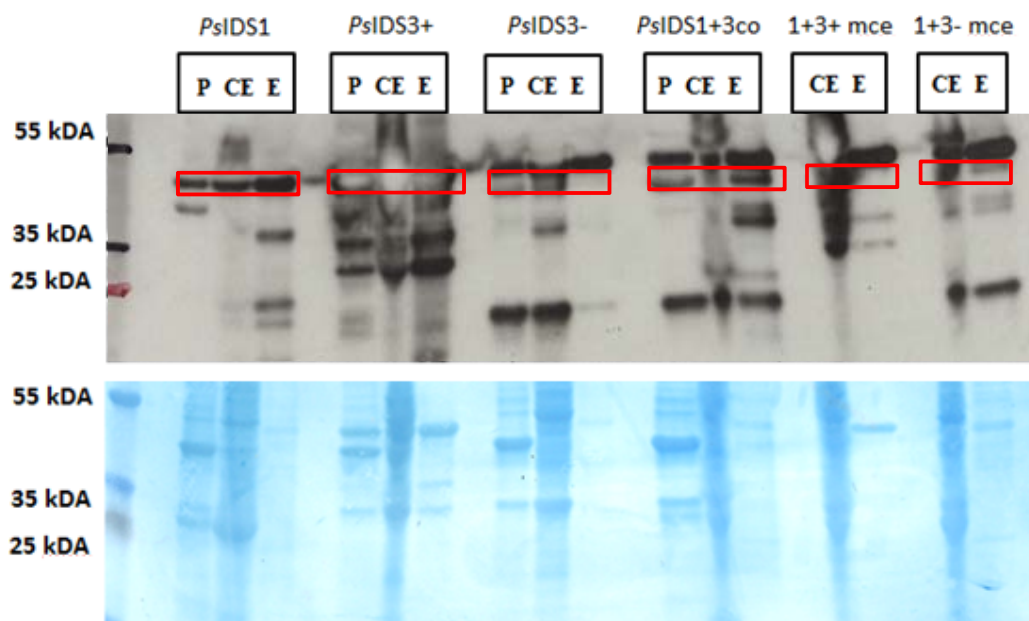


**Figure 22: Protein detection of expressed and co-expressed *PsIDS1* and *PsIDS3***  
 Photo membrane (upper image) and coomassie-staining of the western blot (lower image) are shown. Individually and co-expressed *PsIDS1* and *PsIDS3* were detectable in pellet fractions (P), crude extract (CE) and elution fractions (E), highlighted in red. Coomassie-staining revealed a partially purification via Nickel-resin columns (mce = mixed crude extracts).

### 3.2.1 MS<sup>E</sup> analysis

Elution fractions of recombinant IDS enzymes from *P. striolata* were analyzed for the presence of *PsIDS1* and *PsIDS3*. Crude extracts of individually expressed *PsIDS1* and *PsIDS3* were mixed in the same ratio (1:1 vol/vol) and purified via Ni-resin columns. *PsIDS1* was mixed with *PsIDS3* or *PsIDS3* without His-tag (*PsIDS3*-ht). This was done to test whether *PsIDS3*-ht can form a heterodimer with *PsIDS1* and, therefore, can be detected in elution fractions.

Elution fractions of individually or co-expressed *PsIDS1* and *PsIDS3*, as well as mixed crude extracts of individually expressed *PsIDS1* and *PsIDS3* (with and without His-tag), were separated by SDS-PAGE (**Figure 23**). Samples were cut out of the gel and analyzed via LC-MS<sup>E</sup> (**Table 9**).

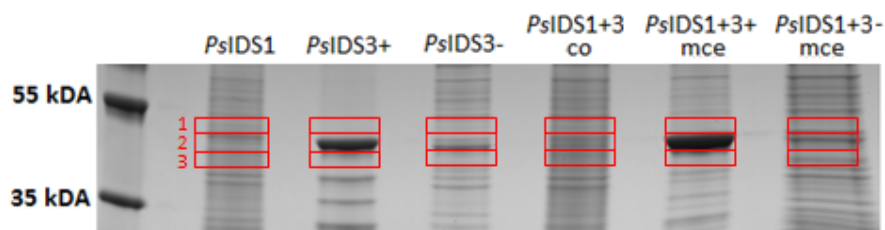


**Figure 23: Coomassie-stained gel used for MS<sup>E</sup> analysis**  
 Protein samples were cut out of the gel (marked in red) and analyzed via MS<sup>E</sup>, to detect heterologously expressed *PsIDS* (mce = mixed crude extracts, co = co-expression, *PsIDS3* labeled with “-“ was expressed without His-tag).

**Table 9: Results MS<sup>E</sup> analysis**

Samples tagged with “-ht” were expressed without His-tag. The number of matched peptides provides rough information about the amount of detected proteins.

Sample	Gel slice	Detected proteins	Matched peptides
<i>PsIDS1</i>	1	<i>PsIDS1</i>	$3 \times 10^{04}$
	2	<i>PsIDS1</i>	$1 \times 10^{05}$
	3	<i>PsIDS1</i>	$3 \times 10^{05}$
<i>PsIDS3</i>	1	<i>PsIDS3</i>	$9 \times 10^{05}$
	2	<i>PsIDS3</i>	$5 \times 10^{06}$
	3	<i>PsIDS3</i>	$4 \times 10^{05}$
<i>PsIDS3-ht</i>	1	<i>PsIDS3</i>	$9 \times 10^{04}$
	2	<i>PsIDS3</i>	$4 \times 10^{05}$
	3	-	-
Co-expressed <i>PsIDS1</i> and <i>PsIDS3</i>	1	<i>PsIDS1</i> / <i>PsIDS3</i>	$2 \times 10^{04}$ / $2 \times 10^{05}$
	2	<i>PsIDS1</i> / <i>PsIDS3</i>	$5 \times 10^{04}$ / $1 \times 10^{05}$
	3	<i>PsIDS1</i> / <i>PsIDS3</i>	$2 \times 10^{05}$ / $2 \times 10^{04}$
Mixed crude extracts (mce) <i>PsIDS1</i> and <i>PsIDS3</i>	1	<i>PsIDS3</i>	$1 \times 10^{06}$
	2	<i>PsIDS1</i> / <i>PsIDS3</i>	$7 \times 10^{04}$ / $1 \times 10^{07}$
	3	<i>PsIDS1</i> / <i>PsIDS3</i>	$5 \times 10^{03}$ / $3 \times 10^{05}$
Mixed crude extracts (mce) <i>PsIDS1</i> and <i>PsIDS3-ht</i>	1	<i>PsIDS3</i>	$6 \times 10^{04}$
	2	<i>PsIDS3</i>	$3 \times 10^{05}$
	3	<i>PsIDS1</i> / <i>PsIDS3</i>	$2 \times 10^{05}$ / $5 \times 10^{05}$

Individually expressed *PsIDS1* or *PsIDS3* were detected in elution fractions. Recombinant *PsIDS3*, expressed without His-tag (*PsIDS3-ht*), was detected in two gel slices, suggesting that the purification via Ni-resin columns did not remove all proteins without His-tag. Both recombinant IDS were detected in elution fractions of co-expressed *PsIDS1* and *PsIDS3*, as well as in samples with mixed crude extracts (1:1 vol/vol) of individually expressed *PsIDS1* and *PsIDS3* (-ht and +ht). The negative control for the interaction studies was *PsIDS3-ht*. The detection of this enzyme in elution fractions makes it difficult to confirm that the detection of both, *PsIDS1* and *PsIDS3-ht* with mixed crude extracts, is due to an interaction of these enzymes. The number of matched peptides for *PsIDS3-ht* was 16 times lower in comparison to *PsIDS3+ht*. In samples with mixed crude extracts, the number of matched peptides for *PsIDS3-ht* was 13-fold lower compared to *PsIDS3+ht*.

### 3.2.2 Enzyme activity of individually expressed *PsIDS1* and *PsIDS3*

The activity of recombinant *PsIDS* enzymes was investigated in assays with concentrations of 5, 10 or 20 µg of recombinant protein. This was done, to test whether higher protein concentrations may affect IDS activity or product specificity. Previous experiments with recombinant IDS have shown that assays with low protein concentrations exhibit no activity or only low activity. Assays were supplied with the substrates DMAPP and IPP.

*PsIDS1* produced GPP and (*E,E*)-FPP under assay conditions. The relative amount of (*E,E*)-FPP was 8-, 16-, or 23 times higher compared to GPP in assays with 5, 10 or 20 µg protein, respectively. These results suggested that (*E,E*)-FPP was the major product of *PsIDS1* and that high protein concentrations slightly shifted the product ratio in favor of FPP (**Figure 24 A**). *PsIDS3* was expressed in two different ways. Treatments labeled with “+tag” were expressed with a His-tag, whereas expressions labeled with “-tag” were expressed without a His-tag.

However, NPP (**Figure 24 B**) and low amounts of (*Z,Z*)-FPP and (*Z,E*)-FPP (**Figure 24 C**) were detected in assays with recombinant *PsIDS3*. The overall enzyme activity was 3- and 25 times higher in assays with 10 and 20 µg of *PsIDS3*, respectively, compared to assays with 5 µg of this protein, suggesting that higher protein concentrations increased the activity of *PsIDS3*. Although *PsIDS3*, expressed without His-tag, was not expected to be present in the elution fraction, NPP and (*Z,E*)-FPP were detected in enzymatic assays. The presence of IDS activity is consistent with the findings from the MS<sup>E</sup>, analysis, in which *PsIDS3* without His-tag was detected in elution fractions. This showed that the purification via Ni-resin columns did not remove all proteins without His-tag. The overall IDS activity with *PsIDS3*-tag was 35 times lower compared to assays with 20 µg of *PsIDS3*+tag, suggesting that only low amounts of *PsIDS3*-tag were present in the respective assays. Although only DMAPP and IPP were provided as substrates, (*Z,E*)-FPP was detected in assays with recombinant *PsIDS3*, implying that GPP, was present in enzymatic assays. It is possible that endogenous GPP from *E. coli* was not removed during the purification step.

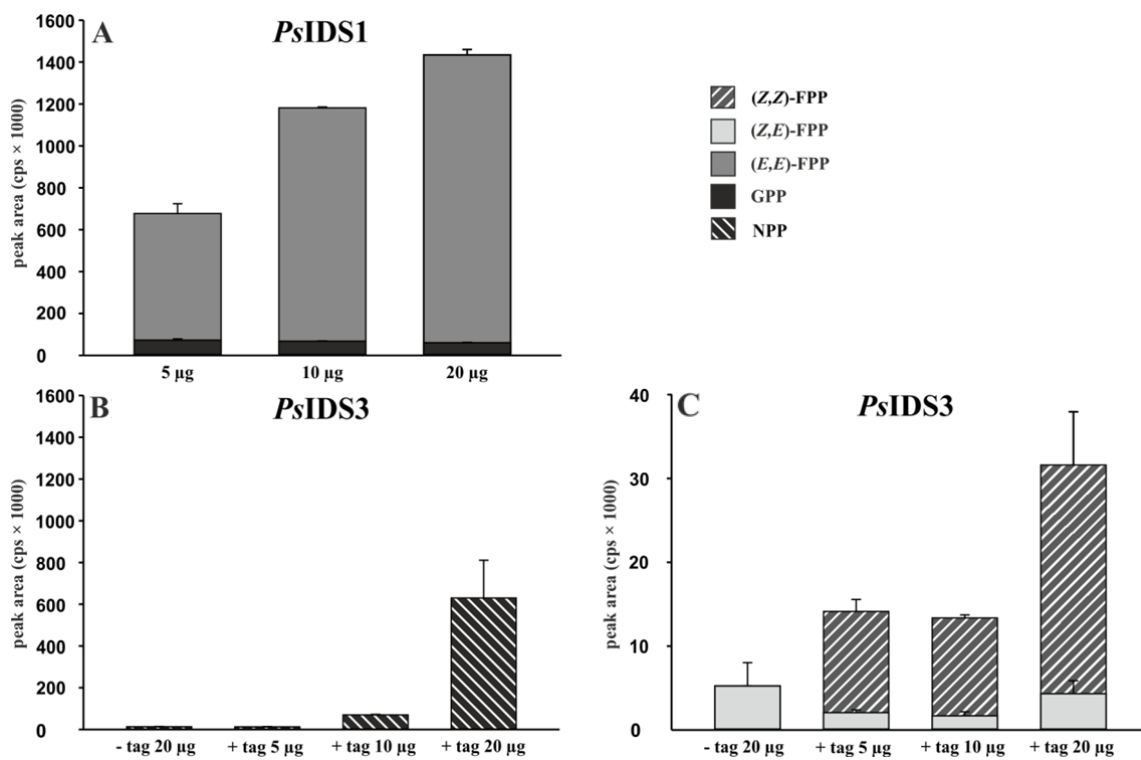


**Figure 24: Relative activity of individually expressed and purified *PsIDS* enzymes**

Activities were measured via LC-MS/MS. Purified *PsIDS1* (A), *PsIDS3* with His-tag (+tag) and *PsIDS3* without His-tag (-tag) were supplied with DMAPP and IPP. NPPS-activity and FPPS-activity of *PsIDS3* are shown in B and C, respectively. Assays with *PsIDS1* and *PsIDS3*+tag were supplied with 5, 10 or 20 µg of recombinant protein ( $N = 3$ ; mean + SD).

### 3.2.3 Identification of co-expressed *PsIDS* products

Three products were detected in activity assays performed with co-expressed *PsIDS1* and *PsIDS3* supplied with DMAPP and IPP. These products were identified as (*Z,E*)-FPP, (*E,E*)-FPP (**Figure 25 A**) and GGPP with a *cis*-conformation (**Figure 25 B**).

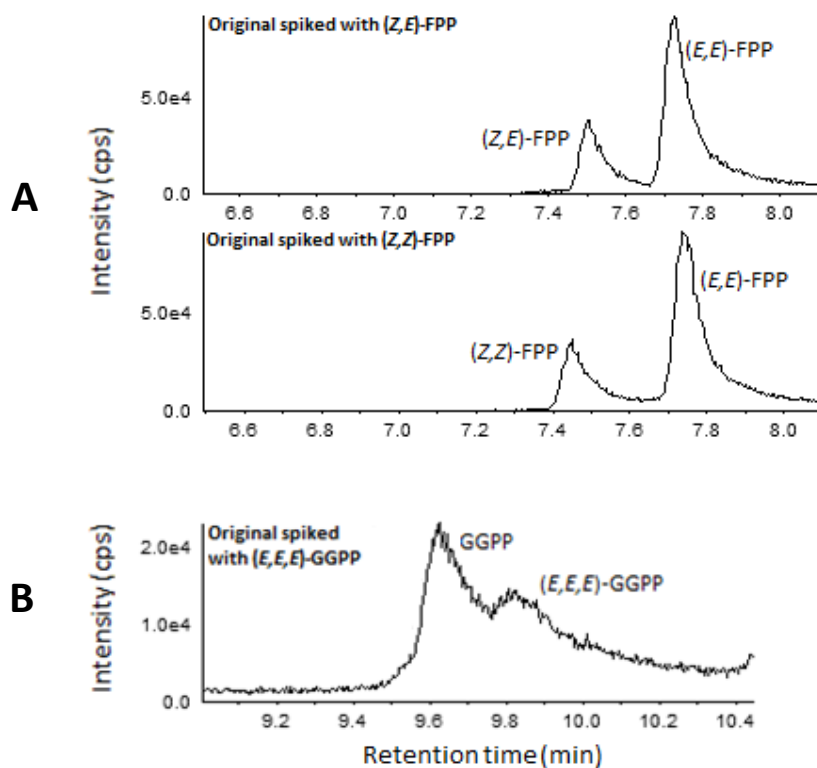


**Figure 25: Spike-in experiments from heterologously co-expressed *PsIDS1* and *PsIDS3***  
Heterologously co-expressed *PsIDS1* and *PsIDS3* produced (*E,E*)- FPP, (*Z,E*)-FPP (A) and GGPP (B). Authentic standards were added to identify assay products.



### 3.2.4 Product identification of individually expressed *PsIDS1* and *PsIDS3*+His-tag with mixed crude extracts

Two products were detected in assays with mixed crude extracts of individually expressed *PsIDS1* and *PsIDS3*. Assays were supplied with DMAPP and IPP as substrates. Products were identified as (*Z,E*)-FPP (**Figure 26 A**) and GGPP with a *cis*-conformation (**Figure 26 B**).

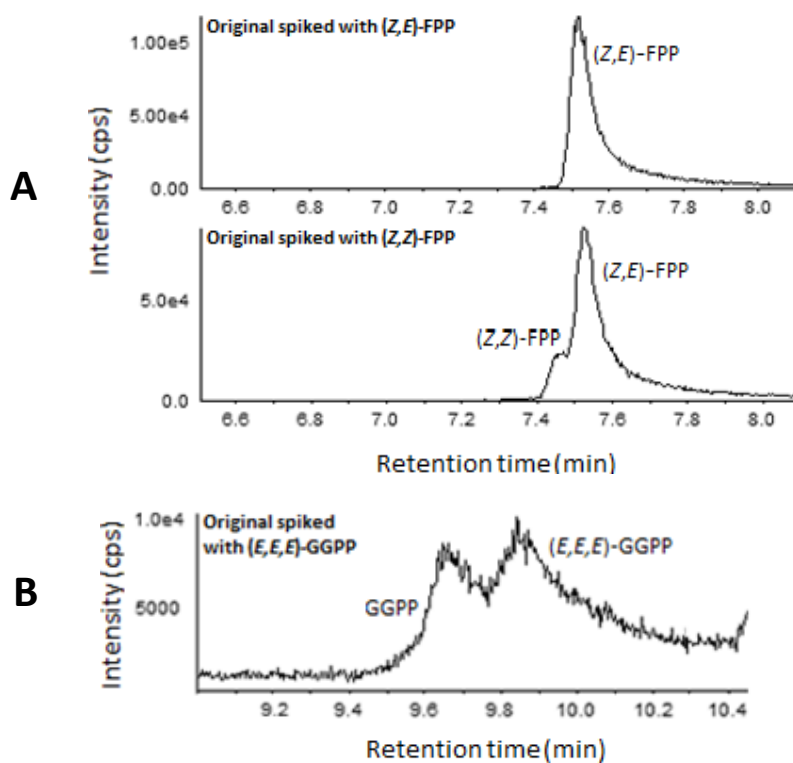


**Figure 26: Spike-in experiments from individually expressed *PsIDS1* and *PsIDS3*+His-tag with mixed crude extracts**

Enzymatic assays with mixed crude extracts of individually expressed *PsIDS1* and *PsIDS3* exhibited (*Z,E*)-FPPS-activity (A) and GGPPS-activity (B). Authentic standards were added to identify products.

### 3.2.5 Product identification of individually expressed *PsIDS1* and *PsIDS3* with mixed elution fractions

Three products were detected in assays with mixed elution fractions of individually expressed and purified *PsIDS1* and *PsIDS3*. Assays were supplied with DMAPP and IPP as substrates. Products were identified as (*E,E*)-FPP, (*Z,E*)-FPP (**Figure 27 A**) and GGPP with a *cis*-conformation (**Figure 27 B**).

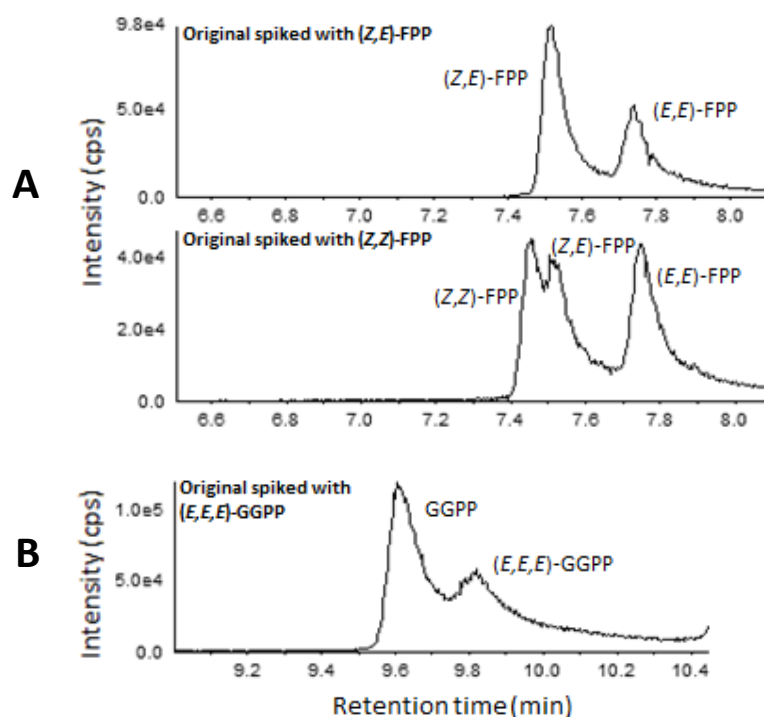


**Figure 27: Spike-in experiments from heterologously expressed *PsIDS1* and *PsIDS3* with mixed elution fractions.**

In enzyme assays with mixed elution fractions of *PsIDS1* and *PsIDS3*, (*E,E*)-FPP, (*Z,E*)-FPP (A) and GGPP (B) were detected. Authentic standards were added to identify products.

### 3.2.6 Enzyme assays with combinations of *PsIDS1* and *PsIDS3*

Enzyme activity of co-expressed *PsIDS1* and *PsIDS3* (**Figure 28 A**), as well as individually expressed *PsIDS1* and *PsIDS3* with mixed crude extracts (**Figure 28 B**) or mixed elution fractions (**Figure 28 C**), were supplied with DMAPP and IPP and tested with different concentrations of recombinant protein. Assays with mixed elution fractions were performed with *PsIDS3* either carrying a His-tag (EM+tag) or without His-tag (EM-tag). These assays were carried out with 20 µg of recombinant protein.

In all assays, the enzyme combination of *PsIDS1* and *PsIDS3* resulted in the production of GGPP. Assays with *PsIDS1* and *PsIDS3* with mixed crude extract or mixed elution fractions produced GGPP and (*Z,E*)-FPP. Both, GGPP and (*Z,E*)-FPP, were not detected as products in enzyme assays with individually expressed *PsIDS1* or *PsIDS3*, suggesting that both enzymes are necessary for GGPPS activity and (*Z,E*)-FPPS activity.

Depending on whether *PsIDS1* and *PsIDS3* were co-expressed, individually expressed and mixed (crude extracts) or purified and mixed (elution fractions), the product ratio in enzyme assays differed. GGPP represented on average 73% and 84% of products in assays performed with co-expressions or mixed crude extracts of *IDS1* and *IDS3*, respectively. In assays with mixed elution fractions (1:1 c/c), GGPP represented 34% of the whole product spectrum. In assays with equal concentrations of *PsIDS1* and *PsIDS3* (mixed elution fractions, *PsIDS1* and *PsIDS3*+His-tag), (*Z,E*)-FPP was the main product, representing 55% of all products. These results showed that the ratio of *PsIDS1* and *PsIDS3* had an influence on the product spectrum. However, no high shift in the product spectrum was evident by increasing the amount of recombinant protein in assays.

In assays with mixed elution fractions of *PsIDS1* and *PsIDS3* (+tag) 16 times more (*Z,E*)-FPP than (*E,E*)-FPP was produced. In contrast, mixed elution fractions of *PsIDS1* and *PsIDS3* (-tag) produced 25 times more (*E,E*)-FPP than (*Z,E*)-FPP.

The main products in assays with mixed elution fractions of *PsIDS1* and *PsIDS3*-His tag was GPP and (*E,E*)-FPP, which should be due to the activity of *PsIDS1*. These findings may show that the purification via Ni-resin-columns removed a major part of *PsIDS3* (-tag) and supports the hypothesis that the ratio of *IDS1* and *IDS3* has an impact on the product spectrum.

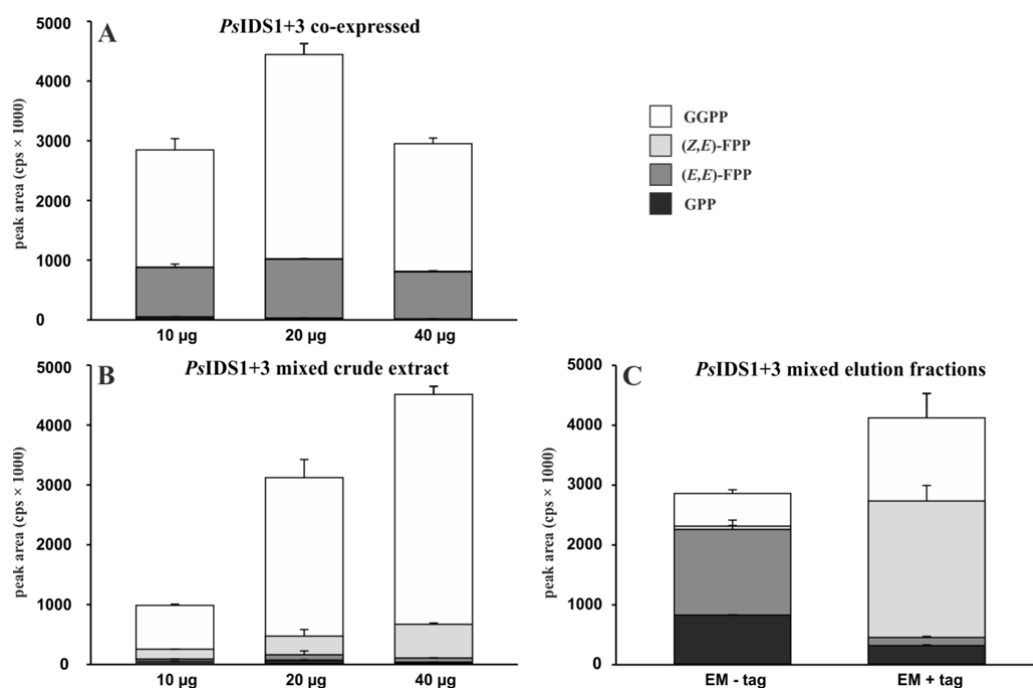


**Figure 28: Relative activity of heterologously expressed and purified *PsIDS1* and *PsIDS3***  
 Activities were measured by LC-MS/MS. Co-expressed *PsIDS1* and *PsIDS3* (A) or individually expressed *PsIDS1* and *PsIDS3* with mixed crude extracts (B) or mixed elution fractions (C) were supplied with DMAPP and IPP and tested with different enzyme concentrations. The protein concentration of mixed elution fractions (EM) was 20 µg ( $N = 3$ ; mean + SD).

### 3.3 Knock-down of *PsIDS1*, *PsIDS2* and *PsIDS3* via RNAi

To investigate the putative role of *PsIDS1*, *PsIDS2* and *PsIDS3* in the biosynthesis of GPP, (*E,E*)-FPP and (*Z,E*)-FPP *in vivo*, the expression of the corresponding genes was down-regulated in male *P. striolata* via RNAi.

#### 3.3.1 Single knock-down of *PsIDS3*

In the first RNAi experiment, males were injected with dsRNA targeting *PsIDS3* to test whether the *cis*-IDS *PsIDS3* is involved in the biosynthesis of (*Z,E*)-FPP. Adults which were injected with dsRNA, targeting *IMPI* and non-injected beetles served as controls. The effects of dsRNA injection were investigated, 14 days after injection, via enzymatic assays with crude beetle protein extracts (**Figure 29**) and volatile collection (**Figure 30**). The transcript levels of *PsIDS1*, *PsIDS2*, *PsIDS3* as well as *PsTPS1* were investigated via qRT-PCR (**Figure 31**). *TPS1* was previously shown to convert (*Z,E*)-FPP into volatile sesquiterpenes (Beran *et al.*, 2016b), thus making it important to verify that *PsTPS1* expression was not affected by RNAi.

The injection of dsRNA targeting *PsIDS3* resulted in significantly reduced (*Z,E*)-FPP formation compared with the negative control IMPI ( $N = 3$ , ANOVA,  $F = 9.811$ ,  $p = 0.018$ ). The difference in (*Z,E*)-FPP activity between ds*PsIDS3* injected beetles and non-injected controls was not statistically significant. RNAi against *PsIDS3* reduced the formation of (*Z,E*)-FPP on average by 71% and 70% compared to the negative control IMPI and the non-injected control, respectively.

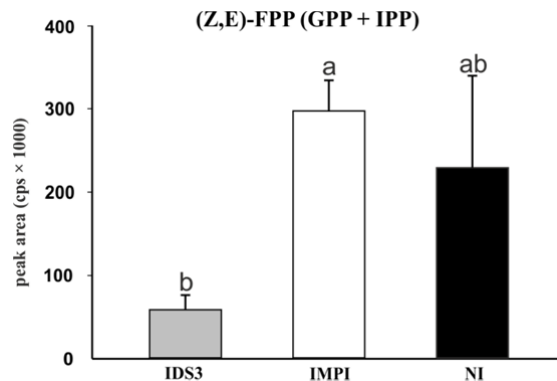


**Figure 29: (*Z,E*)-FPP production in crude beetle extracts after *PsIDS3* knock-down via RNAi**  
RNAi experiments were carried out by injecting dsRNA targeting either *PsIDS3*, or *IMPI* as a negative control. Non-injected beetles were used as a reference control (NI). (*Z,E*)-FPP production in crude beetle extracts was measured via LC-MS/MS. Assays were supplied with GPP and IPP. Bars with different letters are significantly different (One Way ANOVA with square root transformed data; Tukey's test as post-hoc test;  $N = 3$ ; mean + SD). Statistics are shown in **Table 11 (SI)**.

The knock-down of *PsIDS3* resulted in significantly reduced emission of volatile sesquiterpenes in comparison to the non-injected control group ( $N = 3$ , ANOVA,  $F = 4.624$ ,  $p = 0.027$ ). No significant differences between *PsIDS3* and IMPI or the non-injected control group (NI) and IMPI became apparent. The volatile emission was reduced by 76.2% and 49.2% by comparing ds*PsIDS3* injected beetles with the non-injected control or the negative control IMPI, respectively. However, a reduced volatile emission of 52.8% was evident by comparing the non-injected control with the negative control IMPI, which suggests that the injection itself influenced the emission of volatiles. For that reason, and due to the inconsistent volatile emission, further RNAi effects were investigated via enzymatic assays with crude beetle extracts.

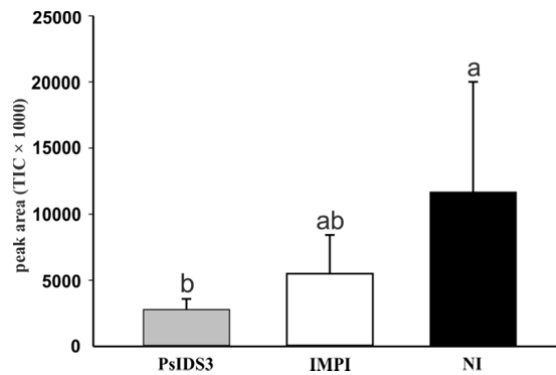


**Figure 30: Volatile emission 14 d after knock-down of *PsIDS3***

Volatile emission was investigated 14 days after dsRNA injection, targeting *PsIDS3* or *IMPI* (negative control). Non-injected beetles (NI) were used as reference group. Volatile emission was measured via GC/MS. Bars represent summed up peak areas of volatile sesquiterpenes, emitted by male *P. striolata*. Bars with different letters are statistically significant (One Way ANOVA; Tukey's test as a post-hoc test ( $N = 6$ ; mean+ SD). Statistics are shown in **Table 11 (SI)**.

The knock-down of *PsIDS3* resulted in significantly reduced transcripts levels for this gene, when compared to the control groups ( $N = 6$ , ANOVA,  $F = 14.722$ ,  $p = 0.001$ ). Transcript levels of *PsIDS3* were 81% and 78% lower compared to the non-injected control and the negative control IMPI, respectively. Transcription levels of *PsIDS1* and *PsIDS2* were not affected by dsRNA injections of ds*PsIDS3*. However, the injection of dsIMPI resulted in 15% lower transcript levels for *PsIDS2*, when compared with the non-injected control group. The expression of *TPS1* was not affected by dsRNA injection.

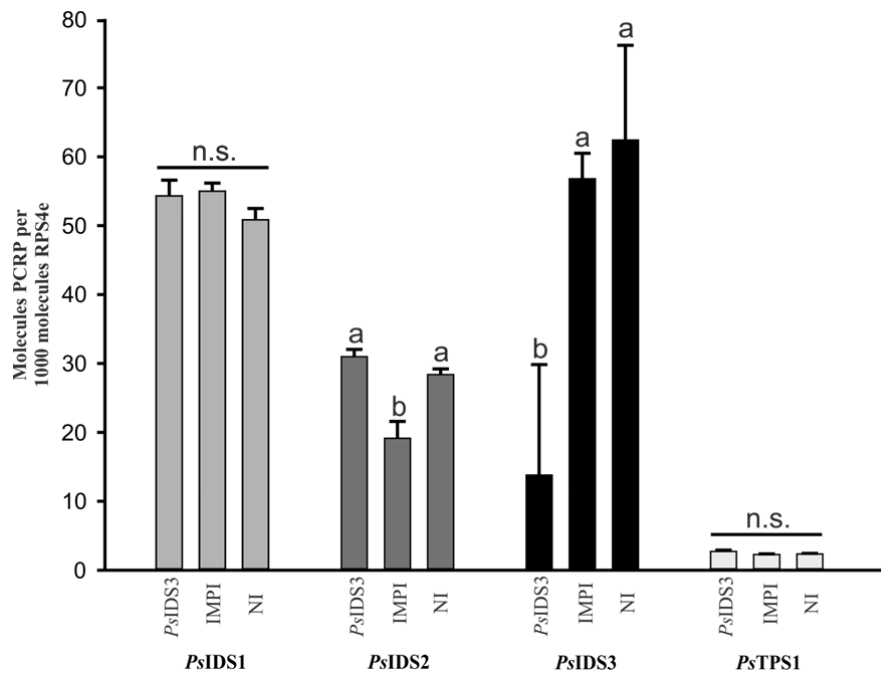


**Figure 31: Transcript levels of *PsIDS* and *TPS1* after *PsIDS3* knock-down**

*PsIDS3* knock-down resulted in a significant reduction (81%) of corresponding transcript levels. Injection of ds*PsIDS3* did not affect other IDS genes or *TPS1*. Injection of dsIMPI resulted in decreased transcript levels of *PsIDS2* ( $N = 6$ , mean + SD; Statistics: ANOVA One Way Analysis and Tukey's test as a post hoc-test) Statistics are shown in **Table 11 (SI)**.

### 3.3.2 Knock-down of *PsIDS1*, *PsIDS2* and *PsIDS3*

After knocking down *PsIDS3* in a first approach, a second RNAi experiment, targeting *PsIDS1*, *PsIDS2* or *PsIDS3*, was performed. The effects of RNAi injection were investigated, 14 d after injection, via enzymatic assays with crude beetle extracts. Crude beetle extracts were tested for GPPS-, (*E,E*)-FPPS and (*Z,E*)-FPPS-activity.

The knock-down of *PsIDS1* resulted in a significantly reduced GPP production (**Figure 32**) compared with non-injected control group or ds*PsIDS3* injected beetles ( $N = 5$ , ANOVA,  $F = 3.319$ ,  $p = 0.028$ ). These results suggested *PsIDS1* being involved in GPP formation in *P. striolata*. No statistically difference was evident when comparing ds*PsIDS1* injected beetles with the negative control IMPI. The GPP formation was 54.5% and 50% lower in ds*PsIDS1* injected beetles, compared to the non-injected beetles and the negative control IMPI, respectively. The silencing of *PsIDS3* and *PsIDS2* did not result in significantly reduced GPP formation compared to control groups.

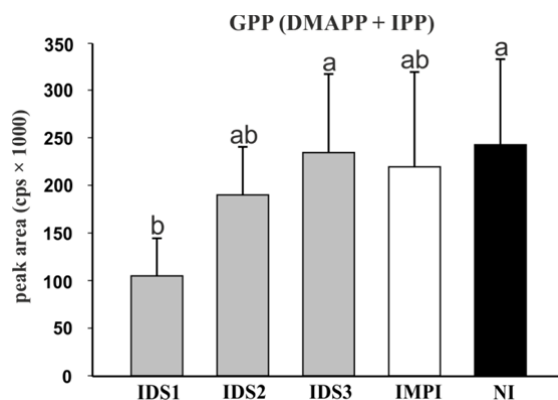


**Figure 32: GPP production in crude beetle extracts after *PsIDS1*, *PsIDS2* or *PsIDS3* knock-down via RNAi**

RNAi experiments were carried out by injecting dsRNA targeting *PsIDS1*, *PsIDS2*, *PsIDS3* or *IMPI* (negative control). Non-injected beetles were used as a reference control (NI). GPP production was measured via LC-MS/MS in enzymatic assays with crude beetle extracts, supplied with the substrates DMAPP and IPP. Bars with different letters are significantly different (One Way ANOVA with log transformed data; Tukey's test as post-hoc test;  $N = 5$  for IDS1; IMPI; NI,  $N = 4$  for IDS2; IDS3 mean + SD). Statistics are shown in **Table 11 (SI)**.



The knock-down of *PsIDS1*, *PsIDS2* or *PsIDS3* did not result in significantly reduced (*E,E*)-FPP formation compared to the negative control IMPI or the non-injected control group. This was neither the case in assays carried out with the canonical substrates DMAPP and IPP (**Figure 33 A**), nor in these, supplied with GPP and IPP (**Figure 33 B**). A statistically significant difference was evident by comparing ds*PsIDS1* injected beetles with ds*PsIDS3* injected beetles ( $N = 5$ , ANOVA,  $F = 3.628$ ,  $p = 0.02$ ).

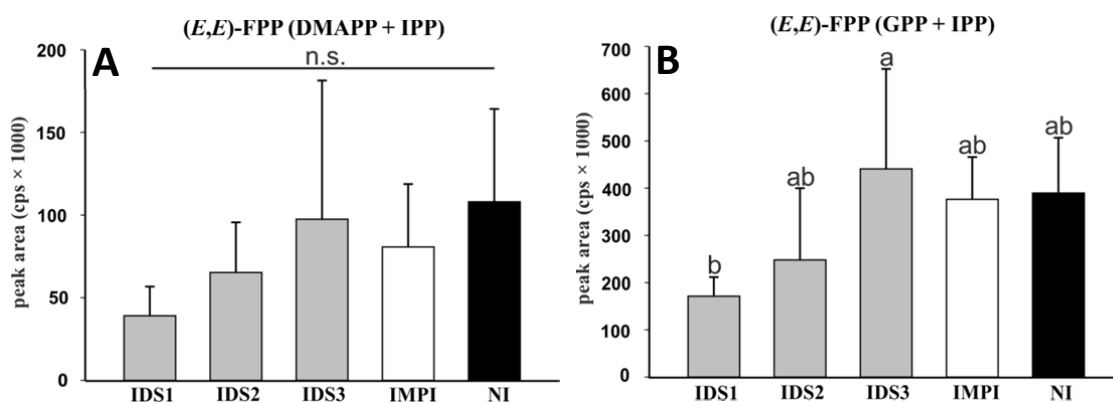


**Figure 33: (*E,E*)-FPP production in crude beetle extracts after *PsIDS1-3* knock-down via RNAi**  
 RNAi experiments were carried out by injecting dsRNA targeting *PsIDS1*, *PsIDS2*, *PsIDS3* or *IMPI* as a negative control. Non-injected beetles were used as a reference control (NI). (*E,E*)-FPP production was measured via LC-MS/MS in enzymatic assays with crude beetle extracts, supplemented with the substrates DMAPP and IPP (A), or GPP and IPP (B). Bars with different letters are significantly different (One Way ANOVA with log transformed data; Tukey's test as post-hoc test;  $N = 6$  for IDS1; IMPI; NI,  $N = 5$  for IDS2; IDS3 mean + SD). Statistics are shown in **Table 11 (SI)**.

The production of (*Z,E*)-FPP in enzymatic assays supplied with DMAPP and IPP (**Figure 34 A**) exhibited significant differences between the non-injected control group and beetles treated with dsRNA targeting *PsIDS1* ( $N = 5$ , Kruskal-Wallis Test,  $H = 10.769$ ,  $p = 0.029$ ). The (*Z,E*)-FPP production in ds*PsIDS1* injected beetles was 76.13% lower compared to the non-injected control group. The negative control IMPI exhibited a high variability in (*Z,E*)-FPP formation, which made it difficult to use IMPI as a comparison to dsIDS-injected groups.

In enzymatic assays which were provided with GPP and IPP (**Figure 34 B**), the injection of dsRNA targeting *PsIDS3* resulted in a significantly reduced production of (*Z,E*)-FPP when compared with the negative control IMPI ( $N = 5$ , ANOVA,  $F = 4.6$ ,  $p = 0.01$ ). The difference between the non-injected control group and treatments with dsRNA targeting *PsIDS1* were not significantly different. A high variability in (*Z,E*)-FPP formation was evident in the non-injected control group.

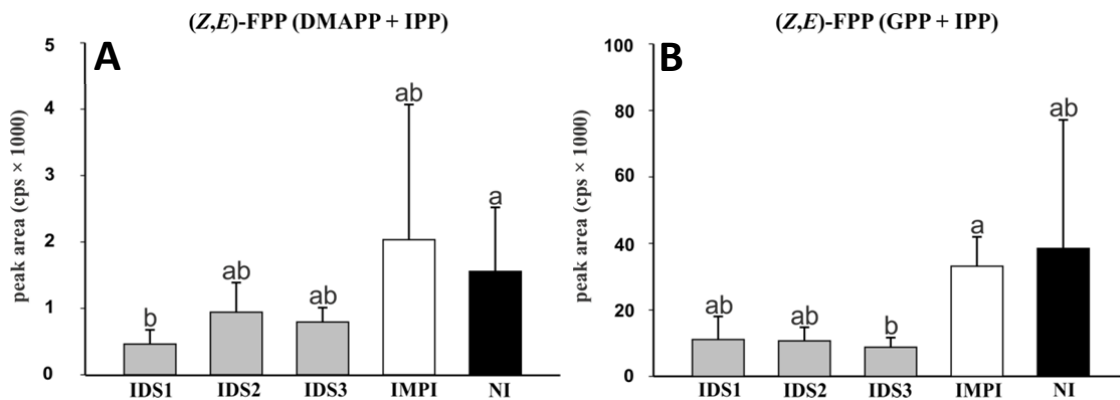


**Figure 34: (*Z,E*)-FPP production in crude beetle extracts after *PsIDS1-3* knock-down via RNAi**  
 RNAi experiments were carried out by injecting dsRNA targeting either *PsIDS1-3* or *IMPI* (negative control). Non-injected beetles were used as a reference control (NI). (*Z,E*)-FPP production was measured via LC-MS/MS in enzymatic assays with crude beetle extracts. DMAPP and IPP (A), or GPP and IPP (B) were supplied as substrates. Bars with different letters are significantly different. **A:** Kruskal-Wallis One Way ANOVA with log transformed data, Dunn's method as post- hoc test,  $N = 6$  for IDS1, IMPI, NI,  $N = 5$  for IDS2; IDS3; **B:** One Way ANOVA with log transformed data; Tukey's test as post- hoc test;  $N = 4$  for IDS1; IDS2; NI,  $N = 5$  for IDS3, IMPI, NI ( mean + SD). Statistics are shown in **Table 11 (SI)**.

The injection of dsRNA targeting *PsIDS1* resulted in significantly reduced transcript levels when compared to treatments targeting *PsIDS2*, *PsIDS3*, *IMPI* or the non-injected control group ( $N = 6$ , ANOVA,  $F = 19.81$ ,  $p < 0.001$ ) (**Figure 35**). The injection of dsIMPI did not affect transcript levels of IDS genes or *TPS1*. Compared with the non-injected control group, the injection of ds*PsIDS1*, ds*PsIDS2* or ds*PsIDS3* exhibited a knock-down effect of 81%, 84% and 94%, respectively. These results suggested that the RNAi experiments targeting their corresponding genes were successful, although no total knock-down was evident. *TPS1* showed no evidence to be affected by dsRNA injection.

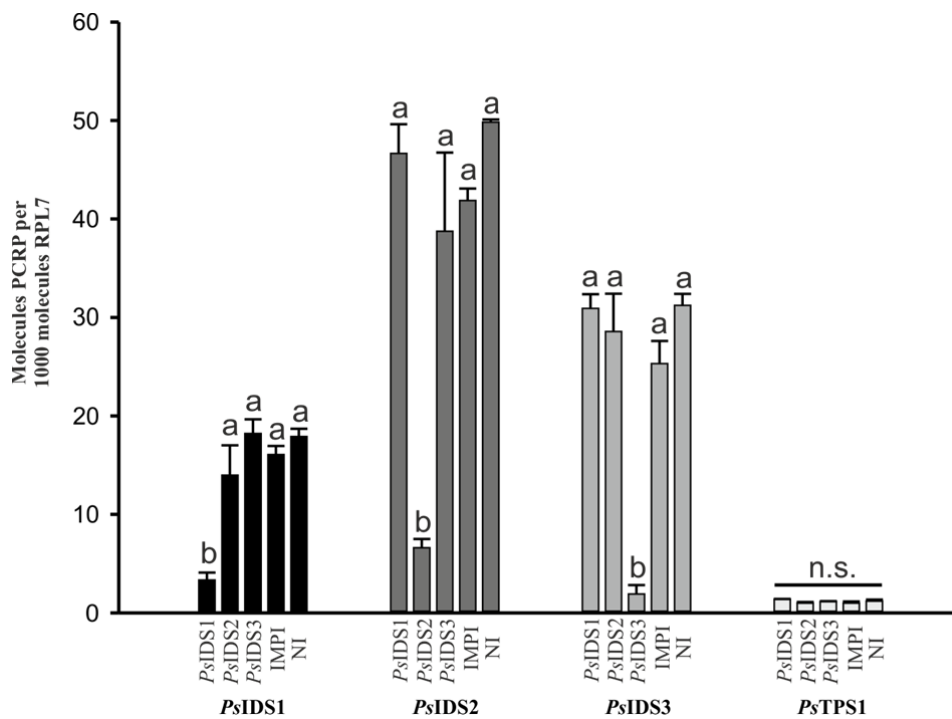


**Figure 35: Transcript levels of *PsIDS1-3* and *TPS1* 14 days after knock-down**

Knock-down via dsRNA injection targeting *PsIDS1*, *PsIDS2* and *PsIDS3* resulted in significantly reduced transcript levels of corresponding genes ( $N = 6$ , mean + SD; Statistics: ANOVA One Way Analysis and Tukey's test as a post-hoc test). Statistics are shown in **Table 11 (SI)**.

## 4 Discussion

### 4.1 *P. armoraciae* and *P. striolata* IDS exhibit similar activities

Phylogenetic analysis of IDS proteins from *P. striolata* and *P. armoraciae* revealed three putative *trans*-IDS enzymes, which are suggested to be orthologues in these flea beetle species (Beran, 2016). When provided with DMAPP and IPP, IDS1 from *P. armoraciae* and *P. striolata* revealed (*E,E*)-FPPS activity. This suggests that these enzymes provide the substrate for juvenile hormone synthesis and protein prenylation (Belles *et al.*, 2005). Although (Beran, 2016) reported no GPPS activity with recombinant *PsIDS1*, small amounts of GPP were detected in enzymatic assays performed with *PaIDS1* and *PsIDS1*. Prenyltransferases are known to catalyze sequential elongation steps by adding C5 subunits until reaching the final chain length of their products (Liang, 2009). Hence, the production of (*E,E*)-FPP presumes the production of GPP, at least as an intermediate. A steady state equilibrium, in which GPP acts as product and substrate simultaneously, may explain the detection of considerably higher amounts of (*E,E*)-FPP in comparison to GPP. In this master's thesis, the incubation time for enzymatic assays with recombinant *PsIDSs* was 15 min. In contrast, Beran *et al.* (2016b) performed enzymatic assays for 2 h. An incubation time of 2 h could be enough for *PsIDS1* to convert GPP completely into (*E,E*)-FPP. This suggestion is consistent with the results from enzymatic assays performed with *PsIDS1* using different concentrations. In that approach, higher concentrations of *PsIDS1* resulted in higher IDS activity and shifted the product ratio in favor of FPP. Although successfully expressed, no enzyme activity of *PaIDS2*, converting DMAPP and IPP into terpenoid precursor molecules was evident. Beran *et al.* (2016b) showed that the SARM motif of *PsIDS2* was altered from DDxxD to KDxxN (**Figure 48, SI**), which may explain the lack of activity of IDS2 in *P. striolata*. Amino acid sequence analysis of *PaIDS2* revealed the same alteration of the SARM motif (**Figure 49, SI**), thus, explaining the lack of activity in *P. armoraciae*. Recombinant *PsIDS3*, predicted to be a *trans*-IDS, produces terpene precursors with a *cis*-conformation. The enzyme converts DMAPP and IPP into NPP as well as (*Z,Z*)-FPP and accepts also GPP and IPP as substrates, which results in the formation of (*Z,E*)-FPP (Beran *et al.*, 2016b). In this master's thesis, activity assays with recombinant *PsIDS3* exhibited the same product spectrum. Assays carried out

with *PaIDS3* showed that this enzyme also accepts GPP and IPP as substrates to produce (*Z,E*)-FPP. The formation of (*Z,E*)-FPP by recombinant *PaIDS3* and *PsIDS3* suggests that both enzymes are involved in the production of volatile sesquiterpenes.

## 4.2 Metal ions regulate overall enzyme activity of IDSs in

### *P. armoraciae*

The production of (*Z,E*)-FPP by IDS3 in *P. armoraciae* and *P. striolata* presumes the presence of GPP as substrate. No recombinant IDS from these beetles was capable to produce high amounts of GPP under assay conditions. IDS1 produced (*E,E*)-FPP as its main product and recombinant IDS2 exhibited no catalytic activity.

Previous studies in plants (*e.g. Abies granda*; (Tholl *et al.*, 2001)) and insects (*e.g. Myzus persicae*; (Vandermoten *et al.*, 2009), *Choristoneura fumiferana*; (Sen *et al.*, 2007b)) reported bifunctional catalytic properties of IDSs. These enzymes produced GPP as well as FPP. Experiments, testing different divalent metal ions, revealed remarkable modulatory effects by these co-factors by regulating the overall enzyme activity in scIDSs. Additionally, a cofactor-dependent chain length regulation has been described in crude extracts of the lepidopteran species *Manduca sexta* (Sen *et al.*, 2007a) or on heterologously expressed *PcIDS1* from the mustard leaf beetle *Phaedon cochleariae* (Frick *et al.*, 2013). Both publications reported a product shift from FPP to GPP, if other divalent metal ions than  $Mg^{2+}$  were provided in enzymatic assays. Especially  $Mn^{2+}$  and  $Co^{2+}$  exhibited a strong impact, shifting the product spectrum from GPP to FPP.

Although no considerable shift in product formation was evident, all enzymatic assays with individually or co-expressed IDS from *P. armoraciae* exhibited an overall increased catalytic activity, when provided with 0.1 and 1 mM  $Mn^{2+}$  instead of  $Mg^{2+}$  (*e.g. PaIDS1* 11-fold higher activity for 0.1 mM  $Mn^{2+}$  compared to  $Mg^{2+}$ ). The major part of enzymatic assays, carried out with low concentrations of  $Co^{2+}$  showed an increased enzyme activity in comparison with assays, performed with similar concentrations of  $Mg^{2+}$ . Here, co-expressed *PaIDS2* and *PaIDS3* were an exception. The enzyme combination exhibited a clear preference for  $Mn^{2+}$  (32-fold; 27-fold increase 1 mM  $Mn^{2+}$  vs.  $Mg^{2+}$  and  $Mn^{2+}$  vs.  $Co^{2+}$ , respectively).

Considering that most assays with a concentration of 10 mM of divalent metal ions showed no substrate peak, makes a comparison on these assays challenging. Especially  $Mn^{2+}$  increased the enzyme activity in a way that substrate limitation

determined the product formation to a certain level. This may explain the similar activities when comparing assays with the same enzymes, although increasing the concentration of  $Mn^{2+}$  from 1 to 10 mM (e.g. *PaIDS1*, *PaIDS1* and *PaIDS2*). To prevent total depletion of substrates, further assays should be carried out with lower amounts of respective IDS enzymes, or in a shorter incubation time.

In comparison with  $Mg^{2+}$ , which are present in relatively high concentrations in eukaryotic cells (10-20 mM; (Romani and Maguire, 2002)),  $Mn^{2+}$  and  $Co^{2+}$  are often mentioned as trace metals. Magnesium ions, for instance, are necessary for ATP activity or as co-factor for polymerases, which demonstrates that Magnesium ions play a variety of important roles inside of a cell.  $Mn^{2+}$ , an essential co-factor of anti-oxidative enzymes, is present in lower intracellular concentrations of 0.04 - 2 mM (Jensen and Jensen, 2015).

Frick *et al.* (2012) investigated the abundance of metal ions in *P. cochleariae* larvae and found considerably higher amounts of  $Mg^{2+}$  (91  $\mu\text{mol/g}$  dry weight (DW)) in contrast to  $Mn^{2+}$  or  $Co^{2+}$  (0.3  $\mu\text{mol/g}$  DW, 4 nmol/g DW, respectively). They reported that *PcIDS1* exhibited a remarkably higher affinity for  $Mn^{2+}$  and  $Co^{2+}$  in comparison to  $Mg^{2+}$ , which indicates that *PcIDS1* compensates the low intracellular concentrations of  $Mn^{2+}$  and  $Co^{2+}$  by higher affinity to these ions.

This may also explain the stronger impact of  $Mn^{2+}$  or  $Co^{2+}$  on *PaIDSs*, when compared to respective assays carried out with 0.1 or 1 mM of  $Mg^{2+}$ .

### **4.3 Co-expressed IDS-isozymes produce (Z,E)-FPP in crucifer flea beetles**

The avian FPPS from the domestic chicken (*Gallus gallus*) was the first scIDS structurally investigated. X-ray analysis revealed that this enzyme exists as a homodimer (Tarshis *et al.*, 1996). Although the medium-chain hexaprenyl diphosphate synthase (Zhang *et al.*, 1998) and the very-long-chain rubber synthase (Light *et al.*, 1989) were identified to act as heterodimers, the idea of FPPS acting as homodimers is widely distributed (Poulter, 2006). Additionally, only few examples of co-expressed IDS isozymes are known, which potentially could show that these proteins can form heterodimers. However, Burke *et al.* (1999) identified two IDS-isozymes from spearmint oil glands. Although there was no activity evident in assays with individually expressed enzymes, co-expressions of these IDS isozymes revealed GPPS activity, suggesting them to act as heterodimers.

Sen and Sperry (2002) described the expression and purification of lepidopteran FPPSs from the spruce bud worm (*Choristoneura fumiferana*) and the armyworm (*Pseudaletia unipuncta*). In both species, two isozymes of FPPS were identified but only one of them exhibited prenyltransferase activity, when expressed individually. An altered FARM (DDxxD to NDxxE) motif explained the lack of activity in the other FPPS. Interestingly, the co-expression of both enzymes resulted in higher production of FPP when compared with individually expressed IDS isozymes. Protein interaction assays identified these lepidopteran FPPS to form heterodimers.

The lack of activity in enzymatic assays with individually expressed *PaIDS2* or *PsIDS2*, led to the hypothesis that these enzymes may form heterodimers with other IDS isozymes to gain activity, especially since *PsIDS2* is the highest expressed IDS in *P. striolata*. Co-expressed *PaIDS1* and *PaIDS2* produced (*E,E*)-FPP and small amounts of GPP in enzymatic assays. Since there are no differences in the product spectrum of individually expressed *PaIDS1* and co-expressed *PaIDS1* and *PaIDS2*, the activity in these assays may be due to *PaIDS1* activity, only. Co-expressed *PaIDS2* and *PaIDS3* exhibited the same product spectrum as individually expressed *PaIDS3*. Accordingly, only (*Z,Z*)-FPP and NPP was detected, suggesting that these enzyme combinations do not play a role in (*Z,E*)-FPP formation.

Co-expressed *PaIDS1* and *PaIDS3* accepted DMAPP and IPP as substrates to produce (*E,E*)-FPP, (*Z,E*)-FPP and the diterpene precursor GGPP. In contrast, individually expressed, neither *PaIDS3* nor *PaIDS1* were able to produce (*Z,E*)-FPP or GGPP when provided with DMAPP and IPP. These results suggest that *PaIDS1* and *PaIDS3* may interact with each other. However, the presence of both enzymes is necessary to convert DMAPP and IPP into (*Z,E*)-FPP.

Activity assays with co-expressed *PsIDS1* and *PsIDS3* resulted in the production of GGPP, a product which was not detected in assays with individually expressed *PsIDSs*. Though only low amounts of (*Z,E*)-FPP were detected with co-expressed *PsIDS1* and *PsIDS3*, enzymatic assays with either mixed crude extracts (1:1 vol/vol) or mixed elution fractions (1:1 c/c) from individually expressed *PsIDS1* and *PsIDS3*, resulted in considerably higher amounts of (*Z,E*)-FPP. These results demonstrate that both, *PsIDS1* and *PsIDS3*, are necessary to produce (*Z,E*)-FPP, the substrate for *PsTPS1* to produce volatile sesquiterpenes in *P. striolata*.

Spike-in experiments from assays with co-expressed IDS1 and IDS3 identified that produced GGPP was not the all-trans-isomer (*E,E,E*)-GGPP. The total conformation

of GGPP was not identified in the process of this master project, but enzymatic assays with co-expressed *PaIDS1* and *PaIDS3*, supplied with  $\text{Co}^{2+}$  (**Figure 19 B**), may give some information about its conformation.

In assays with 0.1 or 1 mM of  $\text{Co}^{2+}$ , (*E,E*)-FPP, (*Z,E*)-FPP and GGPP was produced. Assays with co-expressed *PaIDS1* and *PaIDS3*, supplied with 10 mM of  $\text{Co}^{2+}$  resulted mainly in the production of (*E,E*)-FPP, whereas only low amounts of (*Z,E*)-FPP and GGPP were detected. These results suggest that (*Z,E*)-FPP may serve as the substrate for GGPP synthesis. Concluding from this hypothesis, one could assume that the conformation of the diterpene precursor is either (*E,Z,E*)-GGPP or (*Z,Z,E*)-GGPP, depending on whether *IDS1* or *IDS3* elongate (*Z,E*)-FPP with IPP in *trans*- or *cis*- conformation, respectively.

#### **4.4 RNAi revealed that *PsIDS1* and *PsIDS3* are involved in the biosynthesis of (*Z,E*)-FPP**

Recombinant *PsIDS3*, supplied with GPP and IPP produces (*Z,E*)-FPP. This serves as substrate for *PsTPS1*, which is responsible for the production of volatile sesquiterpenes in male *P. striolata* (Beran, 2016). Some of these sesquiterpenes were identified to act as aggregation pheromones (Beran *et al.*, 2016a). However, enzyme activity of recombinant *PsIDS3* suggests this enzyme being involved in aggregation pheromone synthesis, but *in vivo* evidence is still missing.

The knock-down of *PsIDS3* in the first RNAi experiment resulted in significantly lower (*Z,E*)-FPPS activity in crude beetle extracts compared to the non-injected control group ( $p = 0.017$ ). No statistically significant differences between the non-injected control group and *PsIDS3* knock-down was evident, but a trend was visible ( $p = 0.06$ ). Additionally, the emission of volatile sesquiterpenes was significantly reduced in comparison to the non-injected control group ( $p = 0.004$ ). Quantitative RT-PCR analysis revealed that the dsRNA injection targeting *PsIDS3* did not affect transcript levels of *PsIDS1*, *PsIDS2* and *PsTPS1*. These results suggest *PsIDS3* to be involved in aggregation pheromone synthesis *in vivo*.

The knock-down of *PsIDS1*, *PsIDS2* or *PsIDS3*, in the second RNAi experiment, delivered more challenging results. Although qPCR analysis revealed no off-target effects and significantly reduced transcript levels for the targeted genes (**Figure 35**), the product formation in enzymatic assays with crude beetle extracts revealed a high variability between treatments.



The knock-down of *PsIDS1* resulted in significantly reduced GPPS activity and (*Z,E*)-FPPS activity compared to the non-injected control group and the negative control, respectively. Significantly reduced (*Z,E*)-FPPS activity was also apparent in *dsPsIDS3* injected beetles compared to the negative control. This result is consistent with the results of the first RNAi experiment.

However, the knock-down of *PsIDS2* provided no evidence that *IDS2* in *P. striolata* plays a role in GPP, (*E,E*)-FPP or (*Z,E*)-FPP production. The knock-down of *IDS1* and *IDS3* in *P. striolata* supports the hypothesis that *PsIDS1* produces GPP, which is subsequently used by *PsIDS3* to generate (*Z,E*)-FPP.

## 5 Summary and Outlook

Summarizing, the results of this master's thesis provided new insights into the biosynthesis of (*Z,E*)-FPP in *P. armoraciae* and *P. striolata*.

The respective *IDS* enzymes of both species exhibited similar activities. *IDS1* produced (*E,E*)-FPP, the substrate for the biosynthesis of juvenile hormones. In both beetle species, recombinant *IDS3* produced (*Z,E*)-FPP when supplied with GPP and IPP. Under assay conditions, *PaIDS2* showed no enzyme activity to produce terpenoid precursor molecules. The same was reported for *PsIDS2* (Beran *et al.*, 2016b). The SARM motif in both enzymes is modified in the same way (DDxxD to KDxxN), which may explain the lack of activity. Although highly expressed in both beetles, the role of *IDS2* remains unclear and could be a topic for ongoing research. Enzymatic assays, carried out to investigate the influence of divalent metal ions on *PaIDS* enzymes, showed that  $Mg^{2+}$ ,  $Mn^{2+}$  and  $Co^{2+}$  affected the overall enzyme activity. Only slight changes in the product spectrum were evident in these assays. One major finding of this master's thesis was the verification that both, recombinant *IDS1* and *IDS3*, are necessary to produce (*Z,E*)-FPP by using the canonical substrates DMAPP and IPP. Knock-down of *PsIDS1* or *PsIDS3* via RNAi resulted in reduced (*Z,E*)-FPPS activity in beetle crude extracts, which is consistent with the *in vitro* assay and suggest *PsIDS1* and *PsIDS3* to be involved in (*Z,E*)-FPP production *in vivo*. RNAi experiments, targeting *PsIDS1* reduced GPPS activity in beetle crude extracts, support the hypothesis that *PsIDS1* produces GPP as a substrate for *PsIDS3*. However, the inconsistent *IDS* activity in beetle crude extracts makes it difficult to finally confirm the role of *IDS1* and *IDS3* in *P. striolata*. Quantitative RT-PCR data showed that dsRNA injection did not result in

a total knock-down of IDS genes, which may explain the high variability of IDS activity in beetle crude extracts. An alternative approach would be a knock-out of IDS genes, for instance by using the CRISPR/Cas9 system.

Interaction studies with recombinant *PsIDS1* and *PsIDS3* gave no information that a heterodimerization was necessary for the production of (*Z,E*)-FPP or if simultaneous presence of these enzymes in the same environment is sufficient. Evidence for a putative heterodimerization could be provided by protein protein interaction assays, using two-dimensional SDS-PAGE, yeast-two-hybrid systems or with the help of enzyme-linked immunosorbent assays (ELISA).

## 6 References

- Bartelt, R. J., Cosse, A. A., Zilkowski, B. W., Weisleder, D. and Momany, F. A. (2001) Male-specific sesquiterpenes from *Phyllotreta* and *Aphthona* flea beetles. *Journal of Chemical Ecology* **27**: 2397-2423.
- Belles, X., Martin, D. and Piulachs, M. D. (2005) The mevalonate pathway and the synthesis of juvenile hormone in insects. *Annu Rev Entomol* **50**: 181-199.
- Beran, F., Jiménez-Alemán, G. H., Lin, M.-y., Hsu, Y.-C., Mewis, I., Srinivasan, R., Ulrichs, C., Boland, W., Hansson, B. S. and Reinecke, A. (2016a) The Aggregation Pheromone of *Phyllotreta striolata* (Coleoptera: Chrysomelidae) Revisited. *Journal of Chemical Ecology* **42**: 1-8.
- Beran, F., Mewis, I., Srinivasan, R., Svoboda, J., Vial, C., Mosimann, H., Boland, W., Buttner, C., Ulrichs, C., Hansson, B. S. and Reinecke, A. (2011) Male *Phyllotreta striolata* (F.) produce an aggregation pheromone: identification of male-specific compounds and interaction with host plant volatiles. *J Chem Ecol* **37**: 85-97.
- Beran, F. R., P.; Luck, K.; Nagel, R.; Vogel, H.; Wielsch, N.; Irmisch, S.; Ramasamy, S.; Gershenson, J.; Heckel, D. G.; Köllner, T. G. (2016b) Novel family of terpene synthases evolved from *trans*-isoprenyl diphosphate synthases in a flea beetle. *PNAS* **113**: 2922-2927.
- Boppre, M. (1978) Chemical Communication, Plant Relationships, and Mimicry in the Evolution of Danaid Butterflies. *Entomologia Experimentalis Et Applicata* **24**: 264-277.
- Burgess, L. (1977) Flea beetles (Coleoptera-Chrysomelidae) attacking rape crops in Canadian prairie provinces. *Can Entomol* **109**: 21-32.
- Burke, C. C., Wildung, M. R. and Croteau, R. (1999) Geranyl diphosphate synthase: Cloning, expression, and characterization of this prenyltransferase as a heterodimer. *P Natl Acad Sci USA* **96**: 13062-13067.
- Butenandt, A. and Hecker, E. (1961) Synthese des Bombykols, des Sexual-Lockstoffes des Seidenspinners, und seiner geometrischen Isomeren. *Angew Chem Int Edit* **73**: 349-353.
- Chen, C. C., Shy, J. F., Ko, W. F., Hwang, T. F. and Lin, C. S. (1991) Studies on the ecology and control of *Phyllotreta striolata* (Fab.) (II) Developmental duration and population fluctuation. *Plant Protection Bulletin* **33**: 354-363.
- Cymborowski, B. and Stolarz, G. (1979) Role of juvenile-hormone during larval-pupal transformation of *Spodoptera littoralis* - switchover in the sensitivity of the prothoracic gland to juvenile-hormone. *Journal of Insect Physiology* **25**: 939-942.

- Dossey, A. T., Walse, S. S. and Edison, A. S. (2008) Developmental and geographical variation in the chemical defense of the walking stick insect *Anisomorpha buprestoides*. *Journal of Chemical Ecology* **34**: 584-590.
- Dyer, L. A. and Bowers, M. D. (1996) The importance of sequestered iridoid glycosides as a defense against an ant predator. *Journal of Chemical Ecology* **22**: 1527-1539.
- Fire, A., Xu, S. Q., Montgomery, M. K., Kostas, S. A., Driver, S. E. and Mello, C. C. (1998) Potent and specific genetic interference by double-stranded RNA in *Caenorhabditis elegans*. *Nature* **391**: 806-811.
- Frick, S., Nagel, R., Schmidt, A., Bodemann, R. R., Rahfeld, P., Pauls, G., Brandt, W., Gershenzon, J., Boland, W. and Burse, A. (2013) Metal ions control product specificity of isoprenyl diphosphate synthases in the insect terpenoid pathway. *PNAS* **110**: 4194-4199.
- Fujihashi, M., Zhang, Y. W., Higuchi, Y., Li, X. Y., Koyama, T. and Miki, K. (2001) Crystal structure of *cis*-prenyl chain elongating enzyme, undecaprenyl diphosphate synthase. *P Natl Acad Sci USA* **98**: 4337-4342.
- Fujiwara, S., Yamanaka, A., Hirooka, K., Kobayashi, A., Imanaka, T. and Fukusaki, E. (2004) Temperature-dependent modulation of farnesyl diphosphate/geranylgeranyl diphosphate synthase from hyperthermophilic archaea. *Biochem Biophys Res Commun* **325**: 1066-1074.
- Gao, Y., Honzatko, R. B. and Peters, R. J. (2012) Terpenoid synthase structures: a so far incomplete view of complex catalysis. *Nat Prod Rep* **29**: 1153-1175.
- Gershenzon, J. and Dudareva, N. (2007) The function of terpene natural products in the natural world. *Nature Chemical Biology* **3**: 408-414.
- Goldstein, J. L. and Brown, M. S. (1990) Regulation of the Mevalonate Pathway. *Nature* **343**: 425-430.
- Hosfield, D. J., Zhang, Y. M., Dougan, D. R., Broun, A., Tari, L. W., Swanson, R. V. and Finn, J. (2004) Structural basis for bisphosphonate-mediated inhibition of isoprenoid biosynthesis. *J Biol Chem* **279**: 8526-8529.
- Jensen, A. N. and Jensen, L. T. (2015) Manganese transport, trafficking and function in invertebrates. *Issues Toxicol* **22**: 1-33.
- Lamb, R. J. (1989) Entomology of oilseed brassica crops. *Annu Rev Entomol* **34**: 211-229.
- Li, G. Z., Vissers, J. P., Silva, J. C., Golick, D., Gorenstein, M. V. and Geromanos, S. J. (2009) Database searching and accounting of multiplexed precursor and product ion spectra from the data independent analysis of simple and complex peptide mixtures. *Proteomics* **9**: 1696-1719.

- Liang, P. H. (2009) Reaction kinetics, catalytic mechanisms, conformational changes, and inhibitor design for prenyltransferases. *Biochemistry-U.S.* **48**: 6562-6570.
- Light, D. R., Lazarus, R. A. and Dennis, M. S. (1989) Rubber elongation by Farnesyl pyrophosphate synthases involves a novel switch in enzyme stereospecificity. *J Biol Chem* **264**: 18598-18607.
- Nagel, R., Gershenzon, J. and Schmidt, A. (2012) Nonradioactive assay for detecting isoprenyl diphosphate synthase activity in crude plant extracts using liquid chromatography coupled with tandem mass spectrometry. *Anal Biochem* **422**: 33-38.
- Nielsen, J. K., Larsen, L. M. and Sorensen, H. (1979) Host plant selection of the horseradish flea beetle *Phyllotreta armoraciae* (Coleoptera: Chrysomelidae): identification of two flavonol glycosides stimulating feeding in combination with glycosinolates. *Entomologia Experimentalis et Applicata* **26**: 40-48.
- Picimbon, J. F. and Leal, W. S. (1999) Olfactory soluble proteins of cockroaches. *Insect Biochem Molec* **29**: 973-978.
- Poulter, C. D. (2006) Farnesyl diphosphate synthase. A paradigm for understanding structure and function relationships in *E*-polyprenyl diphosphate synthases. *Phytochemistry Reviews* **5**: 17-26.
- Rohmer, M. (1999) The discovery of a mevalonate-independent pathway for isoprenoid biosynthesis in bacteria, algae and higher plants. *Nat Prod Rep* **16**: 565-574.
- Romani, A. M. P. and Maguire, M. E. (2002) Hormonal regulation of Mg<sup>2+</sup> transport and homeostasis in eukaryotic cells. *Biometals* **15**: 271-283.
- Sen, S. E., Cusson, M., Trobaugh, C., Beliveau, C., Richard, T., Graham, W., Mimms, A. and Roberts, G. (2007a) Purification, properties and heteromeric association of type-1 and type-2 lepidopteran farnesyl diphosphate synthases. *Insect Biochem Mol Biol* **37**: 819-828.
- Sen, S. E. and Sperry, A. E. (2002) Partial purification of a farnesyl diphosphate synthase from whole-body *Manduca sexta*. *Insect Biochem Molec* **32**: 889-899.
- Sen, S. E., Trobaugh, C., Beliveau, C., Richard, T. and Cusson, M. (2007b) Cloning, expression and characterization of a dipteran farnesyl diphosphate synthase. *Insect Biochem Molec* **37**: 1198-1206.
- Shevchenko, A., Tomas, H., Havlis, J., Olsen, J. V. and Mann, M. (2006) In-gel digestion for mass spectrometric characterization of proteins and proteomes. *Nature protocols* **1**: 2856-2860.
- Sobotnik, J., Hanus, R., Kalinova, B., Piskorski, R., Cvacka, J., Bourguignon, T. and Roisin, Y. (2008) (*E,E*)-alpha-Farnesene, an alarm pheromone of the termite *Prorhinotermes canalifrons*. *Journal of Chemical Ecology* **34**: 478-486.

- Steele, C. L., Crock, J., Bohlmann, J. and Croteau, R. (1998) Sesquiterpene synthases from grand fir (*Abies grandis*) - Comparison of constitutive and wound-induced activities, and cDNA isolation, characterization and bacterial expression of delta-selinene synthase and gamma-humulene synthase. *J Biol Chem* **273**: 2078-2089.
- Tarshis, L. C., Proteau, P. J., Kellogg, B. A., Sacchettini, J. C. and Poulter, C. D. (1996) Regulation of product chain length by isoprenyl diphosphate synthases. *P Natl Acad Sci USA* **93**: 15018-15023.
- Tarshis, L. C., Yan, M. J., Poulter, C. D. and Sacchettini, J. C. (1994) Crystal-structure of recombinant Farnesyl diphosphate synthase at 2.6-Angstrom resolution. *Biochemistry-U S* **33**: 10871-10877.
- Tholl, D., Croteau, R. and Gershenzon, J. (2001) Partial purification and characterization of the short-chain prenyltransferases, geranyl diphosphate synthase and farnesyl diphosphate synthase, from *Abies grandis* (grand fir). *Arch Biochem Biophys* **386**: 233-242.
- Vandermoten, S., Charlotiaux, B., Santini, S., Sen, S. E., Beliveau, C., Vandebol, M., Francis, F., Brasseur, R., Cusson, M. and Haubruge, E. (2008) Characterization of a novel aphid prenyltransferase displaying dual Geranyl/Farnesyl diphosphate synthase activity. *Febs Lett* **582**: 2471-2471.
- Vandermoten, S., Santini, S., Haubruge, E., Heuze, F., Francis, F., Brasseur, R., Cusson, M. and Charlotiaux, B. (2009) Structural features conferring dual Geranyl/Farnesyl diphosphate synthase activity to an aphid prenyltransferase. *Insect Biochem Molec* **39**: 707-716.
- Vig, K. (2002) Data on the biology of the crucifer flea beetle, *Phyllotreta cruciferae* (Goeze, 1777) (Coleoptera, Chrysomelidae, Alticinae). *Meded Rijksuniv Gent Fak Landbouwkde Toegep Biol Wet* **67**: 537-546.
- Vig, K. and Verdyck, P. (2001) Data on the host plant selection of the horseradish flea beetle, *Phyllotreta armoraciae* (Koch, 1803) (Coleoptera, Chrysomelidae, Alticinae). *Meded Rijksuniv Gent Fak Landbouwkde Toegep Biol Wet* **66**: 277-283.
- Wang, G. D. and Dixon, R. A. (2009) Heterodimeric Geranyl(geranyl)diphosphate synthase from hop (*Humulus lupulus*) and the evolution of monoterpene biosynthesis. *P Natl Acad Sci USA* **106**: 9914-9919.
- Wientjen, Wh, Lakwijk, A. C. and Vanderma, T (1973) Alarm pheromone of grain aphids. *Experientia* **29**: 658-660.
- Yang, Y., Lu, X., Rong, X. Q., Jiang, W. B., Lai, D. W., Ma, Y., Zhou, K., Fu, G. S. and Xu, S. M. (2015) Inhibition of the mevalonate pathway ameliorates anoxia-induced down-regulation of FKBP12.6 and intracellular calcium handling dysfunction in H9c2 cells. *Journal of Molecular and Cellular Cardiology* **80**: 166-174.

- Zeki, A. A., Ott, S. and Wu, R. (2015) The mevalonate pathway modulates human airway epithelial cell Eotaxin-3 (ccl26) production: implications for the regulation of airway eosinophilia. *American Journal of Respiratory and Critical Care Medicine* **191**.
- Zhang, Y. W., Koyama, T., Marecak, D. M., Prestwich, G. D., Maki, Y. J. and Ogura, K. (1998) Two subunits of heptaprenyl diphosphate synthase of *Bacillus subtilis* form a catalytically active complex. *Biochemistry-Us* **37**: 13411-13420.

## 7 Supplementary Information

**Table 10: dsRNA sequences**

dsRNA	Sequence
ds <i>Ps</i> IDS1	ACGGAAGGAGTAGGTTTAATAGCAGTCAACGATGGAATCCTTCT CGAAAACAGCATTACCTGCTGCTCAAAAAGCATTATCCTCTC TACCCTGCTACGTACCCATCATGGAGCTGTTTCGCGACATCACC TTCAAAACATCCTTGGGACAATCGCTCGATTGCCTTTGTCTCGCC AATGGAAAGCCCGTATTGGATTTGTTACGATGAAAAGGTACAA GACCATCGTCAAGTACAAGACTTCCTATT
ds <i>Ps</i> IDS2	GATCGAACTGTTCCAAGACACGACGCTGAAGAGCGCCATGGGG AAATCCCTCGACTGCGAAATAACTAACGATCTCACTAAAATGAC CATGAAAACTACTCGTTGATATCGAAATACAGGAACGGGTACT GTACGCTACAGTTGCCAGTCGCTGCGGCTATGTATTTAGCGGAA ATGAGCGATCCGGAACAGCATCGGCAAGCTCAGACCCTTTTACT GGAAATGGGGCATTATTTCCAAGTTCAAAAG
ds <i>Ps</i> IDS3	AGCGGCTGATTCCACGAGGCATGCACCAGAAACGATATCACTA GATAAATTCAAGACAATCGCTAAATACAAAACGGGTTTTTACAC ATTCTATTACTCGGTGGGATTGGGGATGTATCTATCCAGGCAAT TCAATAAGGACGTATTGGAGAATCAAATAGCTCCTTTACTGTTT GACATGGGCGAGTACTTCCAAATTAAGAACGATATTAACGACTG TTTCGTTAAGGAAGACATAGCAGGGAAGACGGGTACTGACATA GAGGAGAGTAAGTGCACATGGCTGGCGGTGAAGGCGTTGGAGA AGGGAAATGAGGCTCAAAAAGCGCTGTTTAGAGAAAATTACGG CAAAGCGGATCCGA
dsIMPI	CGGTGGAGCCTGCGATAATGTATGTGCAGATTTACATATACAGA ATAAAACAAACTGTCCCATCATTAATATAAGATGTAATGACAAG TGCTACTGTGAAGATGGCTATGCAAGGGATGTCAATGGCAAATG TATACCGATAAAAGACTGTCTAAAATACGTTTCGCGTTCGTTCCA TTGGGATACCAGTCGACAAGAAATGCTGCACAGGTCCTAACGA ACACTATGACGAAGAGAAAGTAAGCTGTCCTCCAGAAACCTGT ATCTCCCTTGTGGCTAAGTTTTCTGCATTGACTCCCCTCCACCG TCG



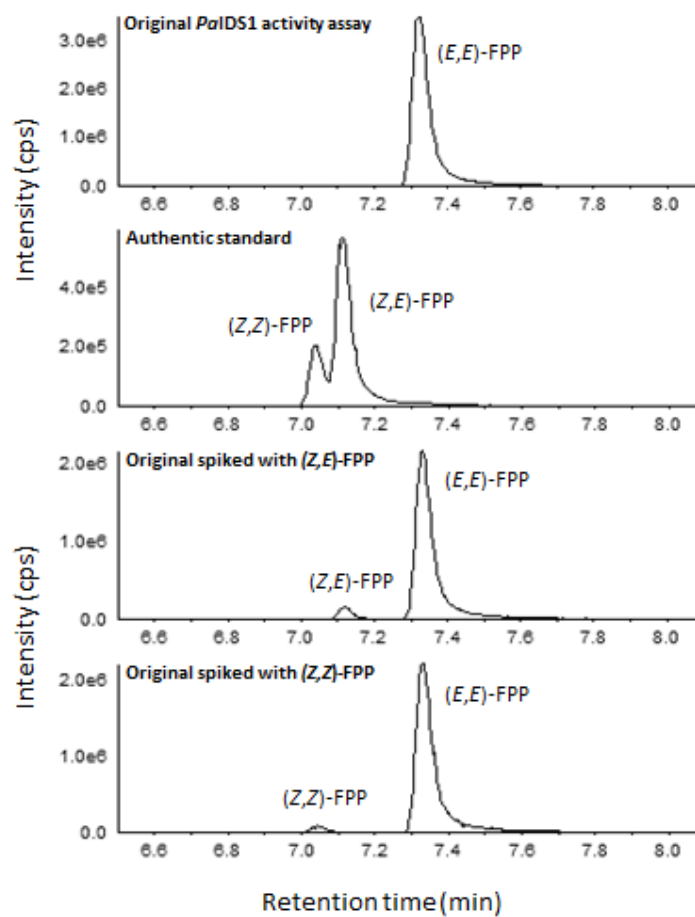
**Table 11: Statistics RNAi targeting *PsIDS3***

Figure	Statistics	Trans-formation	Tested treatments	F-value	p-value
<b>Figure 29:</b> RNAi <i>PsIDS3</i> GPP+IPP → (Z,E)-FPP	One Way ANOVA	square root	-	9.811	0.018
	Tukey's Test		IMPI vs. <i>PsIDS3</i>	-	0.017
			IMPI vs. NI	-	0.569
			NI vs. <i>PsIDS3</i>	-	0.06
<b>Figure 30:</b> RNAi <i>PsIDS3</i> volatile collection	One Way ANOVA		-	4.624	0.027
	Tukey's Test		NI vs. IDS3	-	0.023
			NI vs. IMPI	-	0.171
			IMPI vs. IDS3	-	0.530
RNAi <i>PsIDS3</i> only qPCR IDS1	One Way ANOVA	-	-	1.528	0.249
RNAi <i>PsIDS3</i> only qPCR IDS2	One Way ANOVA	-	-	14.722	0.001
	Tukey's Test		IDS3 vs. IMPI	-	<0.001
			IDS3 vs. NI	-	0.513
			NI vs. IMPI	-	0.003
RNAi <i>PsIDS3</i> only qPCR IDS3 knock-down	One Way ANOVA	-	-	16.77	<0.001
	Tukey's Test		NI vs. IDS3	-	<0.001
			NI vs. IMPI	-	0.873
			IMPI vs. IDS3	-	<0.001
RNAi <i>PsIDS3</i> only qPCR TPS1	One Way ANOVA	-	-	1.109	0.356

**Table 12: Statistics RNAi targeting *PsIDS1*, *PsIDS2* and *PsIDS3***

Figure	Statistics	Transformation	Tested treatments	F-value	p-value
<b>Figure 32:</b> RNAi <i>PsIDS1-3</i> DMAPP+IPP → GPP	One Way ANOVA	log	-	3.319	0.028
	Tukey's Test		IDS3 vs. IDS1	-	0.038
			IDS3 vs. IMPI	-	0.935
			NI vs. IDS1	-	0.042
			IDS2 vs. IDS1	-	0.124
<b>Figure 33-A:</b> RNAi <i>PsIDS1-3</i> DMAPP + IPP → (E,E)-FPP	One Way ANOVA	-	-	1.308	0.258
<b>Figure 33 B:</b> RNAi <i>PsIDS1-3</i> GPP + IPP → (E,E)-FPP	One Way ANOVA	log	-	3.628	0.02
	Tukey's Test		IDS3 vs. IDS1	-	0.032
			NI vs. IDS1	-	0.084
<b>Figure 34 B:</b> RNAi <i>PsIDS1-3</i> GPP + IPP → (Z,E)-FPP	One Way ANOVA	log	-	4.600	0.01
	Tukey's Test		IMPI vs. IDS3	-	0.034
			IMPI vs. IDS1	-	0.059
			NI vs. IDS3	-	0.089
<b>Figure 34 A:</b> RNAi <i>PsIDS1-3</i> DMAPP + IPP → (Z,E)-FPP	Kruskal-Wallis Test	-	-	10.769 (H)	0.029
	Dunn's Method		NI vs. IDS1	-	<0.05
			NI vs. IDS3	-	>0.05
			IMPI vs. IDS1	-	>0.05
Figure 35: RNAi <i>PsIDS1-3</i> qPCR IDS1 knock-down	One Way ANOVA	-	-	13.816	<0.001
	Tukey's Test		IDS3 vs. IDS1	-	<0.001
			NI vs. IDS1	-	<0.001
			IMPI vs. IDS1	-	<0.001
			IDS2 vs. IDS1	-	0.001
Figure 35: RNAi <i>PsIDS1-3</i> qPCR IDS2 knock-down	One Way ANOVA	-	-	22.157	<0.001
	Tukey's Test		NI vs. IDS2	-	<0.001
			IDS1 vs. IDS2	-	<0.001
			IMPI vs. IDS2	-	<0.001
			IDS3 vs. IDS2	-	<0.001
Figure 35: RNAi <i>PsIDS1-3</i> qPCR IDS3 knock-down	One Way ANOVA	-	-	24.642	<0.001
	Tukey's Test		NI vs. IDS3	-	<0.001
			IDS1 vs. IDS3	-	<0.001
			IDS1 vs. IDS2	-	<0.001
			IMPI vs. IDS3	-	<0.001
<b>Figure 35:</b> RNAi <i>PsIDS1-3</i> qPCR TPS1	One Way ANOVA	-	-	1.442	0.25

## *PaIDS1*



**Figure 36: Spike-in experiments with *PaIDS1***

Heterologously expressed *PaIDS1* produced (*E,E*)-FPP when supplied with DMAPP and IPP. Authentic standards were used to identify products.

## *PaIDS1*

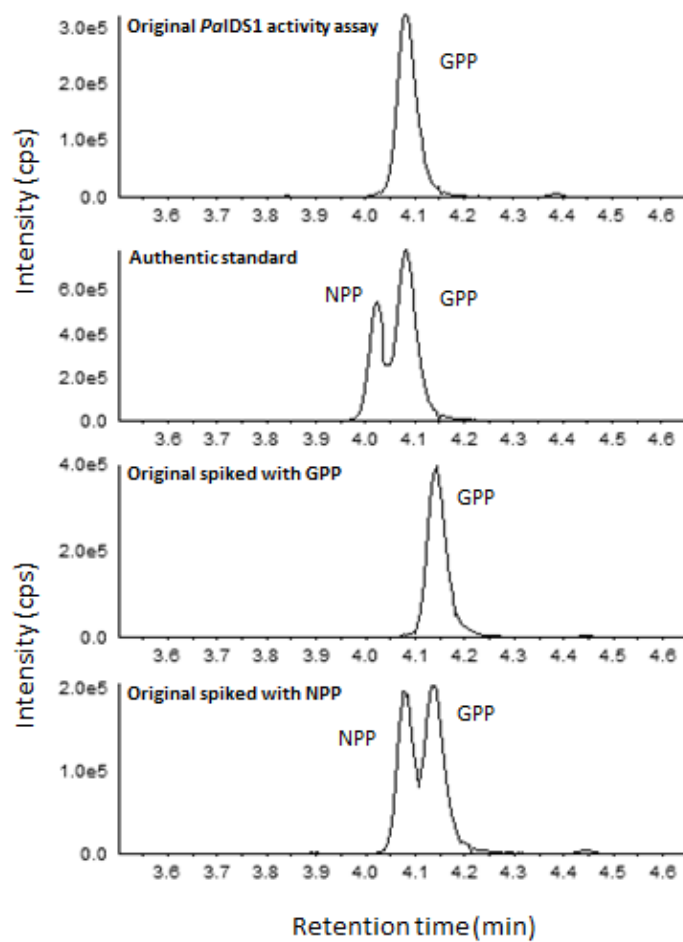


**Figure 37: Spike-in experiments with *PaIDS1***

Heterologously expressed *PaIDS1* produced GPP when supplied with DMAPP and IPP. Authentic standards were added to identify products.

## *PaIDS3*

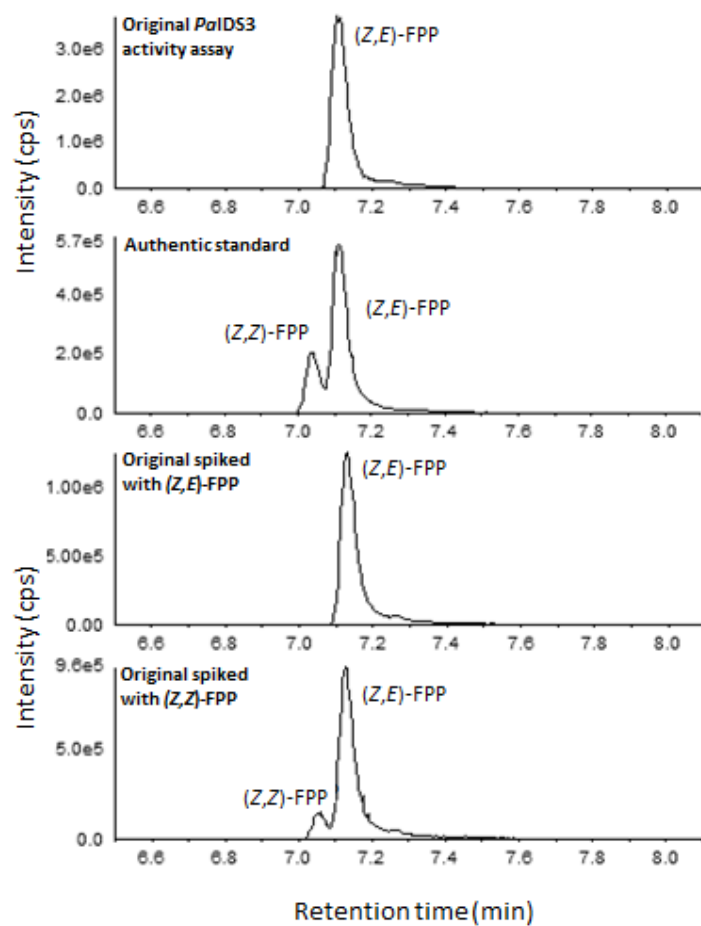


**Figure 38: Spike-in experiments with enzymatic assays with *PaIDS3***

Heterologously expressed *PaIDS3* produces (Z,E)-FPP when supplied with the substrates GPP and IPP. Authentic standards were added to identify products.

## Co-expressed *PaIDS1* and *PaIDS3*

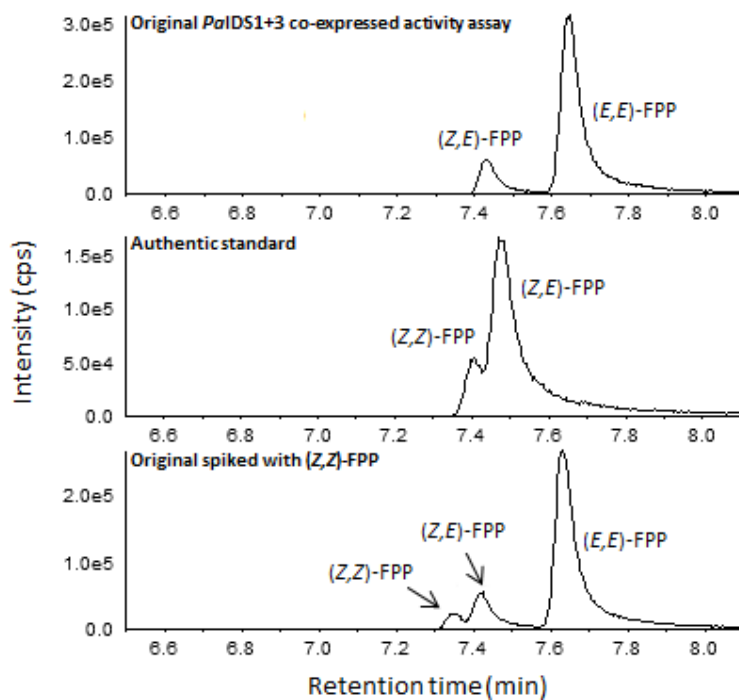


**Figure 39: Spike-in experiments with co-expressed *PaIDS1* and *PaIDS3***

Heterologously co-expressed *PaIDS1* and *PaIDS3* produce (Z,E)-FPP when supplied with the substrates DMAPP and IPP. Authentic standards were added to identify products.

## Co-expressed *PaIDS2* and *PaIDS3*

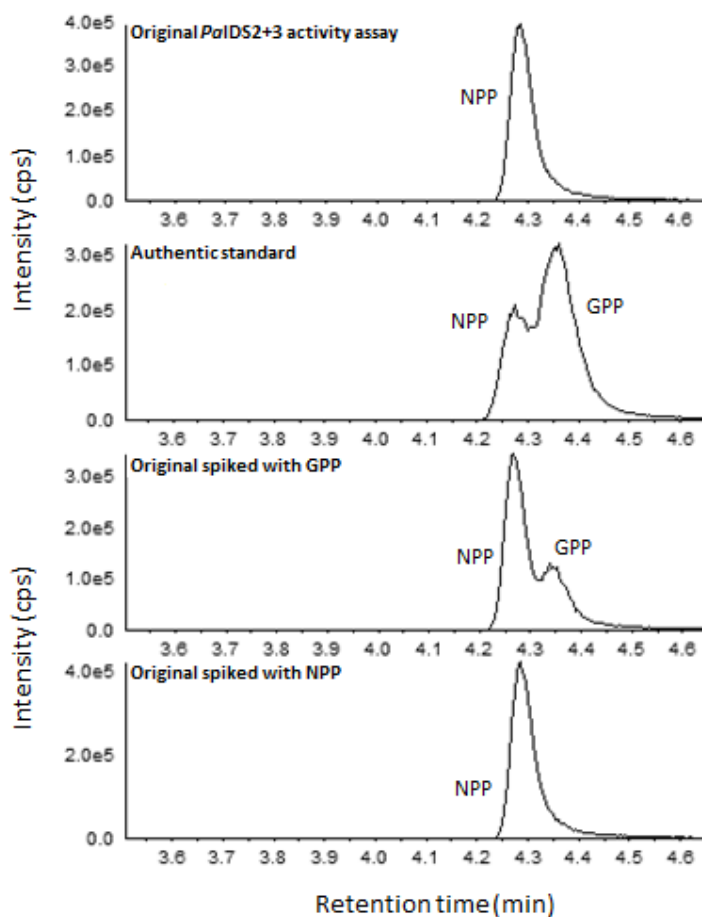


**Figure 40: Spike-in experiments with co-expressed *PaIDS2* and *PaIDS3***

Heterologously co-expressed *PaIDS2* and *PaIDS3* produced NPP when supplied with the substrates DMAPP and IPP. Authentic standards were added to identify products.

## *PsIDS3*

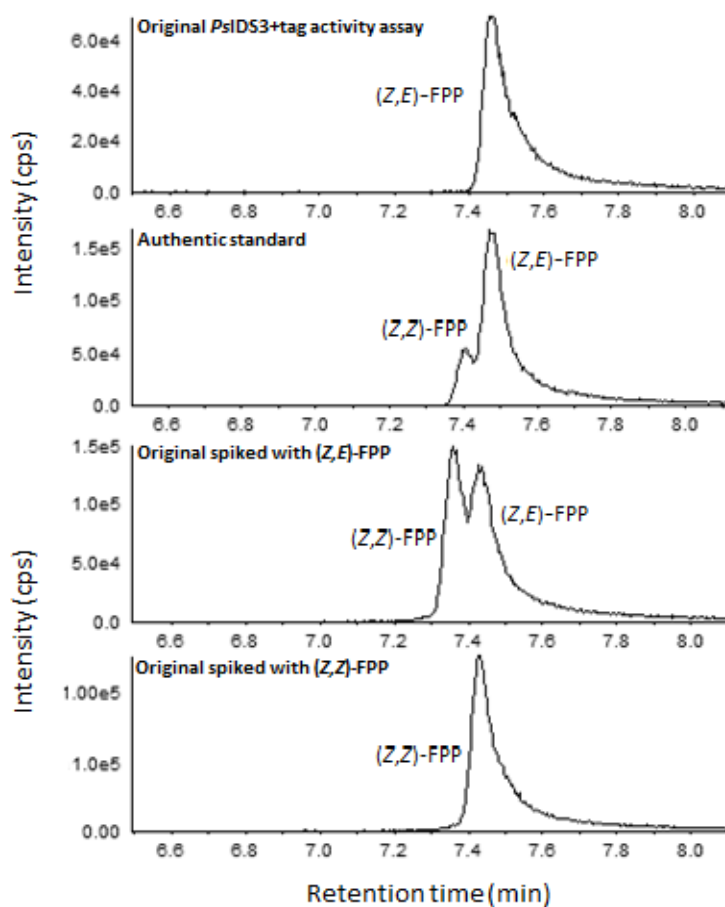


**Figure 41: Spike-in experiments with *PsIDS3***

Heterologously co-expressed *PsIDS3* produced (Z,Z)-FPP when supplied with the substrates GPP and IPP. Authentic standards were added to identify products.



## Co-expressed *PsIDS1* and *PsIDS3*

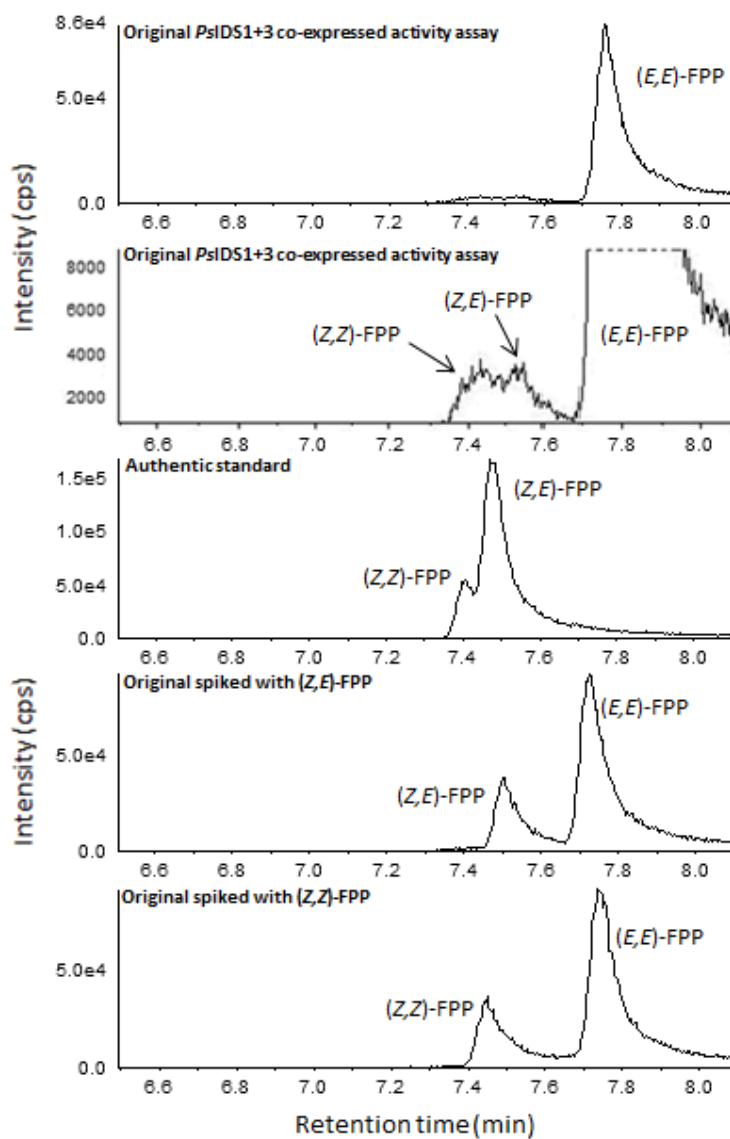


**Figure 42: Spike-in experiments with co-expressed *PsIDS1* and *PsIDS3***

Heterologously co-expressed *PsIDS1* and *PsIDS3* produced FPP when supplied with DMAPP and IPP. Authentic standards were added to identify products.

### Co-expressed *PsIDS1* and *PsIDS3*

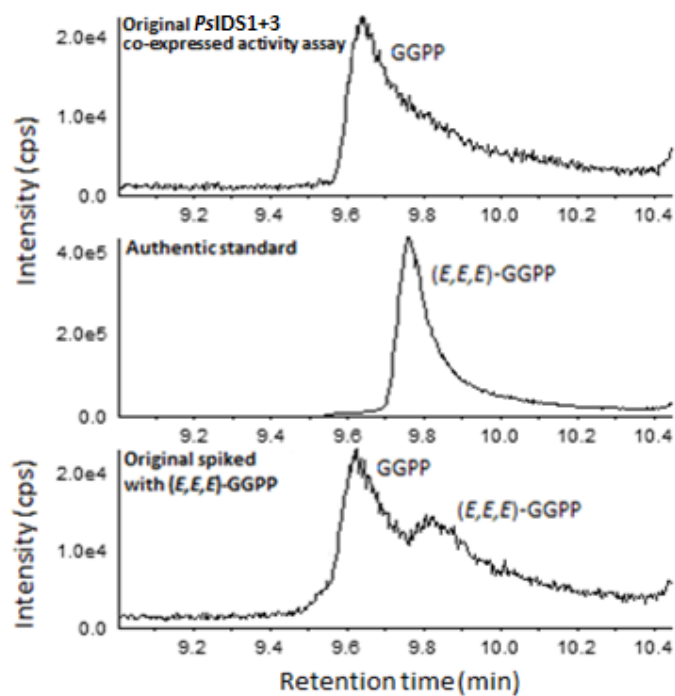


**Figure 43: Spike-in experiments with co-expressed *PsIDS1* and *PsIDS3***

Heterologously co-expressed *PsIDS1* and *PsIDS3* produced GGPP when supplied with DMAPP and IPP. Authentic standards were added to identify products.

### *PsIDS1* and *PsIDS3* with mixed crude extracts

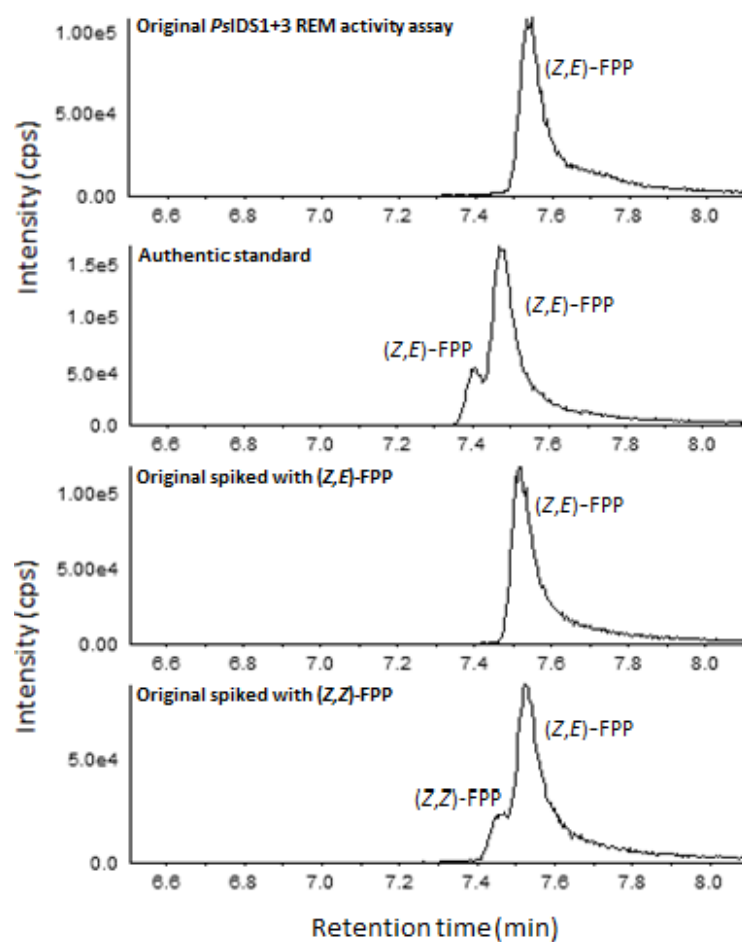


**Figure 44: Spike-in experiments with co-expressed *PsIDS1* and *PsIDS3* with mixed crude extracts**

Enzymatic assays with mixed crude extract fractions of *PsIDS1* and *PsIDS3* produced FPP. Authentic standards were added to products.

### *PsIDS1* and *PsIDS3* with mixed crude extracts

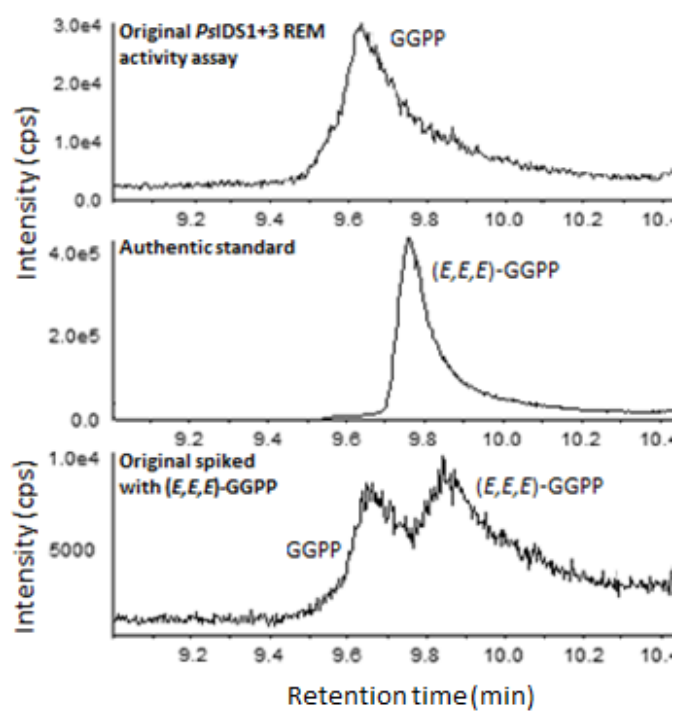


**Figure 45: Spike-in experiments with co-expressed *PsIDS1* and *PsIDS3* with mixed crude extracts**

Enzymatic assays with mixed crude extract fractions of *PsIDS1* and *PsIDS3* produced GGPP. Authentic standards were added to identify products.

### *PsIDS1* and *PsIDS3* with mixed elution fractions

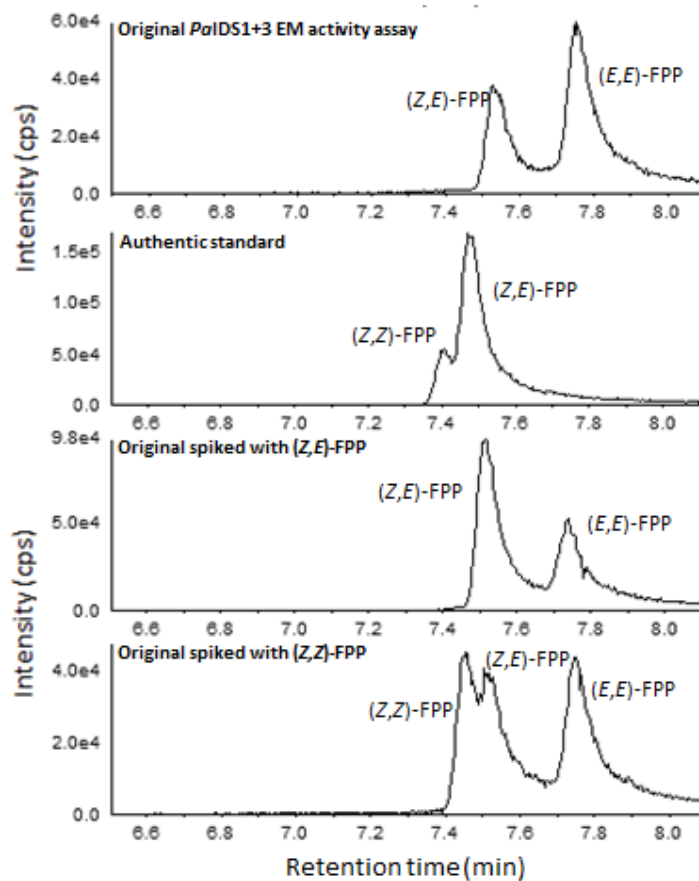


**Figure 46: Spike-in experiments of co-expressed *PsIDS1* and *PsIDS3* with mixed elution fractions**

Enzymatic assays with mixed elution fractions of *PsIDS1* and *PsIDS3* produced two FPP isomers. Authentic standards were added to identify products.

### *PsIDS1* and *PsIDS3* with mixed elution fractions

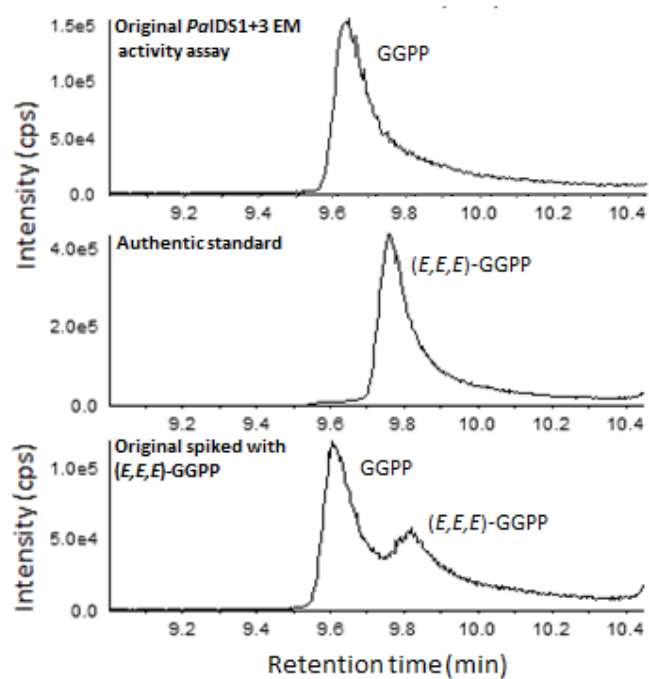


**Figure 47: Spike-in experiments of co-expressed *PsIDS1* and *PsIDS3* with mixed elution fractions**  
Enzymatic assays with mixed elution fractions of *PsIDS1* and *PsIDS3* produced GGPP. Authentic standards were added to identify products.

```

PsIDS1  ILLEMGEFFFOIQDDFLDFVFGSDVDTGK
PsIDS2  LILEMGHYFOVCKDFLNCFGSSESITN
PsIDS3  LLFDMGEYFQIRNDINDCFVKEDIAGK

```

**Figure 48: Cutout from the amino acid sequence alignment of *PsIDS1*, *PsIDS2* and *PsIDS3***  
The SARM motif (DDxxD; highlighted in red) is altered in *PsIDS2* and *PsIDS3* (Beran *et al.*, 2016b).

```

PaIDS1  MFSFNKLPINRASRELRNTLKRQINKTSSAPNSDAVSRKDGQLGANADLKPF SNVRAASDKWTHSKHNNSRALSTIQTK 80
PaIDS2  MFSFNKLPINRASRELRNTLKRQINKTSSAPNSDAVSRKDGQLGANADLKPF SNVRAASDKWTHSKHNNSRALSTIQTK 80
PaIDS3  -----MHSTYCNLLAPVWLRN-----AKCCEKVRFRSSLPKSNATYP 38

PaIDS1  VLPNVSNAFASKEESREFMALFPDIVRDLTDAGRHTDIPEVTKRFAHVLOYNVPNGKKTTRGLTTVIAVKMLEKPENLTP 160
PaIDS2  VLPNVSNAFASKEESREFMALFPDIVRDLTDAGRHTDIPEVTKRFAHVLOYNVPNGKKTTRGLTTVIAVKMLEKPENLTP 160
PaIDS3  TLASFS-----EADTFEFMSHFPTLVSDLSTSMNLENMKQATDRFALCMRNNVPNGKKVIRGLTTVIITVKMLEKPENLTP 112

PaIDS1  ENIRLANILGWCVELLQAYFIVSDDIMDINSISRGRPCWYRNEGVGLTAINDGILLNSLYQLLKKHLSLECYVPIVEL 240
PaIDS2  ENIRLANILGWCVELLQAFGVVDDLIDFSETRHNMACWYKYEDVGMTAVNDSLLPESLFEHLKYYLSNRSHYVSLTEL 240
PaIDS3  DNIRLANILGWFIELFEAAVLEDDLMDVSTRRGGLCWHRQKDVGVLAIDGILNLSGAYLLEKCYFGNHPHFADMSCF 192

PaIDS1  FHDITFKTSLGQSLDCLCLANGKPVLELFTMKRYNTIVKYYKTSHYSLQLPVALGMYLANMTDPEQHR-OAKTILLEGEE 319
PaIDS2  FODITLKSAMGKSLDCEITND----LSKMTMRNYSLISKYRNGYCSLQLPVALRMYLAGMSDPEQHR-OAOTLLEMGHY 315
PaIDS3  SCRVMYNTAIGQVIDSMRHP-----ETISLDKFKALIKYYKTYGYTFYFSVGLGMYLSRQFNKDVLDNQLIAPLLFDMGEY 267

PaIDS1  FOIQDDFLDFVFGDPEVTGKIGTDIRIGKCSWLAVALQRATPAQRKVMEEHYGKDSDESVAIVKNLYEELGLPATYAWVE 399
PaIDS2  FOVCKDFLNCFGDSE SITNIGSDVNEGKCTWLAVALQRANSSQRAVMEEFYGKKGSKAVHVIRNLEVLGLPATYERVE 395
PaIDS3  FOIRNDINDCFVKEDVAGKIGTDIEESKCTWLAVALKALKGNPAKALFRENYGKSDAKSVESIRNLYRELKLOEEFDEYE 347

PaIDS1  EESFNITRTH---IQQISKGLPHELFFKILRKLKLYRDC 434
PaIDS2  EQTNKIITTN---IQQLTRGLPHKLFETILRELYAFE- 429
PaIDS3  ADFFRSLRKRSLSESPYSNVAMVLEKLOHQVYKTVV 385

```

**Figure 49: Full amino acid sequence alignment of *PaIDS1*, *PaIDS2* and *PaIDS3***  
FARM and SARM motifs are highlighted in red. The SARM motif (DDxxD) is altered in *PaIDS2* and *PaIDS3*.  
*PaIDS1* and *PaIDS2* have an identical N-terminus

## 8 Acknowledgements

First, I want to thank my supervisor Dr. Franziska Beran for provision of the topic, guidance and support in the lab, help with the data analysis, proofreading this thesis and great encouragement.

I thank Prof. Dr. Wilhelm Boland for supervision of this master's thesis

I thank Prof. Dr. David G. Heckel and Dr. Franziska Beran for the opportunity to conduct my master's thesis in the Department of Entomology in the Max Planck Institute for Chemical Ecology in the Research Group Sesquestration and Detoxification in Insects of Dr. Franziska Beran.

I want to thank Dr. Michael Reichelt for great support concerning mass spectrometry samples and data analysis, Domenica Schnabelrauch for sequencing, Dr. Natalie Wielsch and Yvonne Hupfer for performing LC-MS<sup>E</sup> analysis.

I thank Dr. Sabine Haenniger, Wiebke Haeger and Johanna Langner for their support and for proofreading this thesis.

Finally, I am deeply thankful for the support from all members of the Department of Entomology. Special thanks to the SD-Group members Franziska Betzin, Susanne Donnerhacke, Theresa Sporer, Matilda Gikonyo and Zhi-Ling Yang for great support and providing a fantastic working atmosphere.



## **9 Statement of Authorship**

### **Eidesstattliche Erklärung**

Hiermit versichere ich, dass ich die Masterarbeit selbstständig verfasst und keine anderen als die angegebenen Quellen und Hilfsmittel benutzt habe, alle Ausführungen, die anderen Schriften wörtlich oder sinngemäß entnommen wurden, kenntlich gemacht sind und die Arbeit in gleicher oder ähnlicher Fassung noch nicht Bestandteil einer Studien- oder Prüfungsleistung war.

\_\_\_\_\_  
Ort, Datum

\_\_\_\_\_  
Unterschrift

